1-1-2014

The Role of Scapular Dyskinesis in Rotator Cuff and Biceps Tendon Pathology

Katherine E. Reuther
University of Pennsylvania, kreuther@seas.upenn.edu

The Role of Scapular Dyskinesis in Rotator Cuff and Biceps Tendon Pathology

Abstract
Shoulder tendon injuries including impingement, rotator cuff disease, and biceps tendon pathology are common clinical conditions and are a significant source of joint pain, instability, and dysfunction. These injuries may progress into partial tears then to complete tendon ruptures, which have limited healing capacity even when surgically repaired. These injuries are frequently seen in the presence of abnormal scapulothoracic joint kinematics (termed scapular dyskinesis). However, the cause and effect relationship between scapular dyskinesis and shoulder injury has not been directly defined. Additionally, while the incidence of shoulder injuries and recurrent failure of repairs is well-documented, the mechanisms behind them are not well-established, making optimal clinical management difficult. Therefore, the objectives of this study were to examine the effect of scapular dyskinesis on the initiation and progression of pathological changes in the rotator cuff and biceps tendon and to define the mechanical processes that lead to these changes. Unfortunately, clinical and cadaveric studies are unable to address the underlying causes of injury and cannot evaluate the injury process over time. Therefore, a rat model of scapular dyskinesis (created by denervating the trapezius and serratus anterior) was developed and used, both alone and in combination with overuse, to investigate the cause and effect relationships between changes in joint loading and alterations in tendon mechanical, histological, organizational, and biological properties. We hypothesized that scapular dyskinesis would result in altered joint loading conditions that would lead to degeneration of the rotator cuff and long head of the biceps. We found that scapular dyskinesis diminished joint function and passive joint mechanics and significantly reduced tendon properties. We also investigated the effect of overuse on tendon properties and found that overuse activity in the presence of scapular dyskinesis resulted in significantly more structural and biological adaptations than scapular dyskinesis alone. We also investigated the effect of scapular dyskinesis on supraspinatus tendon healing and found that scapular dyskinesis was detrimental to tendon properties. These results indicate that scapular dyskinesis is a causative mechanical mechanism of shoulder tendon injury. Identification of scapular dyskinesis as a mechanism of pathological changes will help inform and guide clinicians in developing optimal prevention and long-term rehabilitation strategies.

Degree Type
Dissertation

Degree Name
Doctor of Philosophy (PhD)

Graduate Group
Bioengineering

First Advisor
Louis J. Soslowsky

Keywords
Animal Model, Biceps, Overuse, Rotator Cuff, Scapular Dyskinesis

THE ROLE OF SCAPULAR DYSKINESIS IN ROTATOR CUFF AND BICEPS TENDON PATHOLOGY IN A RAT MODEL

Katherine Reuther

A DISSERTATION

In

Bioengineering

Presented to the Faculties of the University of Pennsylvania

in Partial Fulfillment of the Requirements for the Degree of Doctor of Philosophy

2014

Supervisor of Dissertation

_____

Louis J. Soslowsky, PhD, Fairhill Professor, Orthopaedic Surgery

Graduate Group Chairperson

_____

Jason A. Burdick, PhD, Professor, Bioengineering

Dissertation Committee

Kristy B. Arbogast, PhD, (Committee Chair)
Research Associate Professor, Pediatrics, Children's Hospital of Philadelphia
Mary F. Barbe, PhD
Professor, Anatomy and Cell Biology, Temple University
Kurt D. Hankenson, DVM, PhD
Associate Professor, Animal Biology, University of Pennsylvania
Andrew F. Kuntz, MD
Assistant Professor, Orthopaedic Surgery, University of Pennsylvania
Philip W. McClure, PT, PhD, FAPTA
Professor, Physical Therapy, Arcadia University

Acknowledgements

I would like to thank my advisor, Dr. Louis Soslowsky, for providing mentorship and support throughout my time here. I admire and respect him as a mentor and person and am grateful for his time, patience, commitment to teaching and mentoring, and valuable insight. I would like to thank my committee members for guiding me through my graduate education. I thank Dr. Andrew Kuntz for surgical assistance and clinical insight throughout the development and duration of this project. I also thank Dr. Philip McClure, Dr. Mary Barbe, Dr. Kurt Hankenson, and Dr. Kristy Arbogast for their time and valuable insight and suggestions for this project.

I would also like to thank the entire McKay Orthopaedic Research Laboratory. Dr. Stephen Thomas has been my mentor, Joint Damage partner, and colleague from the beginning and continues to be a close friend. His knowledge, advice, and clinical insight have been instrumental in my graduate education and in this dissertation. I would like to thank Jennica Tucker, Dr. Sarah Yannascoli, Dr. Adam Caro, and Dr. Joshua Gordon for their surgical assistance and willingness to help and discuss ideas. I would like to thank Rameen Vafa for his numerous contributions to this project and for his admirable work ethic and enthusiasm. I would like to thank Adam Pardes, Stephen Liu, Bob Zanes, Julianne Huegel, Pankti Bhatt, and Alex Delong for their contributions to this project. I would like to thank my fellow graduate students, Sarah Rooney, Brianne Connizzo, Ben Freedman, Cori Riggin, and Adam Pardes, for their support and friendship. I would like to thank Kris Miller for her friendship and guidance. I would also like to acknowledge all the past and present graduate students, residents, post-docs, and staff members, for their friendship and valuable insights and discussions.

Finally, I thank my family for their unwavering love and support throughout my life, from the athletic field to the classroom. I thank my parents, Jack and Roxanne, and my sister, Jessica, who have always encouraged and supported me. I thank them for helping to guide me through the highs and lows and for providing comfort, support, and understanding. I thank John, whom I was blessed to share this journey with, for his tremendous understanding and support. I would also like to thank my grandparents, Anne and Tim, for their constant prayers and love. This would not have been possible without them.

ABSTRACT

THE ROLE OF SCAPULAR DYSKINESIS IN ROTATOR CUFF AND BICEPS TENDON PATHOLOGY IN A RAT MODEL

Katherine Reuther

Dr. Louis J. Soslowsky

Shoulder tendon injuries including impingement, rotator cuff disease, and biceps tendon pathology are common clinical conditions and are a significant source of joint pain, instability, and dysfunction. These injuries may progress into partial tears then to complete tendon ruptures, which have limited healing capacity even when surgically repaired. These injuries are frequently seen in the presence of abnormal scapulothoracic joint kinematics (termed scapular dyskinesis). However, the cause and effect relationship between scapular dyskinesis and shoulder injury has not been directly defined. Additionally, while the incidence of shoulder injuries and recurrent failure of repairs is well-documented, the mechanisms behind them are not well-established, making optimal clinical management difficult. Therefore, the objectives of this study were to examine the effect of scapular dyskinesis on the initiation and progression of pathological changes in the rotator cuff and biceps tendon and to define the mechanical processes that lead to these changes. Unfortunately, clinical and cadaveric studies are unable to address the underlying causes of injury and cannot evaluate the injury process over time. Therefore, a rat model of scapular dyskinesis (created by denervating the trapezius and serratus anterior) was developed and used, both alone and in combination with overuse, to

investigate the cause and effect relationships between changes in joint loading and alterations in tendon mechanical, histological, organizational, and biological properties. We hypothesized that scapular dyskinesis would result in altered joint loading conditions that would lead to degeneration of the rotator cuff and long head of the biceps. We found that scapular dyskinesis diminished joint function and passive joint mechanics and significantly reduced tendon properties. We also investigated the effect of overuse on tendon properties and found that overuse activity in the presence of scapular dyskinesis resulted in significantly more structural and biological adaptations than scapular dyskinesis alone. We also investigated the effect of scapular dyskinesis on supraspinatus tendon healing and found that scapular dyskinesis was detrimental to tendon properties. These results indicate that scapular dyskinesis is a causative mechanical mechanism of shoulder tendon injury. Identification of scapular dyskinesis as a mechanism of pathological changes will help inform and guide clinicians in developing optimal prevention and long-term rehabilitation strategies.

TABLE OF CONTENTS

LIST OF TABLES

LIST OF FIGURES

Chapter 1: Introduction

A. Introduction

Shoulder injuries including instability, impingement, rotator cuff disease, and biceps tendon pathology are common clinical conditions and are a significant source of joint pain, instability, and dysfunction. These injuries rank 3rd (behind back and neck pain) in number of musculoskeletal clinical visits, affecting as many as 7.5 million people each year and resulting in significant health-care costs (AAOS). Injuries to the rotator cuff (the network of four muscles that attach the humerus to the shoulder blade and mobilize the shoulder) are particularly common and may include subacromial impingement, partial thickness tears, or complete tendon rupture. Tears may be a result of acute trauma or chronic degeneration and often begin isolated to the supraspinatus tendon with the potential to progress anteriorly to the subscapularis or posteriorly to the infraspinatus over time. In addition, long head of the biceps pathology is often found secondary to rotator cuff tears and is a significant source of pain.[9, 20, 44, 47]

Rotator cuff injuries are frequently seen in the presence of abnormal glenohumeral and scapulothoracic joint kinematics. In particular, combined tears of the supraspinatus and infraspinatus disrupt the subscapularis-infraspinatus force balance (often referred to as "force couple"[6]) and lead to increased joint instability, altered glenohumeral translations, and cause progression of tendon damage to the subscapularis and biceps.[47, 49] Additionally, altered scapular motion and position (termed scapular dyskinesis) has been observed in 68-100% of patients with shoulder injuries.[65] The scapula provides a stable platform for rotator cuff muscle activation in order to achieve normal shoulder movements. However, scapular dyskinesis disrupts the dynamic

restraint of the glenohumeral joint and may contribute to shoulder injury, exacerbate symptoms, and adversely affect outcomes.[26] The causative role scapular dyskinesis plays in injuries to the rotator cuff and biceps is unknown.

Current treatment options for managing rotator cuff injuries include both conservative rehabilitation strategies and surgical intervention. Therapy protocols may be implemented pre-operatively in an attempt to correct deficits and/or post-operatively in an attempt to improve healing and outcomes[24]. When surgical intervention is required to repair rotator cuff tears, success has shown to be mixed, with 5-95% of patients having recurrent tears.[2, 14-17] Current treatment options for managing scapular dyskinesis include rehabilitation strategies[8, 24, 25] to re-educate scapular muscles and correct positional abnormalities and surgical options including neurolysis, nerve transfers, and muscle transfers. However, the benefits of correcting scapular deficits prior to rotator cuff repair have not been evaluated. Therefore, it is unclear how scapular dyskinesis may affect healing of the tendon following repair. Mechanical loading plays an important role in tendon-to-bone healing following repair.[58] It is likely that altered scapulothoracic kinematics (due to scapular dyskinesis) will place abnormal loads on the healing supraspinatus tendon and compromise healing potential. Successful pre-operative scapular rehabilitation may be necessary in order to achieve successful outcomes post-operatively.

While the prevalence of shoulder injuries and their association with scapulothoracic kinematic abnormalities is well-documented[35], the cause and effect relationships behind them are not well-established, making optimal clinical management difficult. Human cadaveric studies have shown that alterations in scapular orientations

and loading of the rotator cuff, deltoid, latissimus dorsi, and pectoralis major (through simulated tears and/or altering applied forces) result in abnormal joint mechanics due to disruption of the normal balance of forces and joint orientations.[28, 31, 42, 59] Additionally, in vivo human studies have identified altered scapular rhythm and position in patients with shoulder injury.[26, 35]However, the in vivo cause and effect relationships that these mechanical alterations and disruptions have on the rotator cuff and biceps properties over time cannot be evaluated using cadaveric studies or in vivo human studies and therefore remains unknown. The underlying mechanisms and cause and effect relationships can only be addressed in an animal model where time from injury can be controlled and evaluated over time. Utilizing an in vivo model of abnormal scapulothoracic joint kinematics will help determine the origin of shoulder tendon injury (initial and recurring) and identify mechanical and biologic events that lead to tendon degeneration and compromised healing.

Therefore, the objective of this study is to use an established animal model to examine scapular dyskinesis as a mechanism for the initiation and progression of pathological changes in the rotator cuff and biceps tendon. The aims of this study have been designed to specifically address common clinical scenarios for which clinicians have insufficient information for understanding and decision-making. For example, Aim 1 will address the question: is scapular dyskinesis a risk factor for the development of rotator cuff and biceps tendinopathy? Aim 2 will help us understand the question: what are the long-term consequences to the day laborer or athlete with scapular dysfunction? Lastly, Aim 3 will answer the question: should a patient with scapular dyskinesis rehabilitate prior to rotator cuff repair in order to increase healing and improve

outcomes? This study will help define the in vivo mechanical processes which lead to tendon degeneration in the shoulder and compromise tendon healing potential following repair. Identification of scapular dysfunction as a mechanism of pathological changes will help guide surgeons in prescribing optimal long term treatment strategies in order to increase scientific understanding of the progression of tendon damage and to improve tendon healing following repair.

B. Background

1. Shoulder Anatomy

The bony architecture of the shoulder is comprised of the humerus, scapula, and clavicle. The shoulder has 4 articulations, including the acromioclavicular, sternoclavicular, glenohumeral, and scapulothoracic joints (Figure 1.1). [51, 67] The

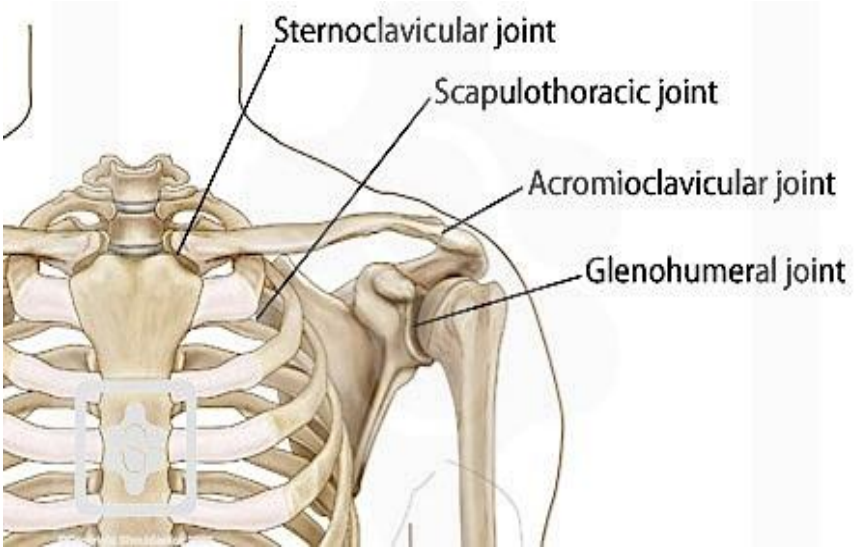

Figure 1.1. Joints of the shoulder.
(Images from shoulderdoc.co.uk)

acromioclavicular and sternoclavicular joints are comprised of the articulation of the clavicle and the acromion (a bony process of the scapula) and sternum, respectively. The acromion, together with the coracoid process (a small hook-like structure on the lateral

edge of the superior anterior portion of the scapula) and coracoacromial ligament, extend laterally over the joint and form a protective arch over the humerus, referred to as the coracoacromial arch (Figure 1.2), or acromial arch.

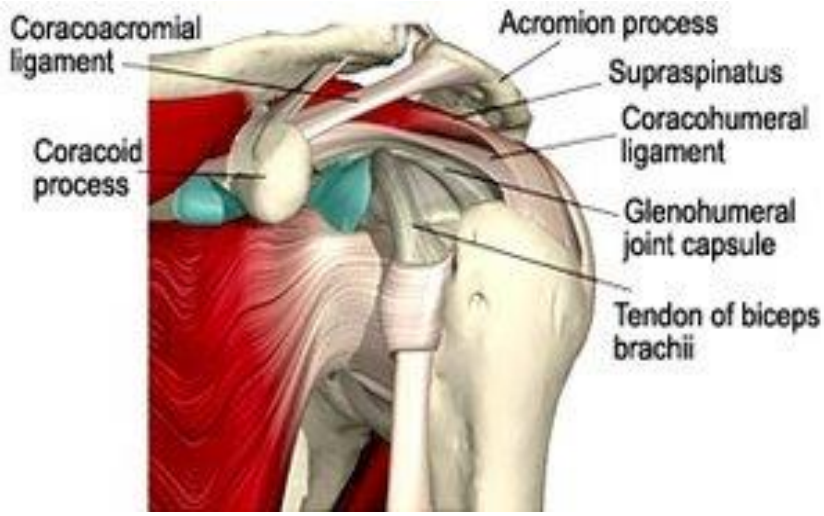

Figure 1.2. Coracoacromial arch.
(Image from massagetoday.com)

a. Glenohumeral Joint

The glenohumeral joint is a multi-axial ball and socket joint, involving the articulation of the glenoid fossa of the scapula and humeral head. It is the most mobile joint in the body and has limited bony constraints. Therefore, it relies on the rotator cuff, biceps tendon, ligaments, glenoid labrum, and joint capsule in order to stabilize and compress the humeral head on the glenoid fossa. The rotator cuff is comprised of four tendons, including the supraspinatus, infraspinatus, subscapularis, and teres minor, that originate on the scapula and insert on the humerus. The subscapularis is located most anteriorly while the infraspinatus and teres minor are located most posteriorly. Lastly, the supraspinatus is located most superiorly under the acromial arch. The biceps tendon is comprised of 2 heads, the long head and the short head. The long head of the biceps crosses the glenohumeral joint and originates on the supraglenoid tubercle while the short

head originates on the coracoid process of the scapula and does not cross the glenohumeral joint. Both heads join at a common insertion on the radius.

b. Scapulothoracic Joint

The scapulothoracic joint is not a true synovial joint (no capsule or ligamentous attachments) and is one of the least congruent articulations in the body.[61] It is formed by the anterior scapula and posterior thoracic rib cage. The only bony stabilization is an indirect connection to the axioskeleton via the clavicle, through ligamentous attachments with the acromion. Therefore, it relies on dynamic muscle attachments for stability. The main stabilizer muscles include the serratus anterior, trapezius, rhomboids, and levator scapulae.

2. Normal Shoulder Function

a. Role of the Glenohumeral Joint

The glenohumeral joint has the largest range of motion of any major joint in the body and relies on static and dynamic restraints to achieve an intricate balance between stability and mobility. Static restraints, such as the bony processes of the scapula and the ligaments and joint capsule, assist in glenohumeral stabilization. Specifically, the coracoacromial arch acts to prevent upward displacement of the humeral head. In addition, the rotator cuff muscles act to achieve stability through concavity compression of the humeral head on the glenoid fossa. The rotator cuff is responsible for many arm motions including humeral abduction and internal and external rotation.[51] Specifically, the supraspinatus assists the deltoid in humeral abduction, the subscapularis assists the pectoralis major in internal rotation, and the infraspinatus and teres minor assist in external rotation. The rotator cuff also acts to maintain an anterior-posterior force

balance at the glenohumeral joint (often referred to as "force couple"[6]) (Figure 1.3). Specifically, the subscapularis anteriorly and infraspinatus posteriorly balance the anterior-posterior forces, maintaining a stable fulcrum at the glenoid fossa; however, disruption of the anterior or posterior portion can result in a shift in the fulcrum and abnormal joint kinematics.[7] The role of the biceps tendon at the shoulder is controversial but it has been suggested to act as a weak shoulder flexor and as a humeral head depressor.[30, 64]

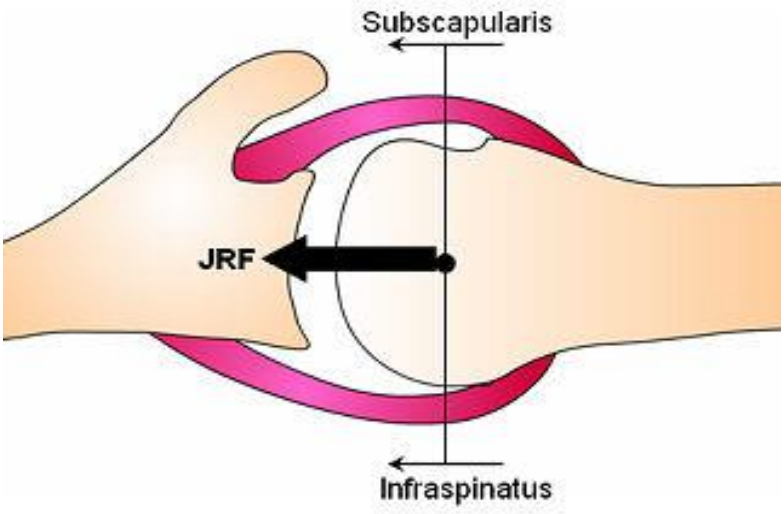

Figure 1.3. Glenohumeral joint anterior-posterior joint balance.
(Image from quizlet.com)

b. Role of the Scapulothoracic Joint

The scapulothoracic joint also relies on the coordinated motion of the surrounding musculature for stabilization and mobilization. Motions of the scapula include elevation, depression, protraction (abduction), retraction (adduction), upward (lateral) rotation, downward (medial) rotation, anterior tipping, and posterior tipping. The serratus anterior and trapezius muscles form an important force couple, defined as 2 resultant forces of equal magnitude and opposite direction which produce rotation of a structure [the

scapula], that serves many functions.[25] In particular, the serratus anterior-trapezius force couple (Figure 1.4) acts to rotate the scapula in order to dynamically position the glenoid and maintain the center of rotation with the humeral head and achieve efficient glenohumeral motion. This relationship has been compared to a seal [the scapula]

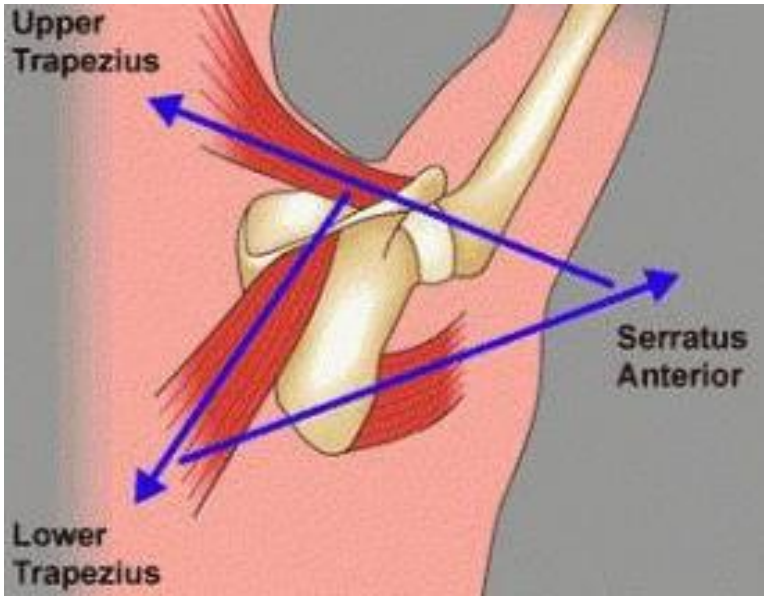

Figure 1.4. Scapulothoracic force couple.
(Image from zachdechant.wordpress.com)

balancing a ball [the humeral head] on its nose [the glenoid fossa].[25] Additionally, the force couple provides a stable base, enabling the glenohumeral muscles to move the arm. If a stable base does not exist, muscles cannot generate appropriate torque which may lead to muscular imbalance and instability. For example, trying to move the humerus without efficient function of the serratus anterior, trapezius, or both is analogous to trying to push against a wall while on roller skates.[22] The force couple also allows for elevation of the acromion, clearing the acromion from the rotator cuff and preventing impingement. Finally, the serratus anterior and trapezius are important in transferring forces from the lower extremity up the kinetic chain to the upper extremity.[24]

c. Scapulohumeral Rhythm

Motion of the scapula in relation to the humerus during shoulder elevation is important to achieve further range of motion. This is referred to as scapulohumeral rhythm[11]. In the human, during the first 30 degrees of shoulder elevation, the movement is largely glenohumeral. However, after the first 30 degrees, the glenohumeral and scapulothoracic joints move simultaneously, with an overall ratio of ~2:1 (glenohumeral : scapulothoracic motion)[19]. It serves two purposes: 1) to preserve the length-tension relationships of the glenohumeral muscles (sustaining force production through a larger range of motion) and 2) to prevent impingement between the humerus and coracoacromial arch.

3. Scapular Dyskinesis

a. Classification

Dysfunction in the scapular musculature leads to an alteration in the normal position or motion of the scapula during coupled scapulohumeral movements. This dysfunction is classified as scapular dyskinesis. Abnormal scapular movements are often found in conjunction with a variety of shoulder injuries and are therefore thought to contribute to these disorders.[26, 35] Clinically, scapular dyskinesis can be identified and classified by visual clinical examination of dysrhythmia or "winging" (Figure 1.5).[38] Abnormalities include prominence of the inferior angle (Type I) or medial border (Type II), excessive superior border elevation (Type III), or symmetrical motion (Type IV).[25, 27].

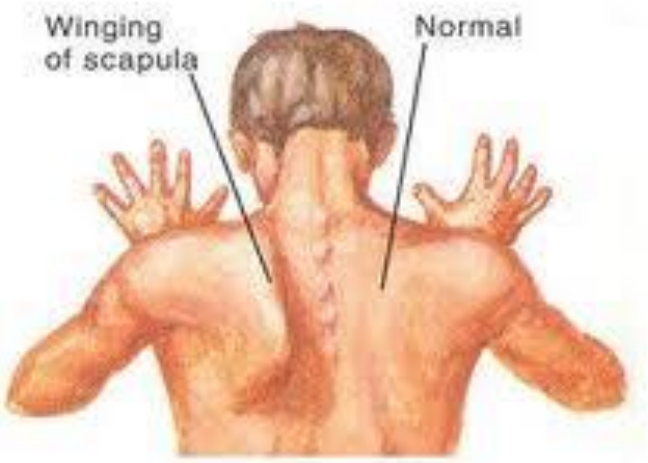

Figure 1.5.Scapular "winging"
(Image from fitnesspainfree.com)

b. Causes

Several factors may contribute to scapular dysfunction including muscle imbalance, nerve injury, postural abnormality, anatomical disruption, capsular contracture, or proprioceptive dysfunction.[24, 25] Specifically, muscular inhibition, impaired coordination, and fatigue of the serratus anterior and lower and middle trapezius is a common cause of scapular dysfunction. This is common in individuals who perform repetitive overuse activity such as athletes (i.e., swimmers and overhead throwers) and laborers.[10, 45, 63, 66] Additionally, nerve injuries such as spinal accessory, long thoracic, or dorsal scapular nerve palsies impair the trapezius, serratus anterior, and rhomboids, respectively, and could lead to abnormal scapular movements.[23, 29, 38] Other mechanisms including postural abnormality due to cervical lordosis or excessive thoracic kyphosis, anatomical disruptions through clavicular fracture or acromioclavicular injury, and capsular stiffness[12, 33] or contracture due to tightness in the pectoralis minor or posterior capsule.[57, 60] Lastly, proprioceptive dysfunction due to malfunction of mechanoreceptors or direct physical trauma may also contribute.

c. Associated Injuries and Impairments

Scapular dyskinesis is present in a larger number of injuries involving the shoulder joint. Specifically, it has been found in conjunction with shoulder pain[25], impingement (involving the supraspinatus, superior joint capsule, subacromial bursa, and biceps)[34, 36, 39, 41, 50, 63], glenohumeral instability[65], biccipital and rotator cuff tendinitis[32, 40], rotator cuff tears[40, 46], adhesive capsulitis[12, 33, 35], and SLAP (superior labral anterior posterior) lesions. Abnormal scapular orientation can alter the center of rotation of the humerus on the glenoid and lead to abnormal shoulder joint kinematics[62], thereby increasing the risk of shoulder injury. However, it is unclear whether scapular dyskinesis is a cause or effect of these injuries. The specific scapular kinematic patterns associated with shoulder injury are mixed. For example, some studies have demonstrated increased upward rotation of the scapula while others have demonstrated reduced upward rotation.[34, 39] Increased upward rotation may be a positive compensation in an attempt to achieve maximum arm elevation and prevent subacromial impingement. Alternatively, reduced upward rotation may alter the subacromial space and contribute to tendon injury.

d. Treatment

The goal of scapular rehabilitation is to achieve a position of optimal scapular function. Most cases of dyskinesis are related to muscle weakness, inhibition, or flexibility and therefore can be treated with rehabilitation. Unfortunately, local injuries, such as nerve damage or muscle detachments, will not respond to therapy unless they are repaired.[13] Therapy protocols focus on re-educating the scapulothoracic muscles, particularly the serratus anterior and trapezius, to achieve dynamic stabilization of the scapula.

4. Tendon Properties

a. Biology and Composition

Tendons are soft connective tissues that connect muscle to bone and allow the transfer of force to enable musculoskeletal motion. The main functional components of tendon are water and extracellular matrix (ECM). Water is the primary constituent, comprising approximately 50% to 60% of tendon weight. The extracellular matrix is comprised of collagen, proteoglycans, and elastin.[5, 43] Collagen makes up approximately 75% of the dry weight with 95% type I collagen and a small amount of type III and other collagens.[5, 43] Proteoglycans, such as decorin, biglycan, aggrecan, fibromodulin, lumican, and versican, are composed of a core protein covalently bound to one or more glycosaminoglycan (GAG) chains and compose ~1-5% of dry weight.[5, 43] Elastin, which functions in tendon elasticity and return to pre-stretched length after loading, composes ~2-3% of dry weight.[5, 43] Tendon cells, or tenocytes, are elongated fibroblast type cells that synthesize the collagen and extra-cellular matrix and are closely packed between bundles of collagen.

The supraspinatus and biceps have different compositions along their length. Specifically, regions that see compressional loading (i.e. the supraspinatus insertion and proximal biceps) typically have a higher proteoglycan content and more rounded (cartilage-like) cells than regions that experience primarily tensional loading (i.e., the supraspinatus mid-substance and distal biceps).

b. Structure and Function

Tendons transmit force between muscle and bone. Collagen is primarily arranged longitudinally and aligned parallel to the long axis of the tendon. Tendon forms a hierarchy, starting with the triple helix of collagen, then microfibrils, fibrils, fascicles, and ultimately the tendon itself. Tendon fibrils also have a wave or crimp pattern that is thought to influence the non-linear mechanical behavior. Another aspect of tendon's morphology is its origin and insertion (its junctions). Tendon has two junction regions: the myotendinous junction, where the muscle transitions to tendon, and the bone-tendon junction, where the tendon transitions to bone. Each is differentially organized and contributes to the varying properties along the length of the tendon. Specifically, the insertion site of tendon has been shown to have different composition, disorganized collagen fiber architecture, and weaker mechanical properties then the tendon mid-substance, or mid-tendon.

The supraspinatus tendon to bone insertion site is a complex transitional region linking tendon and bone (Figure 1.6). The tissue wraps around the humeral head as it inserts into bone and therefore experiences complex loading along its length (tensile loads near tendon, tensile and compressive loads near bone). The tendon to bone insertion is characterized by 4 continuous overlapping zones: tendon, fibrocartilage, calcified fibrocartilage, and bone. This continuous change in tissue composition may alleviate stress concentrations and aid in the efficient transfer of load between two materials of different mechanical properties (tendon and bone). A return to normal composition and structural organization will help support a return to normal function for the insertion site.[58]

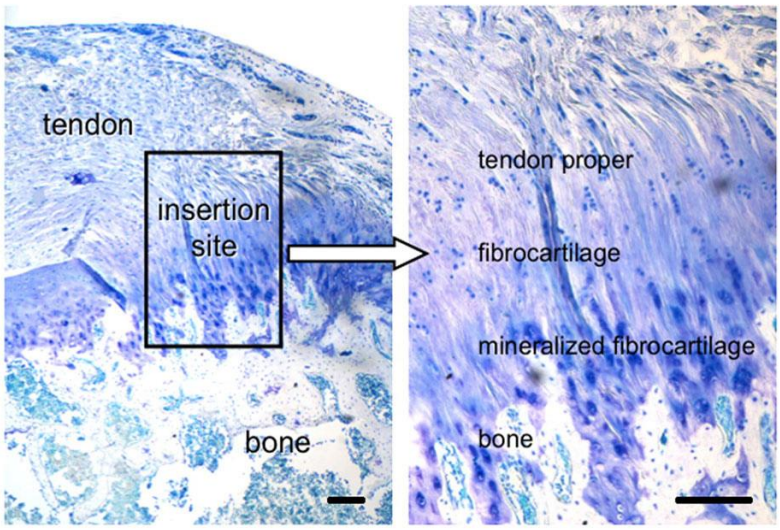

Figure 1.6.Supraspinatus tendon-to-bone insertion site.
(Image from Thomopoulos et al., *J Orthop Res*. 2002 May;20(3):454-63)

The biceps tendon also wraps around the humeral head, resulting in a complex loading environment (tensile loads near tendon, tensile, compressive, and shear loads near bone). As a result, the biceps tendon has varying structural and mechanical properties along its length.

c. Mechanics

Tendon is an inhomogeneous, anisotropic, non-linear, and viscoelastic material. The primary load-bearing component of tendon is collagen I. The stress-strain behavior of tendon exhibits an initial non-linear region at low loads (called the toe region) followed by a linear region, where rate of load development is constant until failure.[5, 43] The toe region has been attributed to the recruitment and realignment of crimped collagen fibrils. In the linear region, fibers are believed to be taut and oriented in the direction of loading. Tendon also exhibits viscoelastic (time and history-dependent) behavior which has been attributed to the inherent viscoelasticity of collagen and the association of water and negatively charged GAGs.

d. Injury and Healing

Tendon healing processes following an acute injury (such as a tear) are characterized by a reactive scar formation that results in tissue that is typically biologically and mechanically inferior to native tissue. In some instances, functional healing is achieved, producing tissue that adequately substitutes for native tissue, whereas in other instances the tissue is significantly compromised, leading to further tendon injury. When innate healing processes fail, surgical repair is often employed in an attempt to accelerate and optimize tendon healing. In this study, we will examine tendon healing following acute surgical repair.

Tendon healing primarily follows the wound healing process for connective tissues, occurring in three intersecting phases: inflammation, proliferation, and remodeling. Immediately after injury, the inflammatory phase begins. Inflammatory cells and erythrocytes migrate to the site of injury and fill the gap between the tendon ends. Next, resorption of the initial hematoma is initialized by monocytes and macrophages that enter the lesion. Various vasoactive and chemotactic factors increase vascularity and recruit more inflammatory cells, triggering both degradative and reparative processes, to remove and replace damaged material. During the final stages of inflammation, tenocytes start to migrate to the injury site and begin to synthesize type III collagen. Within a few days after injury, the proliferative phase begins. Matrix and cellular proliferation predominate at the injury site. This stage is characterized by continuous collagen production and deposition, creating a scar-like fibrous tissue. The synthesis of type III collagen is maximal during this stage, and cellularity remains high. Approximately 6-8 weeks following injury, the remodeling phase begins.[21] This phase is

characterized by a gradual decrease in cellularity and vascularity and the continually increasing organization and maturation of scar tissue over time. During this phase, collagen fibers and fibroblasts attempt to reorient themselves along the length of the tendon. In addition, the synthesis of type I collagen, the main collagen present in uninjured tendons, predominates. The time-scale of each stage of healing may differ depending on the model (e.g., human vs. animal, differing species) being studied. Each of these steps represents an attempt to return to normal tendon characteristics.

Alternatively, chronic tendon injuries (caused by overuse or repetitive microtrauma) have limited propensity for healing and result in disease of the tendon, or tendinopathy. Previous work has shown that tendons with chronic injuries demonstrate disrupted collagen organization[56], increased ECM, increased cellularity, altered cell shape (for example, more rounded)[37], and decreased mechanical properties[52], indicative of a degenerative tissue.

e. Responses to Changes in Loading

Tendon cells can detect their mechanical environment and therefore respond to changes in mechanical loading. Responses to changes in loading include remodeling and changes in collagen organization and composition of ECM, which may affect tendon mechanical properties. Loading environment is important in both uninjured and healing tissues and can differ in amount (i.e., immobilization, exercise, and overuse) and in type (i.e., tensile, compressive, and shear) of loading. For uninjured tissues, the mechanical properties tend to increase with increased loading (during exercise) and decrease with decreased loading (during immobilization) and excessive loading (during overuse).[56, 58] However, the optimal loading conditions in the treatment of healing repair tissues are

unknown. Specifically, previous studies have shown benefits to increased loading while others have shown negative effects.[1, 3, 48, 58] In general, low loading regimens seems to promote healing while excessive loading may have detrimental effects.[4, 18, 48]

Type of loading can also affect the tendon's ability to adapt and respond. Regions of tendon experiencing tensile loading consist of densely aligned collagen fibers and less proteoglycans. Regions of tendon exposed to compressive or shear loading consist of less aligned collagen fibers and more proteoglycans, particularly aggrecan.

5. Cartilage Properties

a. Biology and Composition

Articular cartilage is the connective tissue covering diarthrodial joints that provides for low friction transmission of mechanical loads. It is avascular and therefore has limited intrinsic healing capacity. It is composed of water, a dense ECM (containing collagen and proteoglycans), and sparse distribution of cartilage-cells, called chondrocytes. Water is the most abundant component of cartilage (up to 80% of its wet weight). Collagen, comprises 60% of the dry weight, with 95% classified as type II and the remaining 5% other minor collagens. Proteoglycans, account for 10-15% of the wet weight, with the large proteoglycan aggrecan most abundant and decorin, biglycan, and fibromodulin present in smaller quantities.

b. Structure, Function, and Mechanics

Cartilage can be divided into four zones (each with differing collagen organization and proteoglycan composition): superficial zone, middle/transitional zone, deep zone, and calcified cartilage. The superficial zone contains the highest collagen content with fibers arranged parallel to the articular surface (which resist compressive,

tensile, and shear forces). The middle zone contains more disorganized collagen fibers and higher proteoglycan content than the superficial zone. The deep zone contains the highest proteoglycan and lowest water content and collagen fibers oriented perpendicular to the surface (which provides greatest resistance to compressive forces). The calcified layer anchors the cartilage to bone.

Cartilage is an inhomogeneous, anisotropic, non-linear, and viscoelastic material. It consists of two phases, a solid phase (provided by ECM) and fluid phase (provided by water and inorganic ions). Compressive loading leads to an increase in interstitial pressure and a subsequent redistribution of fluid out of the ECM. However, due to the density of the ECM and frictional drag, permeability of articular cartilage is low, increasing fluid pressure and thereby allowing cartilage to support high loads. Cartilage also exhibits viscoelastic behavior which has been attributed to interstitial fluid flow and intrinsic viscoelasticity of the collagen-proteoglycan matrix.

c. Responses to Changes in Loading

Similar to tendon, mechanical loading induces synthesis and degradation of ECM components. Therefore, alterations in loading patterns can lead to changes in cartilage properties. Specifically, regular cyclic loading has shown positive effects such as enhancement of cartilage mechanical properties while excessive loading may lead to necrosis and tissue damage. Measurement of mechanical properties of cartilage can be used to elucidate differences in loading and contact patterns at articulating surfaces.[53]

6. Rat Model System

a. Justification.

Previous work has identified the rat as an appropriate animal model to study rotator cuff disease.[54] The rat was the only non-primate to satisfy a 34-item checklist that included criteria relating human to animal features such as shoulder musculature, bony anatomy, articulations, and motion. These features are important in order to ask questions related to the rotator cuff. Specifically, bony anatomy (Figure 1.7) is particularly important due to the clinical prevalence of subacromial impingement syndrome, caused by extrinsic compression of the supraspinatus by the coracoacromial arch. Therefore, in order to understand rotator cuff disease, the presence of the coracoacromial arch in an animal model is a critical feature. Additionally, during normal forward locomotion, the supraspinatus tendon passes repetitively under the coracoacromial arch, similar to what occurs in humans during overhead activity. Specifically, previous work has established overuse injury as a significant factor for development of rotator cuff tendinopathy in the rat rotator cuff animal model.[55, 56] Following 8 weeks of overuse activity, the

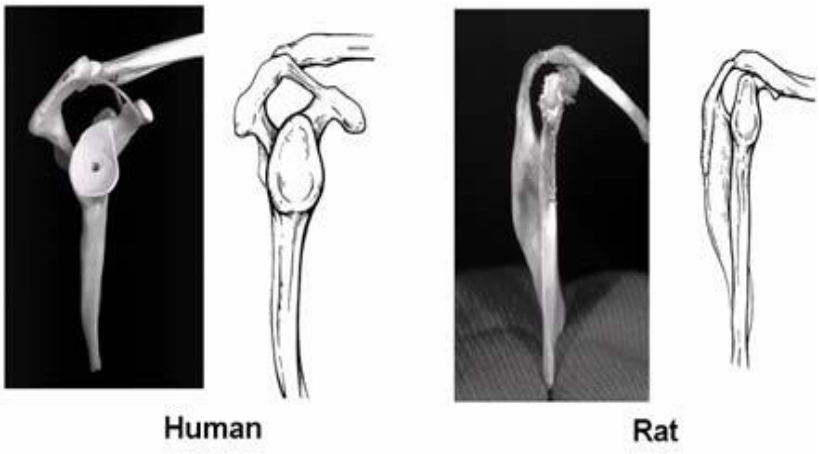

Figure 1.7. Similarities between human and rat.

supraspinatus developed degenerative changes, indicative of tendinopathy, including increased cellularity, decreased collagen organization, and decreased mechanical properties. Lastly, previous studies have also identified clinical parallels in the rat biceps tendon.[47] It has two heads, the long head that passes through the biccipital groove and originates on supraglenoid tubercle, and the short head, that originates on the coracoid process.

b. Investigations for Scapular Dyskinesis in Animal Models

Currently, there are no animal models in use to investigate scapular dyskinesis. An animal model that mimics the clinical situation of scapular dyskinesis would allow examination of changes in shoulder joint function and rotator cuff and biceps tendon properties and elucidate the mechanism by which these changes occur. Additionally, the consequences on rotator cuff healing in the presence of scapular dysfunction are unclear and could be studied in an appropriate animal model. While the rat rotator cuff model has been extensively studied, this is the first study to investigate scapular dyskinesis in this model.

C. Specific Aims

Shoulder injuries including impingement, rotator cuff disease, and biceps tendon pathology are common clinical conditions affecting as many as 7.5 million people each year (according to the American Academy of Orthopaedic Surgeons, AAOS) and are a significant source of joint pain, instability, and dysfunction. These injuries may progress into partial tears then to complete tendon ruptures, which have limited healing capacity even when surgically repaired (5-95% recurrent tears). These injuries are frequently seen in the presence of abnormal glenohumeral and scapulothoracic joint kinematics. Recent studies have shown that disruption of the glenohumeral force couple (combined tears of

the supraspinatus and infraspinatus tendons) leads to abnormal glenohumeral kinematics and causes progression of tendon damage in the subscapularis and biceps tendons.[47, 49] However, it is unclear how abnormal scapulothoracic joint kinematics contributes to (or instead compensates for) these disorders. Additionally, while the incidence of shoulder injuries and recurrent failure of repairs is well documented[14-17], the mechanisms behind them are not well-established, making optimal clinical management difficult. Determining the origin of shoulder tendon injury (initial and recurring) will help define the contributory roles of common mechanical injury mechanisms and identify the mechanical and biologic events that lead to tendon degeneration and compromised healing.

The overall objective of this study is to examine the effect of altered scapulothoracic kinematics (termed scapular dyskinesis) on the initiation and progression of pathological changes in the rotator cuff and biceps tendon in order to define the in vivo mechanical processes which lead to these changes. To accomplish this objective, an animal model of scapular dyskinesis will be used, both alone and in combination with overuse, to investigate the cause and effect relationships between changes in joint function and alterations in tendon mechanical, histological, and biological properties. Our global hypothesis is that scapular dyskinesis results in altered joint loading conditions that lead to degeneration of the rotator cuff and long head of the biceps.

Specific Aim 1: Identify functional, mechanical, and biological changes in the rotator cuff and biceps tendons in the presence of scapular dyskinesis (dennervating the trapezius and serratus anterior) in a rat model.

Hypothesis 1a: Scapular dyskinesis will alter dynamic and static joint mechanics (as measured by joint kinetics, passive shoulder mechanics, and glenoid cartilage properties) due to disruption of the scapulothoracic force couple.

Hypothesis 1b: Scapular dyskinesis will cause degeneration of the rotator cuff and long head of the biceps tendons. Specifically, the altered mechanical loading environment will result in repetitive microtrauma and disruption of tendon structure (loss of normal collagen organization) leading to upregulation of inflammatory cytokines, increased tenocyte proliferation, increased tendon degradation (increased presence of degradative factors, proteoglycans, and chondrogenic markers), and decreased mechanical properties.

Specific Aim 2: Determine the effect of altered loading in combination with scapular dyskinesis on the rotator cuff and biceps tendons.

Hypothesis 2a: Scapular dyskinesis in combination with repetitive overuse will alter dynamic and static joint mechanics (as measured by joint kinetics, passive shoulder mechanics, and glenoid cartilage properties) due to disruption of the scapulothoracic force couple.

Hypothesis 2b: Scapular dyskinesis in combination with repetitive overuse will cause degeneration of the rotator cuff and long head of the biceps due to increased abnormal multi-directional loading demands placed on the tendons.

Hypothesis 2c: Pathologic changes in the rotator cuff and long head of the biceps will be more severe when combined with overuse when compared to changes due to scapular dyskinesis alone. Overuse activity will increase loading demands placed on the tendons and accelerate tendon degeneration.

Hypothesis 2d: Pathologic changes in the rotator cuff and long head of the biceps due to scapular dyskinesis in combination with repetitive overuse will be more severe when compared to changes due to overuse alone. Scapular dyskinesis will increase loading demands placed on the tendons and accelerate tendon degeneration.

Specific Aim 3: Determine the effect of scapular dyskinesis on supraspinatus tendon healing.

Hypothesis 3: Creating scapular dyskinesis will result in decreased supraspinatus tendon to bone healing (decreased collagen organization, altered expression of ECM proteins, and decreased mechanical properties) following tendon repair due to the compromised mechanical environment present during healing.

These studies will help define the in vivo mechanical processes which lead to rotator cuff and biceps tendon degeneration and compromised tendon healing potential following repair. Identification of scapular dyskinesis as a mechanism of pathological changes will help guide surgeons in prescribing optimal long-term treatment strategies. Specifically, future studies will use this animal model to evaluate treatment modalities such as restoration of scapulothoracic function in order to understand the potential for prevention and/or recovery of tendon properties following damage and to improve tendon healing following repair.

D. Study Design

A total of 210 male Sprague-Dawley rats (400-450 g) were used for this Institutional and Animal Care Use Committee (IACUC) approved study. Animals were cared for at the University of Pennsylvania's University Laboratory Animal Resources facility. The study design is shown in Figure 1.8. In this study, accessory and long thoracic nerve transection was performed alone (AIM1) and in combination with overuse

(AIM2) or supraspinatus repair (AIM3). Additionally, organizational, histological, immunohistochemical, and mechanical assays were performed at specific time points. To assess, joint function, forelimb gait and ground reaction forces were recorded in all groups one day prior to surgery (baseline) and at 3, 7, 14, 28, 42, and 56 days post-surgery A total of 70 animals were used for each aim of the study. Animals were used for each aim of the study. Animals were sacrificed at 2, 4, and 8 weeks. At 2 weeks, 10 animals were sacrificed for histological and immunohistochemical assays (N=5). At 4 weeks, 30 animals were sacrificed for histological and immunohistochemical assays (N=5) and mechanics (N=10). At 8 weeks, 30 animals were sacrificed for histological and immunohistochemical assays (N=5) and mechanics (N=10).

.

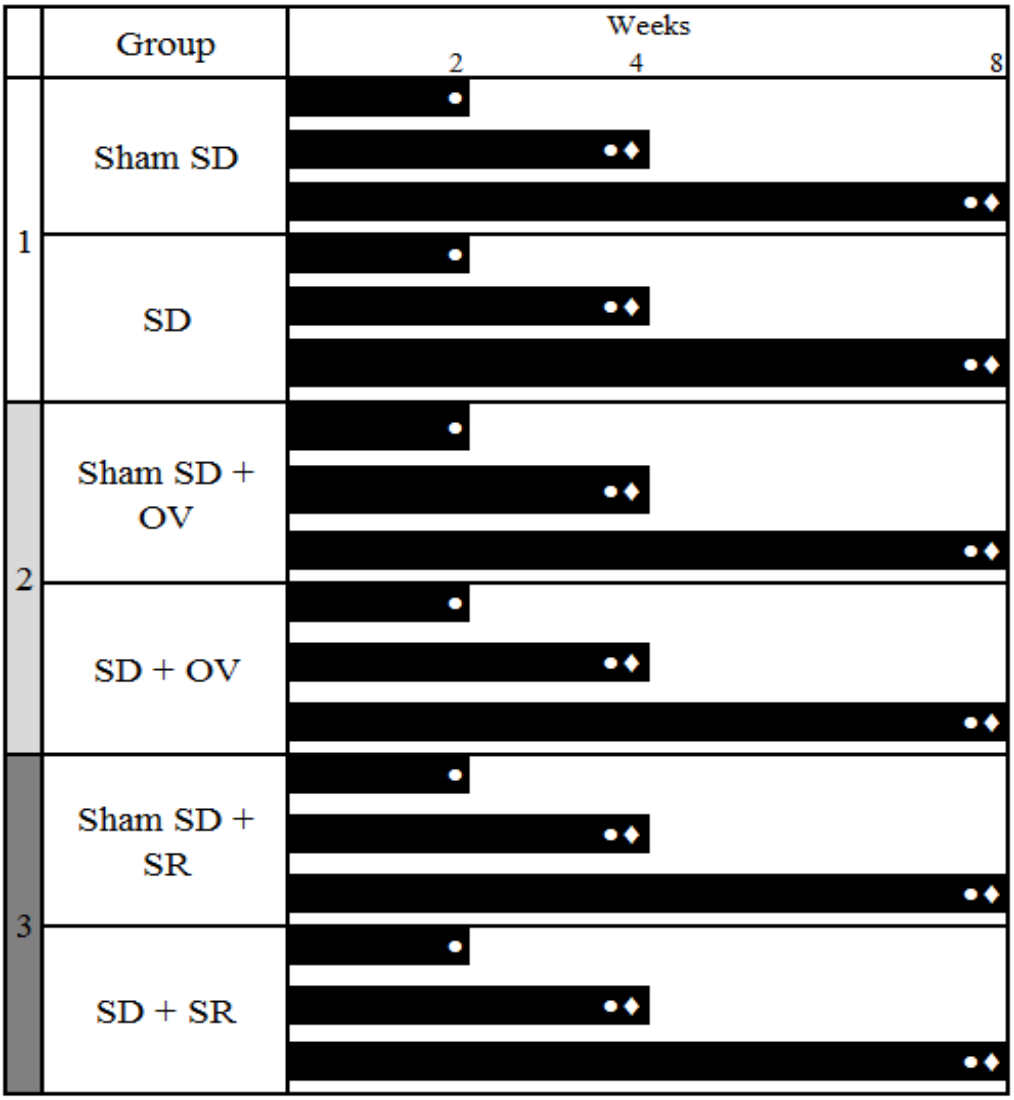

Figure 1.8. Study Design

Aim 1 was to determine the effect of scapular dyskinesis on the supraspinatus and biceps tendons. Specifically, 35 animals underwent transection of the accessory and long thoracic nerves and 35 animals underwent sham transection. Aim 2 was to determine the

effect of scapular dyskinesis in combination with overuse activity on the supraspinatus and biceps tendons. Specifically, 70 animals underwent 2 weeks of overuse treadmill training followed by surgical (N=35) or sham (N=35) transection of the accessory and long thoracic nerve. Both groups then performed overuse activity and were sacrificed 2, 4, or 8 weeks after surgery. Aim 3 was to determine the effect of scapular dyskinesis on supraspinatus tendon healing following repair. Specifically, 70 animals underwent transection of the supraspinatus tendon and immediate repair in combination with surgical (N=35) or sham (N=35) transection of the accessory and long thoracic nerves

E. Chapter Overview

Chapter two describes the development of an animal model of scapular dyskinesis and provides the methods, results, and discussion for the experimental studies performed to characterize the functional consequences and mechanical, histological, organizational, and compositional changes to the supraspinatus and biceps tendon in an animal model. Chapter three provides the methods, results, and discussion for the experimental studies performed to determine the effect of overuse activity in the presence of scapular dyskinesis on the mechanical, histological, organizational and compositional properties of the supraspinatus and biceps tendons. Chapter four provides the methods, results, and discussion for the experimental studies performed to determine the effect of scapular dyskinesis on supraspinatus tendon healing following repair as characterized by mechanical, histological, organizational, and compositional changes in the supraspinatus tendon. Chapter five summarizes the conclusions of the previous chapters and provides potential future directions for this animal model and topic area.

F. References

1. Bedi A, Kovacevic D, Fox AJ, et al. Effect of early and delayed mechanical loading on tendon-to-bone healing after anterior cruciate ligament reconstruction. *J Bone Joint Surg Am.* 2010;92(14):2387-2401.

2. Bigliani LU, Cordasco FA, McIlveen SJ, Musso ES. Operative treatment of failed repairs of the rotator cuff. *J Bone Joint Surg Am.* 1992;74(10):1505-1515.

3. Brophy RH, Kovacevic D, Imhauser CW, et al. Effect of short-duration low-magnitude cyclic loading versus immobilization on tendon-bone healing after ACL reconstruction in a rat model. *J Bone Joint Surg Am.* 2011;93(4):381-393.

4. Buckwalter JA. Effects of early motion on healing of musculoskeletal tissues. *Hand Clin.* 1996;12(1):13-24.

5. Buckwalter JA, Einhorn TA, O'Keefe RJ, American Academy of Orthopaedic Surgeons., Alumni and Friends Memorial Book Fund. *Orthopaedic basic science : foundations of clinical practice*. 3rd ed. Rosemont, IL: American Academy of Orthopaedic Surgeons; 2007.

6. Burkhart SS. Arthroscopic treatment of massive rotator cuff tears. Clinical results and biomechanical rationale. *Clin Orthop Relat Res.* 1991(267):45-56.

7. Burkhart SS. Fluoroscopic comparison of kinematic patterns in massive rotator cuff tears. A suspension bridge model. *Clin Orthop Relat Res.* 1992(284):144-152.

8. Burkhart SS, Morgan CD, Kibler WB. The disabled throwing shoulder: spectrum of pathology Part III: The SICK scapula, scapular dyskinesis, the kinetic chain, and rehabilitation. *Arthroscopy.* 2003;19(6):641-661.

9. Chen CH, Hsu KY, Chen WJ, Shih CH. Incidence and severity of biceps long head tendon lesion in patients with complete rotator cuff tears. *J Trauma.* 2005;58(6):1189-1193.

10. Clarsen B, Bahr R, Andersson S, Kristensen R, Myklebust G. Risk factors for overuse shoulder injuries among male professional handball players. *Br J Sports Med.* 2014;48(7):579.

11. Codman EA. *The Shoulder: Rupture of the Supraspinatus Tendon and Other Lesions in Or about the Subacromial Bursa*: Miller & Medical; 1934.

12. Fayad F, Roby-Brami A, Yazbeck C, et al. Three-dimensional scapular kinematics and scapulohumeral rhythm in patients with glenohumeral osteoarthritis or frozen shoulder. *J Biomech.* 2008;41(2):326-332.

13. Galano GJ, Bigliani LU, Ahmad CS, Levine WN. Surgical treatment of winged scapula. *Clin Orthop Relat Res.* 2008;466(3):652-660.

14. Galatz LM, Ball CM, Teefey SA, Middleton WD, Yamaguchi K. The outcome and repair integrity of completely arthroscopically repaired large and massive rotator cuff tears. *J Bone Joint Surg Am.* 2004;86-A(2):219-224.

15. Gazielly DF, Gleyze P, Montagnon C. Functional and anatomical results after rotator cuff repair. *Clin Orthop Relat Res.* 1994(304):43-53.

16. Gerber C, Fuchs B, Hodler J. The results of repair of massive tears of the rotator cuff. *J Bone Joint Surg Am.* 2000;82(4):505-515.

17. Harryman DT, 2nd, Mack LA, Wang KY, Jackins SE, Richardson ML, Matsen FA, 3rd. Repairs of the rotator cuff. Correlation of functional results with integrity of the cuff. *J Bone Joint Surg Am.* 1991;73(7):982-989.

18. Hettrich CM, Gasinu S, Beamer BS, et al. The effect of mechanical load on tendon-to-bone healing in a rat model. *Am J Sports Med.* 2014;42(5):1233-1241.

19. Inman VT, Saunders JB, Abbott LC. Observations of the function of the shoulder joint. 1944. *Clin Orthop Relat Res.* 1996(330):3-12.

20. Itoi E, Hsu HC, Carmichael SW, Morrey BF, An KN. Morphology of the torn rotator cuff. *J Anat.* 1995;186 (Pt 2):429-434.

21. James R, Kesturu G, Balian G, Chhabra AB. Tendon: biology, biomechanics, repair, growth factors, and evolving treatment options. *J Hand Surg Am.* 2008;33(1):102-112.

22. Kelley MJ, Clark WA. *Orthopedic therapy of the shoulder*. Philadelphia: Lippincott; 1995.

23. Kelley MJ, Kane TE, Leggin BG. Spinal accessory nerve palsy: associated signs and symptoms. *J Orthop Sports Phys Ther.* 2008;38(2):78-86.

24. Kibler WB. The role of the scapula in athletic shoulder function. *Am J Sports Med.* 1998;26(2):325-337.

25. Kibler WB, McMullen J. Scapular dyskinesis and its relation to shoulder pain. *J Am Acad Orthop Surg.* 2003;11(2):142-151.

26. Kibler WB, Sciascia A, Wilkes T. Scapular dyskinesis and its relation to shoulder injury. *J Am Acad Orthop Surg.*20(6):364-372.

27. Kibler WB, Uhl TL, Maddux JW, Brooks PV, Zeller B, McMullen J. Qualitative clinical evaluation of scapular dysfunction: a reliability study. *J Shoulder Elbow Surg.* 2002;11(6):550-556.

28. Konrad GG, Jolly JT, Labriola JE, McMahon PJ, Debski RE. Thoracohumeral muscle activity alters glenohumeral joint biomechanics during active abduction. *J Orthop Res.* 2006;24(4):748-756.

29. Kuhn JE, Plancher KD, Hawkins RJ. Scapular Winging. *J Am Acad Orthop Surg.* 1995;3(6):319-325.

30. Kumar VP, Satku K, Balasubramaniam P. The role of the long head of biceps brachii in the stabilization of the head of the humerus. *Clin Orthop Relat Res.* 1989(244):172-175.

31. Labriola JE, Lee TQ, Debski RE, McMahon PJ. Stability and instability of the glenohumeral joint: the role of shoulder muscles. *J Shoulder Elbow Surg.* 2005;14(1 Suppl S):32S-38S.

32. Lin JJ, Hanten WP, Olson SL, et al. Functional activity characteristics of individuals with shoulder dysfunctions. *J Electromyogr Kinesiol.* 2005;15(6):576-586.

33. Lin JJ, Lim HK, Yang JL. Effect of shoulder tightness on glenohumeral translation, scapular kinematics, and scapulohumeral rhythm in subjects with stiff shoulders. *J Orthop Res.* 2006;24(5):1044-1051.

34. Ludewig PM, Cook TM. Alterations in shoulder kinematics and associated muscle activity in people with symptoms of shoulder impingement. *Phys Ther.* 2000;80(3):276-291.

35. Ludewig PM, Reynolds JF. The association of scapular kinematics and glenohumeral joint pathologies. *J Orthop Sports Phys Ther.* 2009;39(2):90-104.

36. Lukasiewicz AC, McClure P, Michener L, Pratt N, Sennett B. Comparison of 3-dimensional scapular position and orientation between subjects with and without shoulder impingement. *J Orthop Sports Phys Ther.* 1999;29(10):574-583; discussion 584-576.

37. Maffulli N, Wong J, Almekinders LC. Types and epidemiology of tendinopathy. *Clin Sports Med.* 2003;22(4):675-692.

38. Martin RM, Fish DE. Scapular winging: anatomical review, diagnosis, and treatments. *Curr Rev Musculoskelet Med.* 2008;1(1):1-11.

39. McClure PW, Michener LA, Karduna AR. Shoulder function and 3-dimensional scapular kinematics in people with and without shoulder impingement syndrome. *Phys Ther.* 2006;86(8):1075-1090.

40. Mell AG, LaScalza S, Guffey P, et al. Effect of rotator cuff pathology on shoulder rhythm. *J Shoulder Elbow Surg.* 2005;14(1 Suppl S):58S-64S.

41. Michener LA, McClure PW, Karduna AR. Anatomical and biomechanical mechanisms of subacromial impingement syndrome. *Clin Biomech (Bristol, Avon).* 2003;18(5):369-379.

42. Mihata T, Jun BJ, Bui CN, et al. Effect of scapular orientation on shoulder internal impingement in a cadaveric model of the cocking phase of throwing. *J Bone Joint Surg Am.*94(17):1576-1583.

43. Mow VC, Huiskes R. *Basic orthopaedic biomechanics & mechano-biology*. 3rd ed. Philadelphia: Lippincott Williams & Wilkins; 2005.

44. Murthi AM, Vosburgh CL, Neviaser TJ. The incidence of pathologic changes of the long head of the biceps tendon. *J Shoulder Elbow Surg.* 2000;9(5):382-385.

45. Myers JB, Laudner KG, Pasquale MR, Bradley JP, Lephart SM. Scapular position and orientation in throwing athletes. *Am J Sports Med.* 2005;33(2):263-271.

46. Paletta GA, Jr., Warner JJ, Warren RF, Deutsch A, Altchek DW. Shoulder kinematics with two-plane x-ray evaluation in patients with anterior instability or rotator cuff tearing. *J Shoulder Elbow Surg.* 1997;6(6):516-527.

47. Peltz CD, Perry SM, Getz CL, Soslowsky LJ. Mechanical properties of the long-head of the biceps tendon are altered in the presence of rotator cuff tears in a rat model. *J Orthop Res.* 2009;27(3):416-420.

48. Peltz CD, Sarver JJ, Dourte LM, Wurgler-Hauri CC, Williams GR, Soslowsky LJ. Exercise following a short immobilization period is detrimental to tendon properties and joint mechanics in a rat rotator cuff injury model. *J Orthop Res.* 2010;28(7):841-845.

49. Perry SM, Getz CL, Soslowsky LJ. After rotator cuff tears, the remaining (intact) tendons are mechanically altered. *J Shoulder Elbow Surg.* 2009;18(1):52-57.

50. Pribicevic M, Pollard H. Rotator cuff impingement. *J Manipulative Physiol Ther.* 2004;27(9):580-590.

51. Rockwood CA. *The shoulder*. 3rd ed. Philadelphia: Saunders; 2004.

52. Sano H, Ishii H, Yeadon A, Backman DS, Brunet JA, Uhthoff HK. Degeneration at the insertion weakens the tensile strength of the supraspinatus tendon: a comparative mechanical and histologic study of the bone-tendon complex. *J Orthop Res.* 1997;15(5):719-726.

53. Setton LA, Mow VC, Muller FJ, Pita JC, Howell DS. Mechanical properties of canine articular cartilage are significantly altered following transection of the anterior cruciate ligament. *J Orthop Res.* 1994;12(4):451-463.

54. Soslowsky LJ, Carpenter JE, DeBano CM, Banerji I, Moalli MR. Development and use of an animal model for investigations on rotator cuff disease. *J Shoulder Elbow Surg.* 1996;5(5):383-392.

55. Soslowsky LJ, Thomopoulos S, Esmail A, et al. Rotator cuff tendinosis in an animal model: role of extrinsic and overuse factors. *Ann Biomed Eng.* 2002;30(8):1057-1063.

56. Soslowsky LJ, Thomopoulos S, Tun S, et al. Neer Award 1999. Overuse activity injures the supraspinatus tendon in an animal model: a histologic and biomechanical study. *J Shoulder Elbow Surg.* 2000;9(2):79-84.

57. Thomas SJ, Swanik CB, Higginson JS, et al. A bilateral comparison of posterior capsule thickness and its correlation with glenohumeral range of motion and scapular upward rotation in collegiate baseball players. *J Shoulder Elbow Surg.*20(5):708-716.

58. Thomopoulos S, Williams GR, Soslowsky LJ. Tendon to bone healing: differences in biomechanical, structural, and compositional properties due to a range of activity levels. *J Biomech Eng.* 2003;125(1):106-113.

59. Thompson WO, Debski RE, Boardman ND, 3rd, et al. A biomechanical analysis of rotator cuff deficiency in a cadaveric model. *Am J Sports Med.* 1996;24(3):286-292.

60. Tyler TF, Nicholas SJ, Roy T, Gleim GW. Quantification of posterior capsule tightness and motion loss in patients with shoulder impingement. *Am J Sports Med.* 2000;28(5):668-673.

61. Voight ML, Thomson BC. The role of the scapula in the rehabilitation of shoulder injuries. *J Athl Train.* 2000;35(3):364-372.

62. von Eisenhart-Rothe R, Matsen FA, 3rd, Eckstein F, Vogl T, Graichen H. Pathomechanics in atraumatic shoulder instability: scapular positioning correlates with humeral head centering. *Clin Orthop Relat Res.* 2005(433):82-89.

63. Wadsworth DJ, Bullock-Saxton JE. Recruitment patterns of the scapular rotator muscles in freestyle swimmers with subacromial impingement. *Int J Sports Med.* 1997;18(8):618-624.

64. Warner JJ, McMahon PJ. The role of the long head of the biceps brachii in superior stability of the glenohumeral joint. *J Bone Joint Surg Am.* 1995;77(3):366-372.

65. Warner JJ, Micheli LJ, Arslanian LE, Kennedy J, Kennedy R. Scapulothoracic motion in normal shoulders and shoulders with glenohumeral instability and impingement syndrome. A study using Moire topographic analysis. *Clin Orthop Relat Res.* 1992(285):191-199.

66. Weldon EJ, 3rd, Richardson AB. Upper extremity overuse injuries in swimming. A discussion of swimmer's shoulder. *Clin Sports Med.* 2001;20(3):423-438.

67. Wilk KE, Reinold MM, Andrews JR. *The athlete's shoulder*. 2nd ed. Philadelphia, PA: Churchill Livingstone Elsevier; 2009.

Chapter 2: Scapular Dyskinesis is Detrimental to Shoulder Tendon Properties and Joint Mechanics in a Rat Model

A. Introduction

This chapter will discuss the development of an animal model for scapular dyskinesis and characterize the functional consequences and mechanical, histological, organizational, and compositional changes to the supraspinatus and biceps tendon in a rat model.

Shoulder injuries including impingement, rotator cuff disease, and biceps tendon pathology are common clinical conditions and are a significant source of joint pain, instability, and dysfunction. Injuries to the rotator cuff are particularly common and may include impingement (subacromial and internal), partial thickness tears, or complete tendon rupture. Tears may be a result of acute trauma or chronic degeneration and often begin isolated to the supraspinatus tendon with the potential to progress anteriorly to the subscapularis or posteriorly to the infraspinatus over time. In addition, long head of the biceps pathology can be found in isolation or secondary to rotator cuff tears and can be a significant source of pain.

Rotator cuff injuries are frequently seen in the presence of abnormal scapulothoracic joint kinematics. Specifically, altered scapular motion and position (termed scapular dyskinesis) has been observed in 68-100% of patients with shoulder injuries.[32] The scapula provides a stable platform for rotator cuff muscle activation in order to achieve normal shoulder movements. Specifically, the rotator cuff muscles act to achieve stability through concavity compression of the humeral head on the glenoid fossa. It has been hypothesized that if a stable base does not exist, as in the case of scapular dyskinesis, the rotator cuff muscles may not be able to efficiently generate

appropriate torque which may lead to muscular imbalance and instability. An unstable scapula could reduce the dynamic restraint of the glenohumeral joint provided by the rotator cuff, leading to increased joint translations, and placing the joint at increased risk for secondary injuries, including impingement and biceps pathology.[13] Additionally, abnormal scapular position, such as increased protraction[26], reduced upward scapular rotation, and subsequent loss of appropriate acromial elevation, may lead to compression of the rotator cuff under the acromial arch[24], leading to shoulder injury. Alternatively, scapular dyskinesis may occur as a result of or in response to the shoulder injury (as a form of compensation). Therefore, the causative role scapular dyskinesis plays in injuries to the rotator cuff and biceps is still unknown.

While the prevalence of shoulder injuries and their association with scapulothoracic kinematic abnormalities is well-documented[16], the cause and effect relationships between the two are not well-established, making optimal clinical management difficult. Human cadaveric studies have shown that alterations in scapular orientations and loading of the rotator cuff, deltoid, latissimus dorsi, and pectoralis major (through simulated tears and/or altering applied forces) result in abnormal joint mechanics due to disruption of the normal balance of forces and joint orientations. [14, 15, 17, 31] [14, 15, 17] Additionally, in vivo human studies have identified altered scapular rhythm and position in patients with shoulder injury.[13, 16] However, the in vivo cause and effect relationships that these mechanical alterations and disruptions have on the rotator cuff and biceps properties over time cannot be evaluated using cadaveric studies or in vivo human studies and therefore remains unknown. The underlying mechanisms and cause and effect relationships can only be addressed in an animal model where time from injury

can be controlled and evaluated over time. Utilizing an animal model of abnormal scapulothoracic joint kinematics will help determine the origin of shoulder tendon injury (initial and recurring) while providing insight into the mechanical and biologic events that lead to tendon degeneration and compromised healing.

Therefore, the objective of this study was to develop and use a rat model of scapular dyskinesis to examine the initiation and progression of pathological changes in the rotator cuff and biceps tendon. We hypothesized that scapular dyskinesis would: H1) diminish shoulder function, passive joint mechanics, and cartilage properties, H2) diminish supraspinatus and biceps tendon histological, compositional, and mechanical properties, and H3) result in increased serum concentration of inflammatory cytokines, which has been previously associated with tendon injury.[1]

B. Methods

Study Design and Surgical Technique. A rat model of scapular dyskinesis was developed and used. This study was approved by the Institutional Animal Care and Use Committee (IACUC). Sixty male Sprague-Dawley rats (400-450 g) underwent unilateral surgical transection (N=30) (or sham transection (N=30)) of the spinal accessory and long thoracic nerves resulting in denervation of the trapezius and serratus anterior muscles, respectively. The rats were administered buprenorphine subcutaneously as a pre- (0.05 mg/kg) and post- (0.05 mg/kg) operative analgesia. Pre-surgical buprenorphine was administered 30 minutes prior to surgery and a local injection of lidocaine (1 mg/kg) was administered at both sites of incision. Post-surgical buprenorphine was administered 6-8 hours after surgery, then every 12 hours for the following 2 days. Briefly, animals were anesthetized and a 2 cm vertical incision was made 1 cm posterior to the left ear.

The cervical nerve, clavo-trapezius, and acromio-trapezius muscles were identified. The clavo-trapezius and acromio-trapezius muscles were separated cranial to the cervical nerve using blunt dissection with Iris scissors to expose the spinal accessory nerve, located above the omotransversarius muscle. The spinal accessory nerve was transected 2 mm and 5 mm proximal to the acromio-trapezius and removed. The surgical site was irrigated with sterile saline and the overlying skin was closed with staples. Next, the animal's forelimb was abducted and internally rotated and a 3 cm axillary incision was made in the caudal direction along the abdominal fascia, exposing the serratus anterior muscle. Next, the latissimus dorsi muscle was identified and an incision was made along the fascial interface and blunt dissection was performed between the latissimus dorsi muscle and serratus anterior to gain proximal exposure to the serratus anterior muscle and long thoracic nerve. The long thoracic nerve was transected 2 mm and 5 mm proximal to the serratus anterior and removed. The abdominal fascia was sutured closed with 4-0 Vicryl suture (Ethicon, Inc., Blue Ash, Ohio, USA). The surgical site was irrigated with sterile saline and the overlying skin was then sutured closed. Animals were returned to un-restricted cage activity. At 4 and 8 weeks after surgery, animals were sacrificed for mechanical testing (N=10 at each time point) or for histological and immunohistochemical assays (N=5 at each time point) for the control and SD groups. Blood was collected via cardiac puncture at time of sacrifice and centrifuged at 1000 x g for 20 minutes at 4 °C. Serum was collected, flash frozen, and stored at -80 °C in order for biomarker assays. For mechanical testing, the animals were frozen at -20° C until testing and for histological and immunohistochemical assays, the supraspinatus and biceps tendons were harvested immediately and fixed in formalin.

Quantitative Ambulatory Assessment. Forelimb ground reaction forces (medial/lateral, braking, propulsion, and vertical) and spatio-temporal parameters (step width, stride length, and speed) were quantified using an instrumented walkway, as described previously.[22] Briefly, the system consists of two 6 degree-of-freedom force/torque cells mounted to clear, acrylic force plates and incorporated into a walkway. Rats were acclimated to walk freely along the instrumented walkway over a period of 1 week prior to formal recording of ambulatory data. For all groups, data was collected one day prior to surgery to obtain baseline, uninjured values. Post-surgery data was collected at days 5, 7, 14, 28, 42, and 56. All data was normalized by body-weight.

Passive Joint Mechanics. Passive range of motion measurements were performed utilizing the instruments and methodology, as previously described.[23] Measurements were taken under anesthesia prior to nerve transection, and at 2, 4, and 8 weeks following surgery. Under anesthesia, the forelimb was placed through a fixture and secured into the rotating clamp at 90° of elbow flexion and 90° of glenohumeral forward flexion. The scapula was manually stabilized to isolate glenohumeral motion and prevent scapulothoracic motion. The forelimb was then rotated through full range of internal and external rotation three times. The ROM was calculated as the difference in the average of three measures of maximal internal and external rotation. A bilinear fit utilizing least-squares optimization was applied to calculate joint stiffness in the toe and linear regions in both directions. All parameters were normalized to baseline values.

Sample Preparation for Mechanical Testing. At the time of testing, the animals were thawed and the scapula and humerus were dissected out with the biceps and supraspinatus tendons intact. For biceps testing, the tendon was isolated while still

attached to the scapula at the superior aspect of the glenoid. For supraspinatus testing, the tendon was isolated while still attached to the humerus. The tendons were fine dissected under a microscope to remove muscle and excess tissue. Cross-sectional area was measured using a custom laser device.[29]

Tendon Mechanical Testing. Elastic and viscoelastic mechanical properties of the biceps and supraspinatus tendon were determined using uniaxial tensile testing, as previously described.[19] Verhoeff stain lines were placed along the length of each tendon to divide the insertion and mid-substance regions for local optical strain measurements. The scapula and humerus were embedded in a holding fixture using polymethylmethacrylate (PMMA) and inserted into a custom testing fixture. The proximal end of the tendon was gripped with cyanoacrylate annealed sand paper in custom grips. The specimen was immersed in PBS at 37°C during testing. Tensile testing of the tendon was performed as follows: preconditioning for 10 cycles from 0.1 N to 0.5 N, stress relaxation to 4% (biceps) or 5% (supraspinatus) strain at a rate of 5 %/sec for 600 sec, and ramp to failure at 0.3%/sec (Figure 2.1). Stress was calculated as force divided by initial area and 2D Lagrangian strain was determined from the stain line displacements, using custom texture tracking software. Elastic properties were calculated using a linear regression from the linear region of the stress-strain curves. For viscoelastic parameters, the stress-relaxation curve was analyzed and percent relaxation was determined using the peak and equilibrium loads.

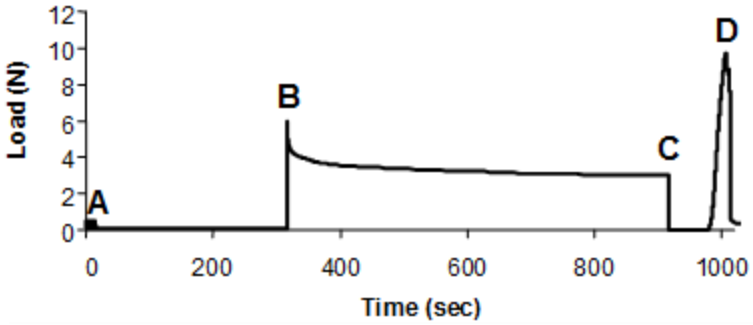

Figure 2.1. Mechanical testing protocol: (A) pre-conditioning (B) stress-relaxation (C) return to pre-load displacement (D) ramp to failure. (Image from http://repository.upenn.edu/edissertations/222)

Tendon Histology. Histologic analysis was performed to examine cellular and organizational changes in the biceps and supraspinatus tendons. Tissues were harvested immediately after sacrifice and processed using standard paraffin procedures. Sagittal sections (7 um) were collected, and stained with Hematoxylin–Eosin (H&E). Stained supraspinatus tendon sections were imaged at the insertion site and mid-substance using a microscope at 200X and 100X magnification using traditional and polarized light, respectively. Due to the unique anatomy of the biceps, it was subdivided into four regions: insertion site (INS), intra-articular space (INTRA), proximal groove (PROX), and distal groove (DIS). Cell density (number of cells/mm^2) and cell shape (aspect ratio; 0–1, with 1 being a circle) were quantified in the traditional light images using a bioquantification software system (Bioquant Osteo II; BIOQUANT Image Analysis Corp, Nashville, TN, USA). Polarized light images were analyzed using custom software to evaluate tendon organization, as previously described.[6] The angular deviation (AD) of the collagen orientation for each specimen, a measure of the fiber distribution spread, was calculated in each tendon location.

Tendon Immunohistochemistry. The distribution of ECM proteins was localized using immunohistochemical techniques. The same tissue specimens from histology were

used and stained for collagens type II and III, the proteoglycan decorin, and the inflammatory marker, IL1-β (Table 2.1). The proteins were visualized using DAB, making the antibody-protein conjugate turn brown. The insertion site and mid-substance (with biceps mid-substance region subdivided into intra-articular space, proximal groove, and distal groove) of each tendon were evaluated separately. Staining results were independently graded by three blinded investigators, who were provided with previously prepared standard images, using a scale of 0-3 (0=undetectable, 1=low, 2=medium, 3=high), and the mode was used as the final score.

Table 2.1. Primary antibodies used for immunohistochemical staining.

Protein Target	Antibody	Host	Type	Enzyme pretreatment	Dilution	Incubation period (h)	Source
Collagen II	II-116B3	Mouse	Monoclonal	Hyaluronidase	1:4	16	DSHB, Iowa City, IA, USA
Collagen III	c7805	Mouse	Monoclonal	Hyaluronidase	1:500	38	Sigma, St. Louis, MO, USA
Decorin	LF-113	Rabbit	Polyclonal	Chondroitinase ABC	1:300	38	L. Fisher, Bethesda, MD, USA
IL1-β	AB1832	Rabbit	Polyclonal	Pepsin	1:250	16	Millipore, Billerica, MA, USA

Cartilage Mechanical Testing. Glenoid cartilage properties were examined to elucidate changes in joint loading in the presence of scapular dyskinesis. Following completion of biceps testing, the glenoid cartilage was prepared for mechanical testing, as previously described.[20, 21] Briefly, the biceps was sharply detached at its insertion on the superior rim of the glenoid using a scalpel blade. The glenoid was then preserved by wrapping in soft tissue and refreezing (-20°C).

For cartilage thickness measurement[20], each scapula was thawed and immersed in PBS containing a protease inhibitor cocktail (5 mM Benz-HCl, 1mM PMSF, 1 M NEM) at room temperature. Specimens were scanned at 0.25 mm increments using a 55 MHz ultrasound probe (Visualsonics, Inc) in plane with the scapula. Captured B-mode images of each scan were manually segmented (three times and averaged) by selecting the cartilage and bony surfaces of the glenoid. The 3D positions of these surfaces were reconstructed with a custom program (MATLAB, MathWorks, Inc., Natick, Massachusetts) and used to determine cartilage thickness maps. Each thickness map was divided into six regions (center (C), posterior-superior (PS), posterior-inferior (PI), anterior-superior (AS), anterior-inferior (AI), and superior (S)) and an average thickness was computed for each region (Figure 2.2). Following ultrasound scanning, specimens were again preserved by wrapping in soft tissue and refreezing (-20°C) until mechanical testing.

For cartilage mechanical testing[20], each scapula was thawed and immersed in PBS containing the protease inhibitor cocktail at room temperature. Utilizing a 0.5 mm diameter, non-porous spherical indenter tip, cartilage indentation testing was performed as previously described.[20] Briefly, a preload (0.005 N) was set followed by 8 step-wise

stress relaxation tests (8 μm ramp at 2 μm/s followed by a 300 second hold). The scapula was repositioned for each localized region using angular, rotational, and linear stages such that the indenter tip was perpendicular to the cartilage surface in each region (Figure 2.3). Cartilage thickness for indentation testing was determined by identifying the indentation location on each cartilage thickness map. Equilibrium elastic modulus was calculated using a mathematical solution for the elasticity problem of indentation of a thin, elastic, homogeneous layer of material bonded to a rigid half space:[9]

$$E = \frac{(1 - v^2)}{2aK(v, \frac{a}{h})} \frac{P}{w}$$

where P is the applied force, w is the indentation depth, a is the radius of the indentor, v is Poisson's ratio, h is the tissue thickness, and K is a scaling factor, that depends on the aspect ratio ($\frac{a}{h}$) and Poisson's ratio(v). Indentation depth was defined as 20% of cartilage thickness and Poisson's ratio was assumed (v=0.30), as previously described.[20]

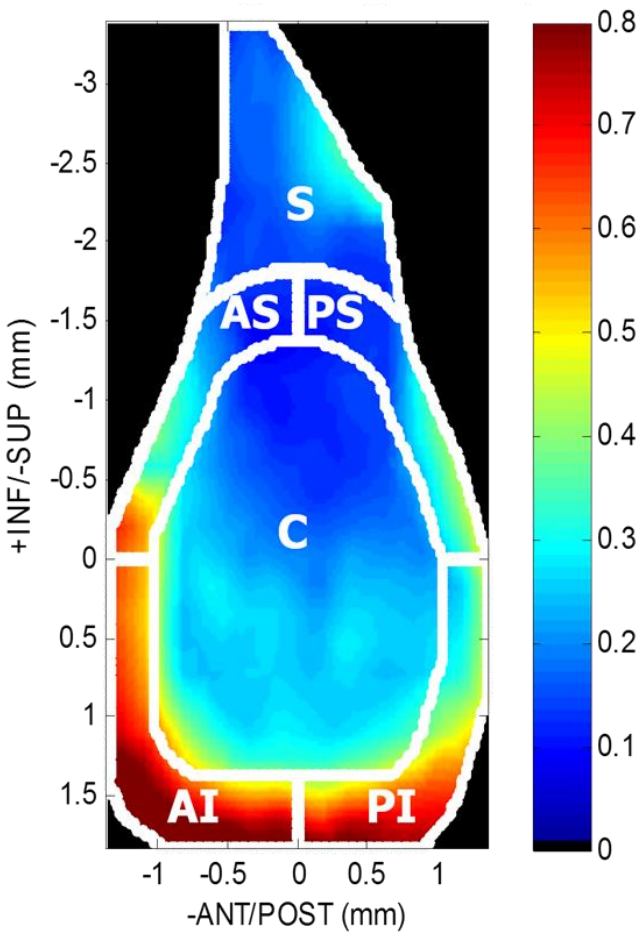

Figure 2.2. Glenoid cartilage thickness measurement. Each thickness map was divided into six regions (center (C), posterior-superior (PS), posterior-inferior (PI), anterior-superior (AS), anterior-inferior (AI), and superior (S)) and an average thickness was computed for each region.

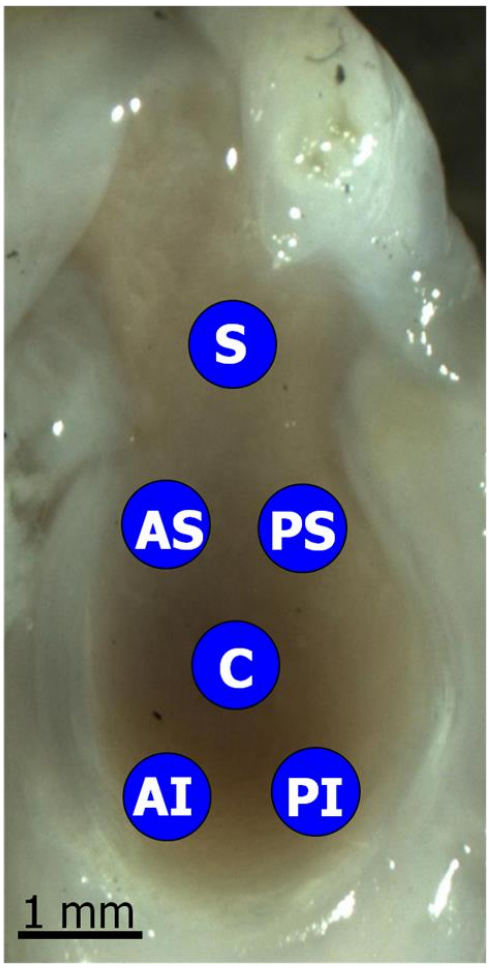

Figure 2.3. Glenoid cartilage indentation locations. Six regions (center (C), posterior-superior (PS), posterior-inferior (PI), anterior-superior (AS), anterior-inferior (AI), and superior (S)) were mechanically tested.

Serum Biomarkers. Serum inflammatory cytokines (IL1α, IL1β, TNFα, IL-6, IL-10, MIP-2, and MCP-1) were identified using a Milliplex Magnetic Bead Panel (EMD Millipore, Billerica, MA, USA) and levels were analyzed in triplicate using a Luminex System (Luminex, Austin, TX, USA).

Statistical Analysis. Statistical analysis was performed using SPSS version 20 (IBM, Armonk, NY). For the ambulatory assessment, multiple imputations were conducted using the Markov chain Monte Carlo method for missing data points (~10%). For both ambulatory assessment and passive joint mechanics, significance was assessed using a 2-

way ANOVA with repeated measures on time with follow-up t-tests between groups at each time point. Tissue mechanics and histologic parameters between groups were assessed using a t-test. Immunohistochemistry scores and cartilage thickness were evaluated using a Mann-Whitney test. Significance was set at $p<0.05$, trends at $p\leq0.1$.

C. Results

Ambulatory Data. Gross observational examination demonstrated clear alterations in scapular movements during forward locomotion in the rat, consistent with scapular "winging" in the human and characterized by entire medial border prominence in the closed kinetic chain activity. Additionally, shoulder function was significantly altered in the SD group. Specifically, the SD group had a significantly decreased vertical force and significantly increased propulsion force compared to control at all time-points (Figure 2.4, 2.5). No differences between groups were observed in braking force (Figure 2.6). Medial-lateral force was significantly altered at early time points (5 and 7 days post-transection), with the SD group demonstrating a more medially directed force than control (Figure 2.7). No significant differences in spatio-temporal parameters (step width, stride length, or speed) were observed between groups.

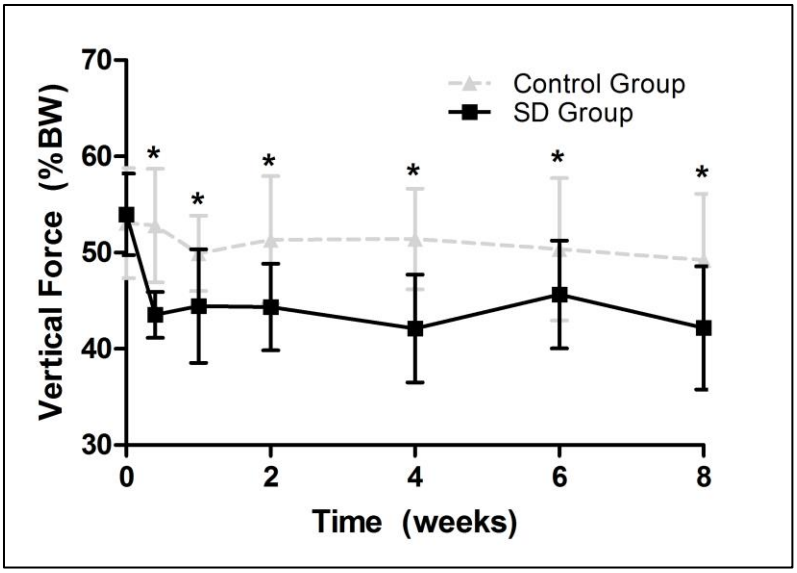

Figure 2.4. The SD group had a significantly decreased vertical force compared to control at all time-points. Data shown as mean ± standard deviation (*p<0.05). (SD=scapular dyskinesis)

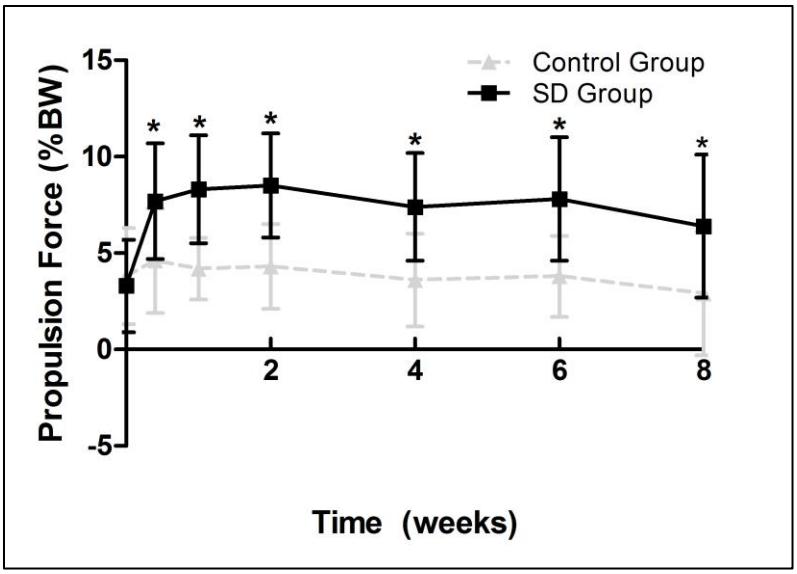

Figure 2.5. The SD group had a significantly increased propulsion force compared to control at all time-points. Data shown as mean ± standard deviation (*p<0.05). (SD=scapular dyskinesis)

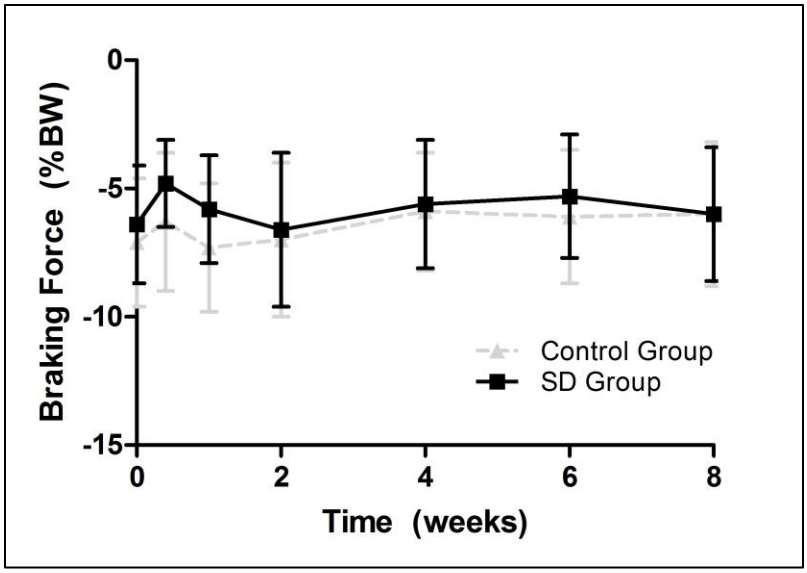

Figure 2.6. No differences were observed in braking force. Data shown as mean ± standard deviation. (SD=scapular dyskinesis)

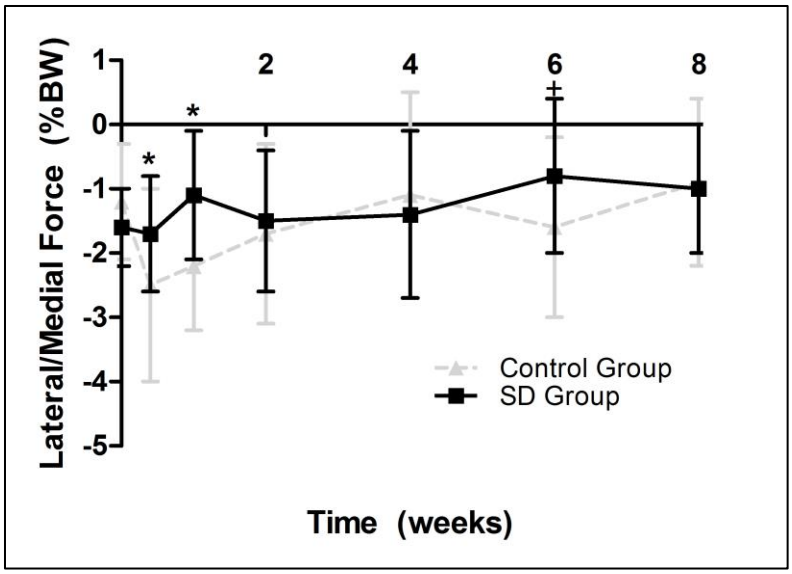

Figure 2.7. The SD group had a more medially directed force at 5 and 7 days compared to control. Data shown as mean ± standard deviation (*p<0.05). (SD=scapular dyskinesis)

Passive Joint Mechanics. Passive joint mechanics were also significantly altered (Table 2.2). Specifically, internal range of motion was significantly greater in the SD group compared to control at 4 and 8 weeks post-surgery, with a similar trend at 2 weeks. No other differences were observed, except for an increase in toe region stiffness in external rotation in the SD group compared to control at 4 weeks post-surgery.

Direction	Measurement	Time (wks)	Control	SD
Internal	**ROM (degrees)**	**2**	-8.93±24.20	7.37±18.17^{+}
		4	-11.98±7.99	-0.22±17.29*
		8	-14.65±12.99	1.35±16.28*
	Toe Stiffness (N/mm)	**2**	0.12±0.13	-0.03±0.11
		4	0.10 ±0.08	0.01±0.11
		8	0.05±0.13	-0.02±0.12
	Linear Stiffness (N/mm)	**2**	0.22±0.36	0.16±0.12
		4	0.21 ±0.13	0.13±0.11
		8	0.29±0.26	0.24±0.07
External	**ROM (degrees)**	**2**	19.12±11.49	16.03±7.42
		4	2.92 ±9.88	-2.58±9.51
		8	24.53±14.25	18.21±10.61
	Toe Stiffness (N/mm)	**2**	-0.04±0.13	-0.10±0.14
		4	-0.06±0.09	0.06±0.19*
		8	-0.05±0.10	-0.04±0.13
	Linear Stiffness (N/mm)	**2**	0.05±0.16	0.04±0.20
		4	0.08±0.18	-0.06±0.16
		8	0.12±0.23	0.13±0.19

Table 2.2. Results for passive joint mechanics demonstrated increased internal range of motion (ROM) in the SD group compared to control at 4 and 8 weeks, with a similar trend at 2 weeks. External toe-stiffness was also increased at 4 weeks in the SD group compared to control. Data normalized by baseline value (change from baseline) and as mean ± standard deviation (*$p<0.05$, +$p\leq0.1$). (SD=scapular dyskinesis)

Tendon Mechanics. In the presence of scapular dyskinesis, mechanical parameters (viscoelastic and elastic) were significantly altered. Specifically, tendon percent relaxation was significantly greater in the SD group compared to control at 8 weeks, for both the biceps and supraspinatus tendons, indicative of inferior tissue properties (Figure 2.8). No differences were observed in any tendon for cross-sectional area (Figure 2.9, 2.10) or insertion elastic modulus (Figure 2.11). However, tendon mid-substance elastic parameters were significantly altered. Specifically, tendon mid-substance elastic modulus was significantly decreased in the SD group compared to control, at both 4 and 8 weeks for the supraspinatus and at 8 weeks for the biceps, also indicative of inferior tissue properties (Figure 2.12).

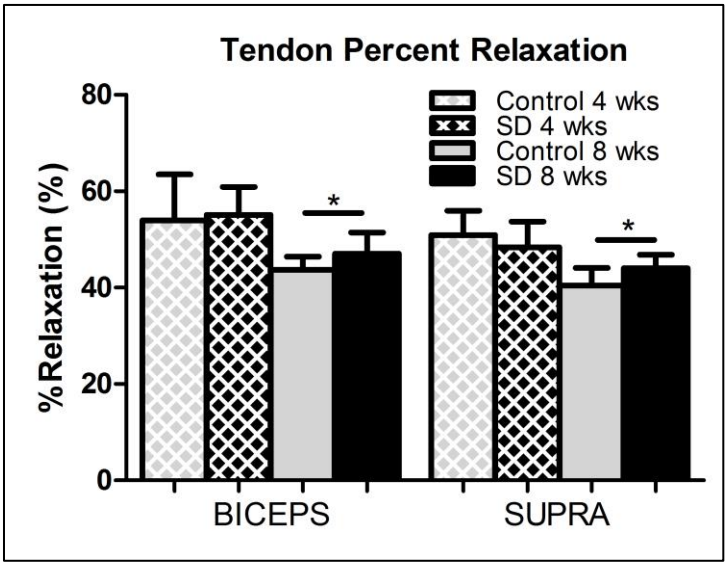

Figure 2.8. The biceps and supraspinatus tendons demonstrated significantly increased percent relaxation at 8 weeks post-surgery in the SD group compared to control. Data shown as mean + standard deviation (*$p<0.05$). (SD=scapular dyskinesis)

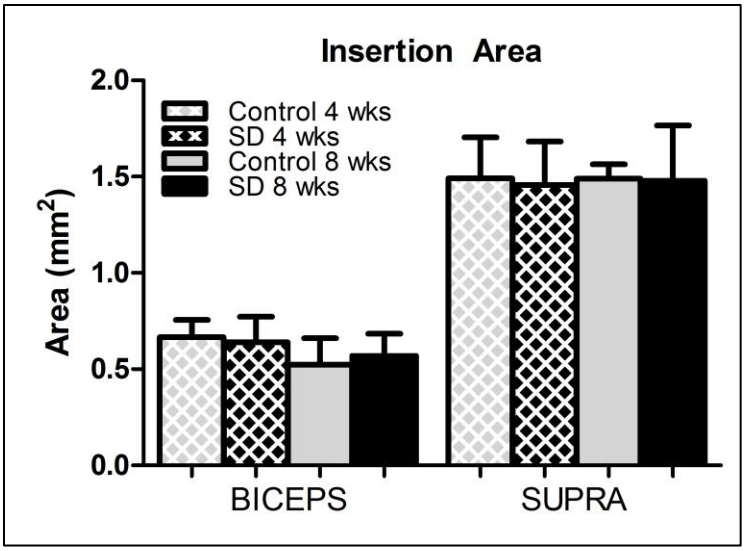

Figure 2.9. No differences in insertion cross-sectional area were observed in either tendon. Data shown as mean + standard deviation. (SD=scapular dyskinesis)

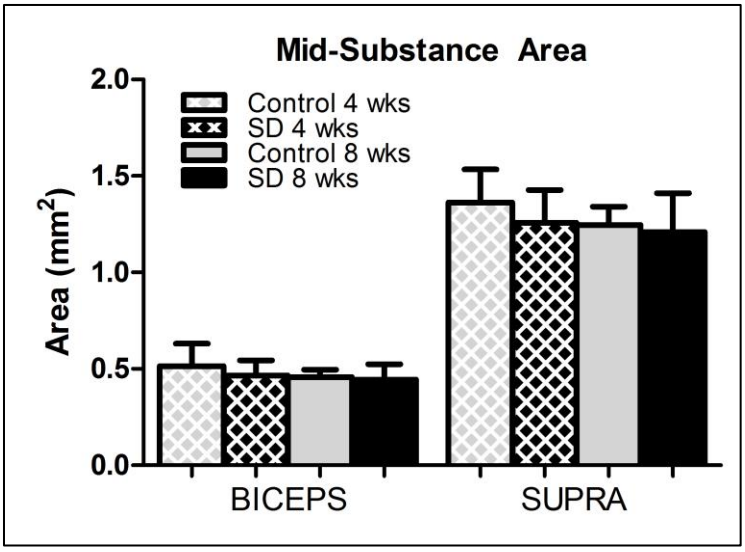

Figure 2.10. No differences in mid-substance cross-sectional area were observed in either tendon. Data shown as mean + standard deviation. (SD=scapular dyskinesis)

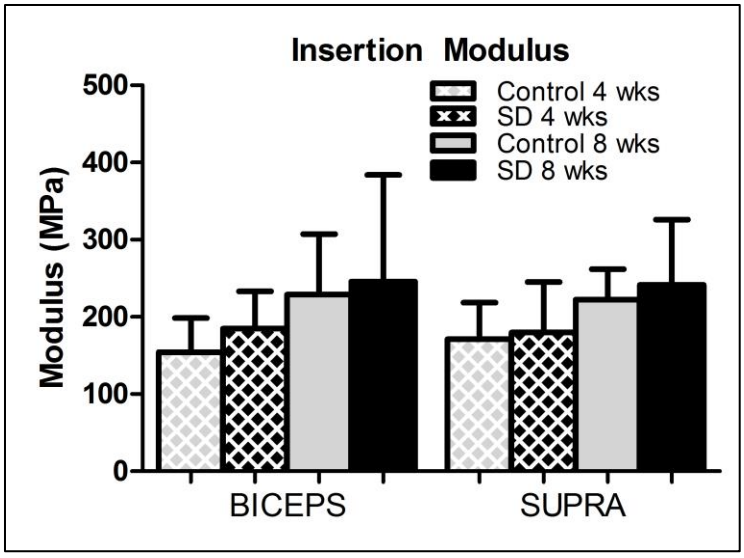

Figure 2.11. No differences in insertion modulus were observed in either tendon. Data shown as mean + standard deviation (*p<0.05). (SD=scapular dyskinesis)

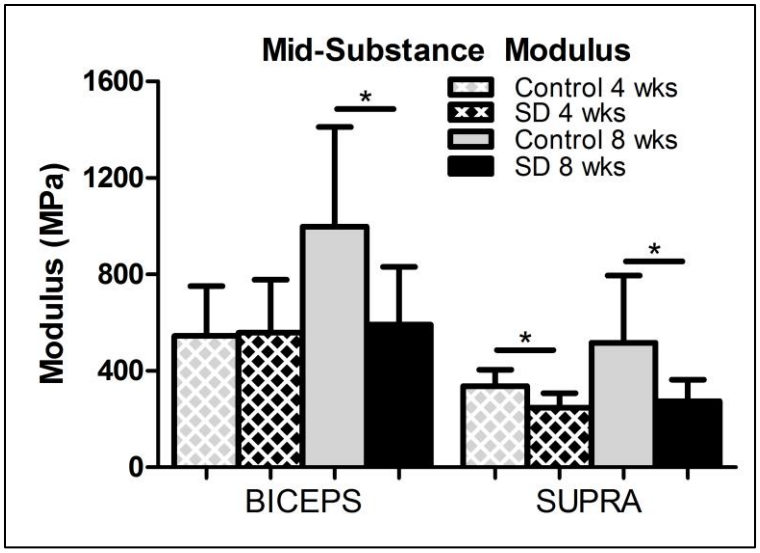

Figure 2.12. The biceps and supraspinatus tendons demonstrated significantly decreased tendon modulus at 8 weeks and both 4 and 8 weeks, respectively, in the SD group compared to control. Data shown as mean + standard deviation (*p<0.05). (SD=scapular dyskinesis)

Tendon Histology. A significantly more rounded cell shape was observed in the SD group in the distal groove of the biceps tendon at 8 weeks, with similar trends at the insertion, intra-articular space, and proximal groove regions at 8 weeks (Table 2.3). A significantly less rounded cell shape was observed at the insertion of the supraspinatus tendon in the SD group compared to control at 8 weeks. No other differences in cell shape were observed along the length of the supraspinatus tendon at any time point. A trend toward decreased cell density was observed at the insertion of the biceps at 8 weeks compared to control (Table 2.4). Cell density was significantly increased in the SD group at the insertion of the supraspinatus tendon at 8 weeks compared to control (Figure 2.13), with a similar trend at the insertion at 4 weeks and mid-substance at 8 weeks. Changes in tissue organization were observed with polarized light microscopy. Surprisingly, a significant decrease in angular deviation (indicative of more highly aligned collagen fibers) was observed in the proximal groove of the biceps at 4 weeks in the SD group compared to control, with a similar trend in the intra-articular region at 2 and 4 weeks (Figure 2.14). An additional trend toward increased angular deviation (indicative of greater collagen disorganization) was observed in the insertion of the biceps at 8 weeks in the SD group compared to control. For the supraspinatus tendon, a significant increase in angular deviation was observed at the insertion site at 2 weeks in the SD group compared to control (Figure 2.15). No other differences in tissue organization were observed in the supraspinatus tendon at either time point.

Tendon	Group	Region	2 weeks (mm/mm)	4 weeks (mm/mm)	8 weeks (mm/mm)
Biceps	SD	INS	0.754 ± 0.09	0.685 ± 0.08	0.623 ± 0.05^{+}
	Control		0.764 ± 0.06	0.711 ± 0.08	0.580 ± 0.04
	SD	INTRA	0.689 ± 0.04	0.689 ± 0.08	0.598 ± 0.10^{+}
	Control		0.660 ± 0.05	0.699 ± 0.09	0.537 ± 0.07
	SD	PROX	0.598 ± 0.04	0.645 ± 0.08	0.609 ± 0.11^{+}
	Control		0.622 ± 0.06	0.667 ± 0.09	0.522 ± 0.05
	SD	DIS	0.494 ± 0.06	0.577 ± 0.04	0.556 ± 0.14*
	Control		0.494 ± 0.11	0.602 ± 0.13	0.403 ± 0.11
Supra	SD	INS	0.695 ± 0.04	0.646 ± 0.09	0.650 ± 0.03*
	Control		0.654 ± 0.07	0.698 ± 0.03	0.722 ± 0.04
	SD	MID	0.662 ± 0.03	0.502 ± 0.06	0.402 ± 0.07
	Control		0.652 ± 0.06	0.534 ± 0.04	0.461 ± 0.07

Table 2.3. At 2 and 4 weeks, no differences were observed between groups. At 8 weeks, cell shape was significantly more rounded at the biceps distal groove (DIS) with similar trends at the insertion (INS), intra-articular space (INTRA), and proximal groove (PROX), in the SD group compared to control. At 8 weeks, cell shape was significantly less rounded at the supraspinatus (Supra) insertion in the SD group compared to control. Data shown as mean ± standard deviation (*$p<0.05$, $+p\leq0.1$). (SD=scapular dyskinesis)

Tendon	Group	Region	2 weeks (cells/mm^2)	4 weeks (cells/mm^2)	8 weeks (cells/mm^2)
Biceps	SD	INS	300 ± 53	184 ± 94^{+}	276 ± 52
	Control		284 ± 33	249 ± 57	298 ± 92
	SD	INTRA	331 ± 108	328 ± 64	255 ± 27
	Control		287 ± 31	290 ± 75	277 ± 51
	SD	PROX	426 ± 181	295 ± 65	321 ± 130
	Control		519 ± 216	285 ± 41	300 ± 96
	SD	DIS	351 ± 199	327 ± 89	334 ± 152
	Control		357 ± 97	309 ± 85	345 ± 130
Supra	SD	INS	448 ± 306	387 ± 59^{+}	461 ± 87*
	Control		454 ± 314	318 ± 81	322 ± 46
	SD	MID	282 ± 121	431± 111	594 ± 23^{+}
	Control		349 ± 70	406 ± 147	431 ± 83

Table 2.4. At 2 weeks, no differences were observed between groups. At 4 weeks, a trend toward decreased cell density was observed at the biceps insertion (INS) in the SD group compared to control. At 8 weeks, cell density was significantly increased at the supraspinatus (Supra) insertion, with similar trends at the insertion at 4 weeks and at the mid-substance (MID) at 8 weeks, in the SD group compared to control. Data shown as mean ± standard deviation (*$p<0.05$, $^{+}p\leq0.1$). (SD=scapular dyskinesis)

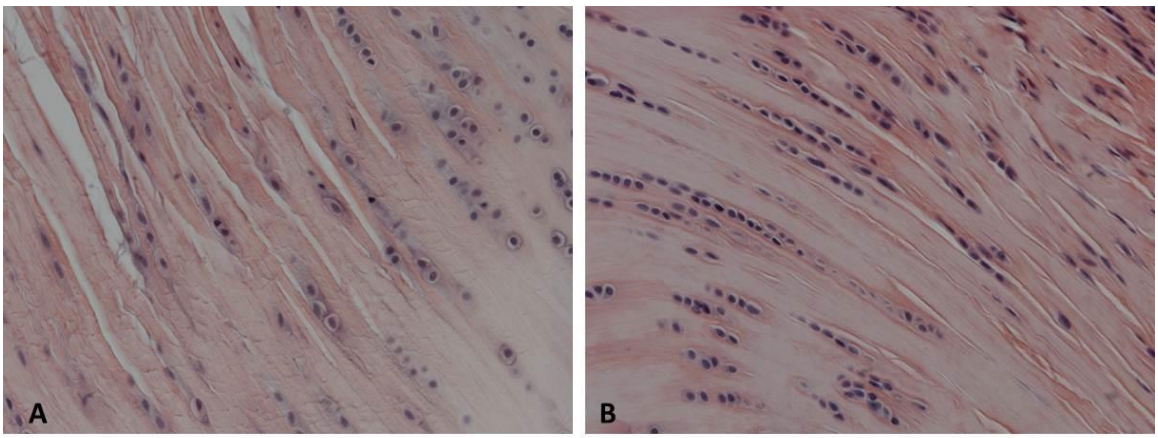

Figure 2.13. Tendon histology (supraspinatus and biceps) was quantified for cell shape and cell density at the insertion and mid-substance regions. A representative image for the supraspinatus insertion is displayed. Cell density was significantly increased (*$p<0.05$) in the SD group (B) compared to the control group (A). (SD=scapular dyskinesis)

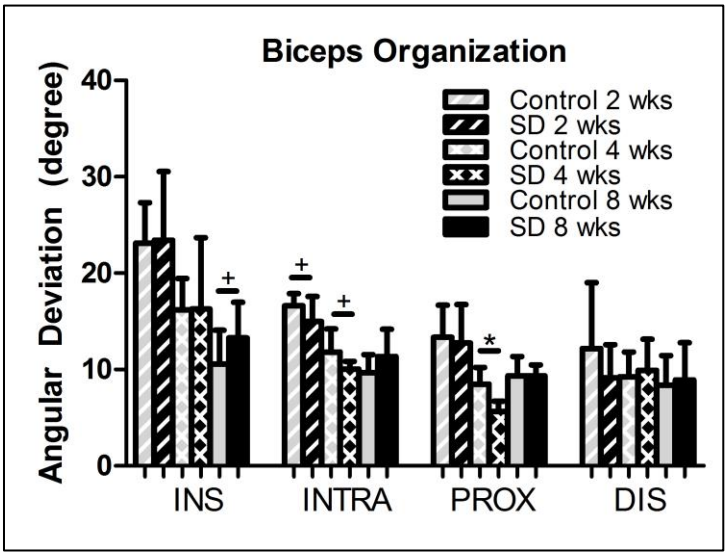

Figure 2.14. At 2 weeks, a trend toward decreased angular deviation was observed at the intra-articular space (INTRA), in the SD group compared to control. At 4 weeks, biceps angular deviation was significantly decreased at the proximal groove (PROX), with a similar trend at the intra-articular space, in the SD group compared to control. At 8 weeks, a trend toward increased angular deviation was observed at the biceps insertion (INS) in the SD group compared to control. Data shown as mean + standard deviation (*$p<0.05$, +$p\leq0.1$). (SD=scapular dyskinesis)

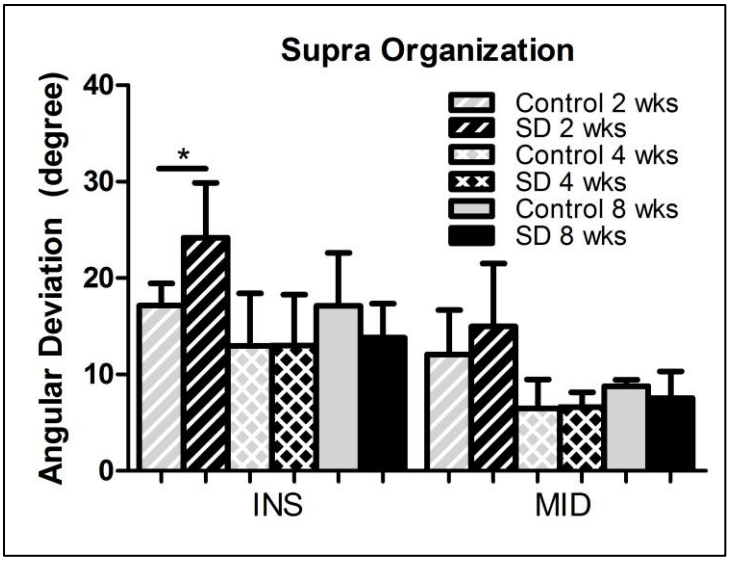

Figure 2.15. At 2 weeks, a significant increase in angular deviation was observed at the supraspinatus insertion in the SD group compared to control. Data shown as mean + standard deviation (*$p<0.05$, +$p\leq0.1$). (SD=scapular dyskinesis)

Tendon Immunohistochemistry. Changes in protein expression were observed with immunohistochemical staining. Compared to control, collagen III was significantly increased in the SD group at the supraspinatus insertion at 4 weeks, with a similar trend at the supraspinatus insertion and mid-substance and biceps insertion at 8 weeks (Table 2.5). However, collagen III was significantly decreased in the SD group compared to control at the distal groove of the biceps at 8 weeks. Decorin was significantly decreased in the SD group compared to control at the biceps insertion and distal groove at 4 weeks (Table 2.5). Interestingly, however, decorin was significantly increased in the SD group compared to control at the biceps insertion at 8 weeks, with a similar trend in the supraspinatus mid-substance at 8 weeks. No differences in collagen II or IL1-β were observed (Table 2.6).

Tendon	Region	Col III						Decorin					
		2 weeks		4 weeks		8 weeks		2 weeks		4 weeks		8 weeks	
		Control	SD	Control	SD	Control	SD	Control	SD	Control	SD	Control	SD
Biceps	INS	1.5(0.75-2.25)	0.5(0-1.25)	2 (1-2)	1 (1-1)	1 (1-2)	2 (2-2)+	1(0.5-1.5)	1.5(1-2.25)	2.5 (2-3)	1 (1-1.25)*	1 (1-2)	3 (2-3)*
	INTRA	2(1.5-2.5)	2(1.75-2)	1 (1-1)	1 (0-1)	2 (1-2)	2 (1-2)	1.5(1.25-1.75)	2(1-2)	2 (1.5-2.5)	1.5 (1-2)	2 (1.5-2.5)	2 (2-3)
	PROX	0.5(0-1.25)	0(0-0)	0 (0-1)	0 (0-1)	1 (1-1)	1 (1-1)	1(1-1.25)	1(0.5-1)	2 (1-2)	1 (1-1.25)	2 (1-2)	1 (1-2)
	DIS	0(0-0.5)	0(0-0)	0 (0-1)	0 (0-1)	1 (1-1)	0 (0-1)*	1.5(0.75-2)	1(0.5-1)	2 (2-2.25)	1 (1-1)*	1 (1-2)	2 (1-2)
Supra	INS	0.5(0-1.5)	0(0-0)	0.5 (0-1)	1 (1-2)*	1.5 (0.75-2)	2 (2-2)+	1(1-1.25)	1(1-2)	2 (1.75-2)	3 (2-3)	2 (2-2.5)	2.5 (1.75-3)
	MID	0.5(0-1)	0(0-0.25)	0.5 (0-1)	0 (0-1)	0.5 (0-1)	2 (1-1)+	1(1-1.25)	1(1-2)	2 (1.5-2.25)	3 (2.5-3)	2 (1-2)	2 (2-2.25)+

Table 2.5. At 8 weeks, collagen III staining was decreased at the biceps distal groove (DIS) in the SD group compared to control. A trend toward increased collagen III staining was also observed at the biceps insertion in the SD group compared to control. At 4 weeks, collagen III staining was increased at the supraspinatus insertion, with similar trends at the insertion and mid-substance at 8 weeks, in the SD group compared to control. At 4 weeks, decorin staining was decreased at the biceps insertion and distal groove in the SD group compared to control. At 8 weeks, decorin staining was increased at the biceps insertion in the SD group compared to control, with a similar trend at the supraspinatus mid-substance. Data is shown as median and interquartile range (*$p<0.05$, +$p\leq0.1$). (SD=scapular dyskinesis)

Tendon	Region	Col II						IL1-β					
		2 weeks		4 weeks		8 weeks		2 weeks		4 weeks		8 weeks	
		Control	SD	Control	SD	Control	SD	Control	SD	Control	SD	Control	SD
Biceps	INS	1(0.75-1)	0(0-1)	0(0-0)	0(0-0)	0(0-0)	0(0-0)	1(1-1.5)	1.5(1-2)	0(0-0)	0(0-0)	0(0-0)	0(0-0)
	INTRA	1(0.75-1.25)	1(1-2)	0(0-0)	0(0-0)	0(0-0)	0(0-0)	1.5(0.75-2)	1(1-2)	0(0-0)	0(0-0)	0(0-0)	0(0-0)
	PROX	0.5(0-1.25)	0(0-2)	0(0-0)	0(0-0)	0(0-0)	0(0-1)	1.5(0.75-2)	1(1-1.25)	1(0-1)	1(0-2)	2(1-2)	1(1-2)
	DIS	0(0-0.25)	0(0-1)	0(0-0)	0(0-0)	0(0-0)	0(0-0)	1(1-1)	0.5(0-1.25)	1(1-1)	0(0-1)	2(1-2)	1.5(1-2)
Supra	INS	0(0-0)	0(0-0)	0(0-0)	0(0-1)	1(1-1)	1(0-1)	2(1-2)	1(1-1)	2(1-2)	1(1-2)	2(2-2)	2(2-2)
	MID	0(0-0)	0(0-0)	0(0-0)	0(0-0)	1(1-1)	1(0-1)	1(0-1)	1(1-1)	1(1-1.25)	1(1-1)	1.5(1-2)	2(2-2)

Table 2.6. No differences in Col II or IL1-β were observed. Data is shown as median and interquartile range (SD=scapular dyskinesis).

Cartilage Mechanics and Thickness. No differences in cartilage equilibrium elastic modulus were observed in any region and any time point, except a small but significant increase in the posterior-superior region at 8 weeks in the SD group compared to control (Figure 2.16). No differences in cartilage thickness were observed in any region and any time point. Trends toward increased cartilage thickness were observed in the center at 4 weeks and posterior-superior and posterior-inferior regions at 8 weeks in the SD group compared to control (Figure 2.17).

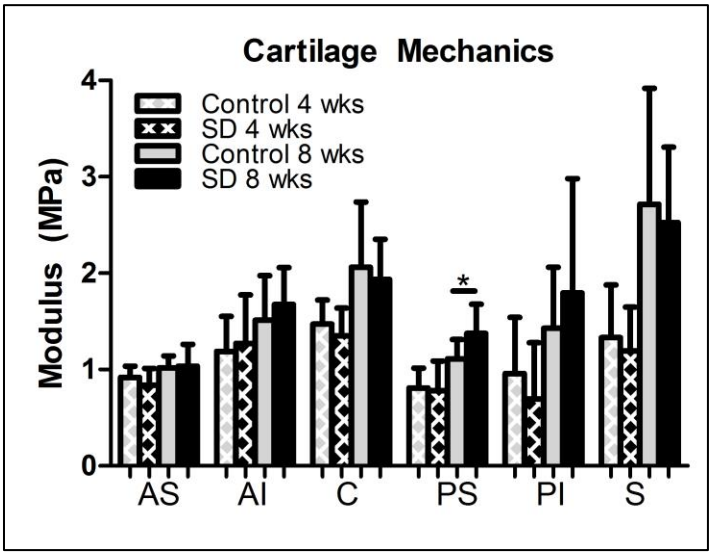

Figure 2.16. A significant increase in equilibrium elastic modulus was observed in posterior-superior region in the SD group compared to control at 8 weeks. Data shown as mean + standard deviation (*$p<0.05$). (SD=scapular dyskinesis)

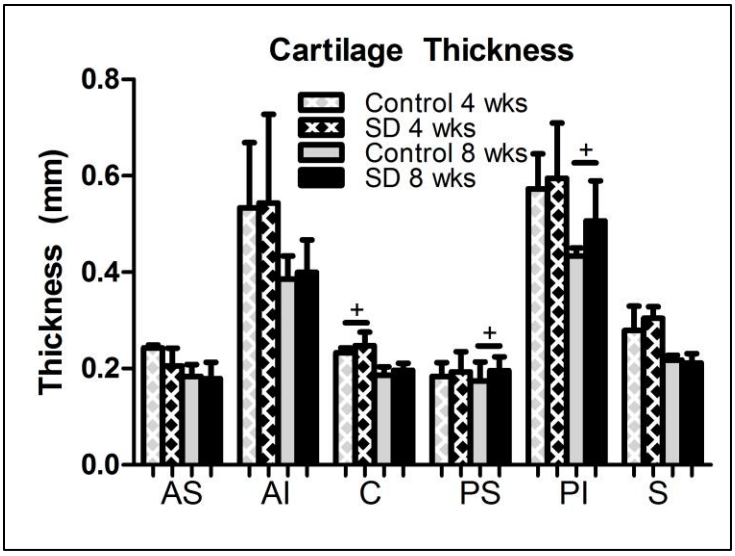

Figure 2.17. No significant differences in cartilage thickness were observed in any region. Data shown as median + interquartile range (+p≤0.1). (SD=scapular dyskinesis)

Serum Biomarkers. Results demonstrated no significant differences in serum inflammatory biomarkers (Figures 2.18-24).

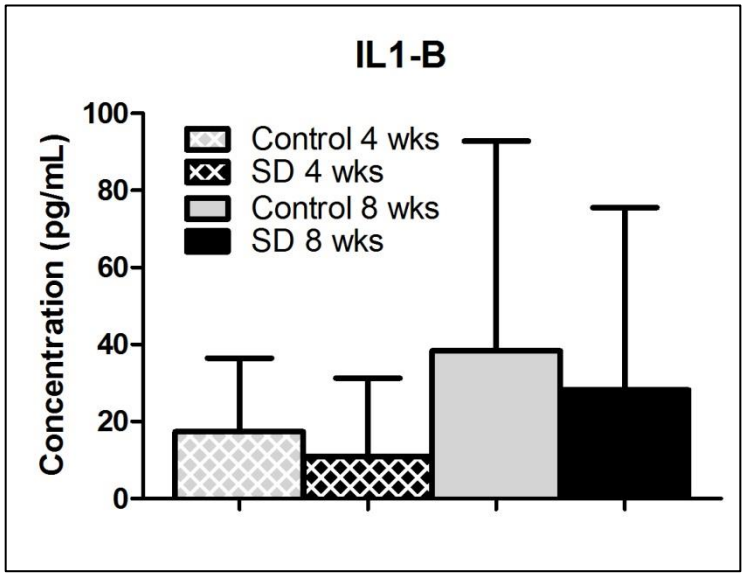

Figure 2.18. No differences were observed in IL1-β.

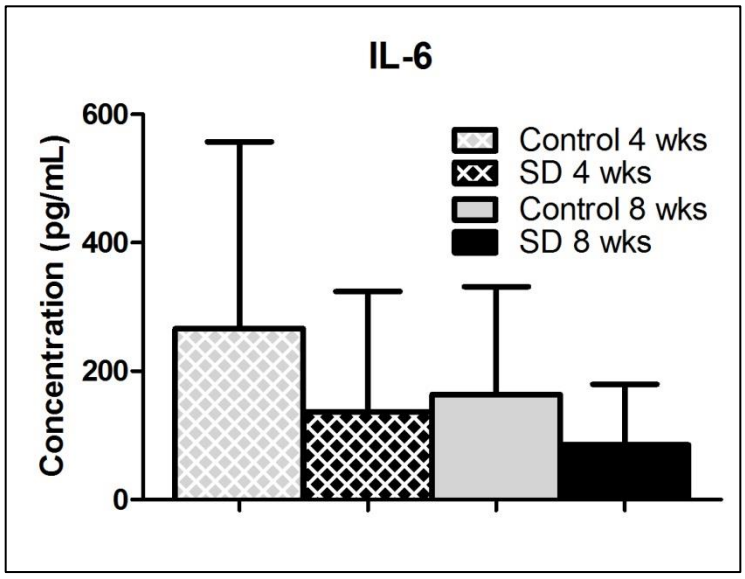

Figure 2.19. No differences were observed in IL-6.

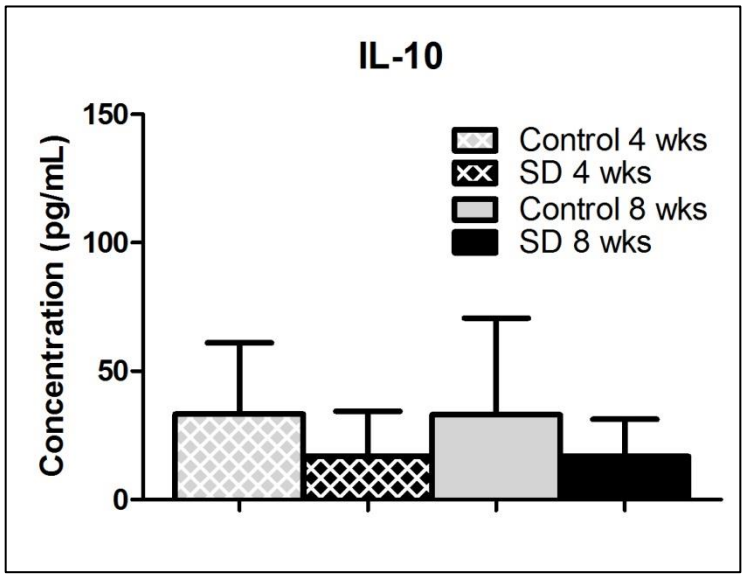

Figure 2.20. No differences were observed in IL-10.

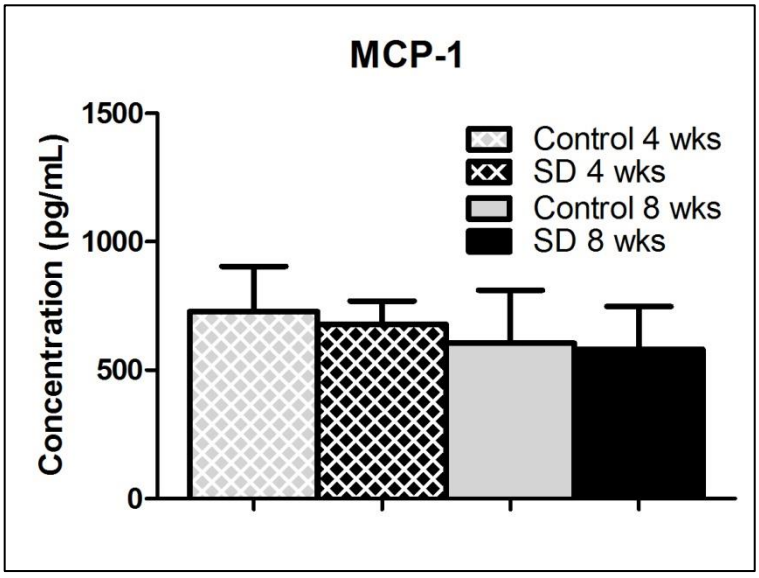

F**igure 2.21**. No differences were observed in MCP-1.

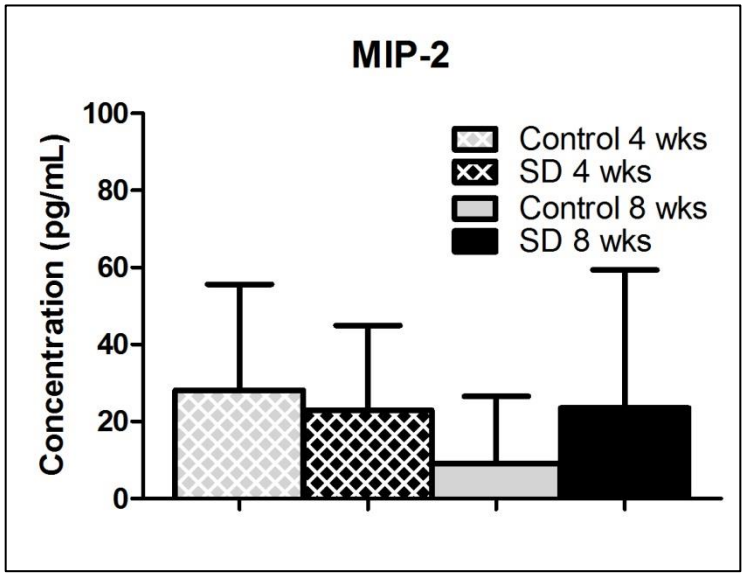

Figure 2.22. No differences were observed in MIP-2.

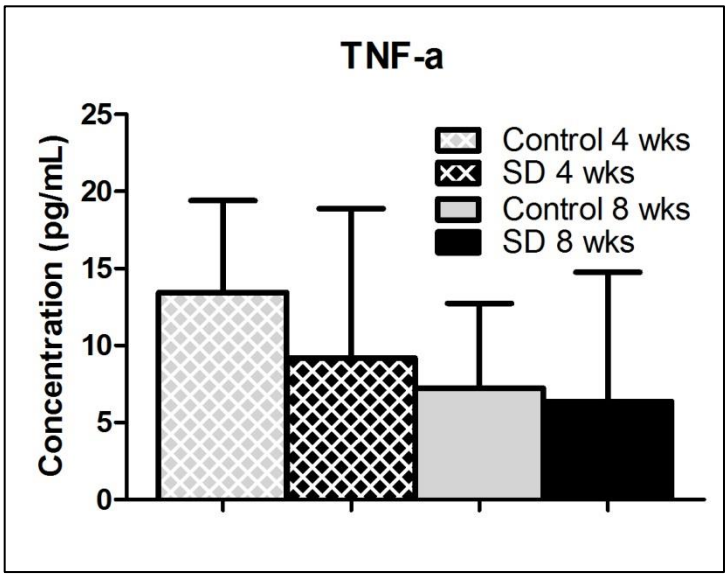

Figure 2.23. No differences were observed in TNF-α.

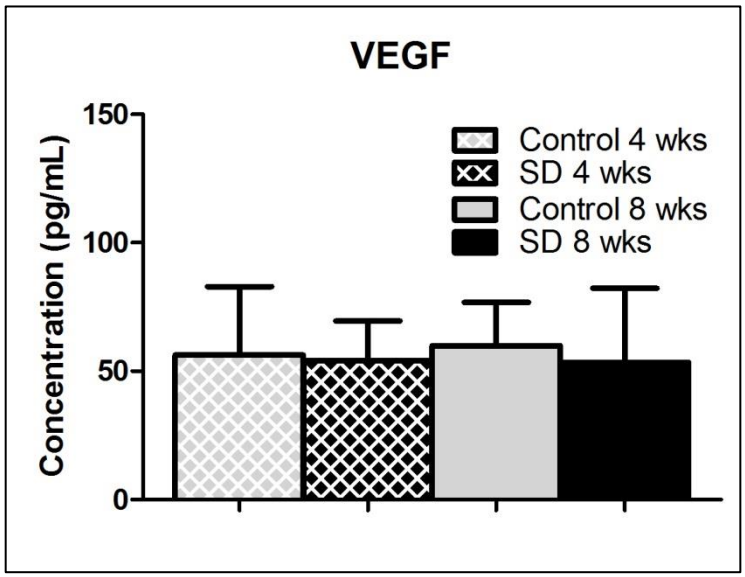

Figure 2.24. No differences were observed in VEGF.

D. Discussion

While the prevalence of shoulder impingement and its association with scapulothoracic kinematic abnormalities is well-documented, the cause and effect relationships remain unknown, making optimal clinical management difficult. In this animal model, we were able to prescribe scapular dyskinesis and evaluate the effect on the supraspinatus and the long head of the biceps in a controlled manner.

Results of this study demonstrate that scapular dyskinesis alters shoulder function and passive joint mechanics. Specifically, vertical force decreased and propulsion force increased in the SD group compared to control. The increased propulsion force may be due to the reduced upward rotation of the scapula and subsequent abrupt compressive contact force at the glenohumeral joint during forward locomotion. Alternatively, increased propulsion may be an attempt by the scapula to "catch up" with the humerus. Additionally, gross observational examination demonstrated clear alterations in scapular movements during forward locomotion, consistent with scapular "winging" in the human and characterized by entire medial border prominence in the closed kinetic chain activity. These changes indicate an alteration in the loading environment of this model and may place the glenohumeral joint at increased risk for degenerative injury. Specifically, altered scapular orientation infers altered acromial position which may lead to mechanical impingement of the rotator cuff and biceps and subsequent deficits in mechanical properties.[26] Additionally, passive joint mechanics were significantly altered in the SD group, with the SD group having increased internal range of motion. This may be due to a capsular inefficiency as a result of the reduced dynamic restraint. Previous studies have demonstrated that abnormal scapular orientation, specifically excessive

protraction, may place increased strains on the joint capsule, increasing risk of injury.[33] Additionally, the unstable scapula may diminish the ability of the rotator cuff to effectively compress the humeral head into the glenoid fossa thereby requiring the joint to rely on additional support from the static restraints, such as the joint capsule for stability. The resultant increased stress on the capsule could progress to the observed increased joint laxity.

Scapular dyskinesis also led to compromised tendon properties. Specifically, in the SD group, tendon elastic modulus was diminished in the mid-substance of both tendons. Additionally, percent relaxation, a viscoelastic parameter, was significantly increased. Previous studies have demonstrated that diminished elastic modulus and increased percent relaxation are indicative of inferior tissue properties as observed in injured and tendinopathic tendons.[3, 28] The changes observed in the presence of scapular dyskinesis may be a result of altered acromial position and subsequently reduced subacromial space, leading to tendon mechanical abrasion and wear. Alternatively, these changes could be a result of the increased demand (overload and overuse) placed on the rotator cuff and biceps in an attempt to restore dynamic stability to the glenohumeral joint, despite the presence of an unstable scapula. The location specific tendon changes (mid-substance region) may be due to its anatomic location under the acromial arch during forward flexion, resulting in impingement.

Histologic changes, consistent with tendon pathology, were also observed in each tendon. Specifically, the SD group had more rounded cell morphology in the biceps tendon at 8 weeks. These changes have been observed previously in injured tendon and may be indicative of increased cellular activity and/or a compressive loading

environment. Surprisingly, the SD group had a less rounded cell shape at the supraspinatus tendon insertion. The cellular changes observed in the supraspinatus tendon of the SD group are less than 10% different compared to controls and therefore may not be scientifically relevant, despite statistical significance. The changes observed in the biceps tendon were greater (~30% change) and therefore may be indicative of changes in cell behavior. Additionally, the SD group had a greater cell density at the supraspinatus tendon insertion, which may be indicative of increased cellular metabolic activity in response to the altered loading environment. It is important to note that cell density was only quantified in the tendon proper and the epitenon, a connective tissue sheet surrounding the tendon, was not included. Previous studies have demonstrated accumulation of epitenon cells in response to tendon injury and therefore further studies are warranted to evaluate cellular changes in the epitenon due to scapular dyskinesis.[35] Tendon collagen organization was also altered at the supraspinatus insertion at 2 weeks, with greater disorganization observed in the SD group compared to control. Additionally, the biceps tendon had greater organization in the SD group in the proximal groove at 4 weeks and intra-articular space at 2 and 4 weeks. However, at 8 weeks there was greater disorganization in the SD group compared to control at the insertion. The tendon's differential organization at each time point may be associated with a varied adaptation in response to changes in loading over time.

Structural changes were accompanied by changes in protein expression. Specifically, collagen III was significantly altered in both tendons. Collagen III was increased in the supraspinatus tendon and at the insertion of the biceps tendon in the SD group. Accumulation of collagen III in tendon has been associated with microtrauma,

scar formation, and a decrease in mechanical strength.[2, 5] Additionally, collagen III was decreased in the distal groove of the biceps tendon in the SD group. The location of this change is consistent with the location of differences in cell morphology in the biceps tendon and may be indicative of alterations in cellular function and subsequent extracellular-matrix deposition. Decorin was also significantly altered in both tendons. Specifically, decorin was decreased at the biceps insertion and distal groove at 4 weeks and interestingly, increased at the biceps insertion and supraspinatus mid-substance at 8 weeks, in the SD group. Decorin is the primary proteoglycan found in tendon and is involved in regulation of fibrillogenesis and may play a role in the tendon response to injury.[4] The initial decrease in decorin observed at 4 weeks is consistent with previous studies that have demonstrated that decorin is initially downregulated in injured tendon.[2] Interestingly, the increase in decorin observed at 8 weeks may be a result of the tendon's adaptive response to the change in loading and is consistent with the increased proteoglycan content observed with tendinopathy.[10] No differences in the cartilage marker, collagen II, or the pro-inflammatory cytokine, IL1-β, were observed. Previous studies have identified IL1-β as a possible initiator of tendinopathy and therefore IL1-β was selected for this study as an important inflammatory marker to be examined.[7, 8] Additionally, no differences in serum inflammatory biomarkers were observed. Previous studies have identified increased concentration of serum inflammatory biomarkers in the presence of soft tissue damage.[1] Taken together, the immunohistochemical results for IL1-β and biochemical results for serum biomarkers indicate that chronic inflammation may not play a role in the mechanical changes observed in this study; however, future

studies are warranted to further elucidate the acute and chronic inflammatory responses following injury.

Mechanical properties and geometry of the glenoid cartilage in the presence of scapular dyskinesis was examined. Measurement of mechanical properties of cartilage can be used to elucidate differences in loading and contact patterns at articulating surfaces.[25] Results from this study suggest that scapular dyskinesis alone is not detrimental to cartilage properties.

This study has several limitations. First, the use of a quadruped animal does not exactly replicate the human condition. However, it has been well-established that the rat shoulder has similar bony architecture and soft tissue anatomy as the human.[27] The presence of the acromial arch in the rat is particularly important because during forward locomotion, the supraspinatus passes repetitively under it, leading to supraspinatus tendinopathy. This is similar to what occurs in humans during repetitive overhead activity[28]. Secondly, acute transection of both the spinal accessory and long thoracic nerves to induce scapular dyskinesis does not exactly mimic the clinical scenario. Specifically, several factors may contribute to scapular dysfunction clinically including muscle imbalance, nerve injury, postural abnormality, anatomical disruption, capsular contracture, or proprioceptive dysfunction [11, 12]. For this model, we utilized a nerve injury mechanism and were able to successfully and repeatably create scapular "winging", which is consistent with observations found clinically in patients with scapular dyskinesis. Additionally, by utilizing an animal model, we were able to rigorously evaluate its effect in a controlled manner. Additionally, while nerve transection was performed to induce atrophy in the scapular muscles, it may also have secondary effects

on the surrounding bone, leading to altered skeletal homeostasis and changes in the microarchitecture.[30, 34] These changes should be further characterized through sophisticated imaging in future studies. Despite these limitations, results clearly demonstrate that scapular dyskinesis caused mechanical and structural consequences in the supraspinatus and biceps tendons.

This is the first study to directly identify scapular dyskinesis as a causative mechanical mechanism for the development of pathological changes in the supraspinatus and biceps tendons. Specifically, scapular dyskinesis permanently diminished shoulder function and tendon mechanical, structural, and compositional properties. Identification of scapular dyskinesis as a mechanism of pathological changes will help inform and guide clinicians in developing optimal long-term rehabilitation strategies. Alternatively, early interventions, such as preventative neuromuscular training, can also be considered, as has been successfully demonstrated in prevention of anterior-cruciate ligament (ACL) injuries[18]. Future chapters will examine the effect of scapular dyskinesis in the presence of overuse and following supraspinatus tendon repair in order to help define the in vivo mechanical processes which lead to rotator cuff and biceps tendon degeneration and compromise tendon healing potential following repair.

E. References

1. Barbe MF, Barr AE, Gorzelany I, Amin M, Gaughan JP, Safadi FF. Chronic repetitive reaching and grasping results in decreased motor performance and widespread tissue responses in a rat model of MSD. *J Orthop Res.* 2003;21(1):167-176.

2. Berglund M, Reno C, Hart DA, Wiig M. Patterns of mRNA Expression for Matrix Molecules and Growth Factors in Flexor Tendon Injury: Differences in the Regulation Between Tendon and Tendon Sheath. *The Journal of Hand Surgery.* 2006;31(8):1279-1287.

3. Dourte LM, Perry SM, Getz CL, Soslowsky LJ. Tendon properties remain altered in a chronic rat rotator cuff model. *Clin Orthop Relat Res.* 2010;468(6):1485-1492.

4. Dunkman A, Buckley M, Mienaltowski M, et al. The Tendon Injury Response is Influenced by Decorin and Biglycan. *Annals of Biomedical Engineering.* 2013;42(3):619-630.

5. Eriksen HA, Pajala A, Leppilahti J, Risteli J. Increased content of type III collagen at the rupture site of human Achilles tendon. *Journal of Orthopaedic Research.* 2002;20(6):1352-1357.

6. Gimbel JA, Van Kleunen JP, Mehta S, Perry SM, Williams GR, Soslowsky LJ. Supraspinatus tendon organizational and mechanical properties in a chronic rotator cuff tear animal model. *J Biomech.* 2004;37(5):739-749.

7. Gotoh M, Hamada K, Yamakawa H, Tomonaga A, Inoue A, Fukuda H. Significance of granulation tissue in torn supraspinatus insertions: an

immunohistochemical study with antibodies against interleukin-1 beta, cathepsin D, and matrix metalloprotease-1. *J Orthop Res.* 1997;15(1):33-39.

8. Green RA, Taylor NF, Watson L, Ardern C. Altered scapula position in elite young cricketers with shoulder problems. *J Sci Med Sport.* 2013;16(1):22-27.

9. Hayes WC, Keer LM, Herrmann G, Mockros LF. A mathematical analysis for indentation tests of articular cartilage. *J Biomech.* 1972;5(5):541-551.

10. Joseph M, Maresh CM, McCarthy MB, et al. Histological and molecular analysis of the biceps tendon long head post-tenotomy. *Journal of Orthopaedic Research.* 2009;27(10):1379-1385.

11. Kibler WB. The role of the scapula in athletic shoulder function. *Am J Sports Med.* 1998;26(2):325-337.

12. Kibler WB, McMullen J. Scapular dyskinesis and its relation to shoulder pain. *J Am Acad Orthop Surg.* 2003;11(2):142-151.

13. Kibler WB, Sciascia A, Wilkes T. Scapular dyskinesis and its relation to shoulder injury. *J Am Acad Orthop Surg.*20(6):364-372.

14. Konrad GG, Jolly JT, Labriola JE, McMahon PJ, Debski RE. Thoracohumeral muscle activity alters glenohumeral joint biomechanics during active abduction. *J Orthop Res.* 2006;24(4):748-756.

15. Labriola JE, Lee TQ, Debski RE, McMahon PJ. Stability and instability of the glenohumeral joint: the role of shoulder muscles. *J Shoulder Elbow Surg.* 2005;14(1 Suppl S):32S-38S.

16. Ludewig PM, Reynolds JF. The association of scapular kinematics and glenohumeral joint pathologies. *J Orthop Sports Phys Ther.* 2009;39(2):90-104.

17. Mihata T, Jun BJ, Bui CN, et al. Effect of scapular orientation on shoulder internal impingement in a cadaveric model of the cocking phase of throwing. *J Bone Joint Surg Am.*94(17):1576-1583.

18. Myklebust G, Engebretsen L, Braekken IH, Skjolberg A, Olsen OE, Bahr R. Prevention of anterior cruciate ligament injuries in female team handball players: a prospective intervention study over three seasons. *Clin J Sport Med.* 2003;13(2):71-78.

19. Peltz CD, Perry SM, Getz CL, Soslowsky LJ. Mechanical properties of the long-head of the biceps tendon are altered in the presence of rotator cuff tears in a rat model. *J Orthop Res.* 2009;27(3):416-420.

20. Reuther KE, Sarver JJ, Schultz SM, et al. Glenoid cartilage mechanical properties decrease after rotator cuff tears in a rat model. *J Orthop Res.* 2012;30(9):1435-1439.

21. Reuther KE, Thomas SJ, Sarver JJ, et al. Effect of return to overuse activity following an isolated supraspinatus tendon tear on adjacent intact tendons and glenoid cartilage in a rat model. *J Orthop Res.*

22. Sarver JJ, Dishowitz MI, Kim SY, Soslowsky LJ. Transient decreases in forelimb gait and ground reaction forces following rotator cuff injury and repair in a rat model. *J Biomech.*43(4):778-782.

23. Sarver JJ, Peltz CD, Dourte L, Reddy S, Williams GR, Soslowsky LJ. After rotator cuff repair, stiffness--but not the loss in range of motion--increased transiently for immobilized shoulders in a rat model. *J Shoulder Elbow Surg.* 2008;17(1 Suppl):108S-113S.

24. Seitz AL, McClure PW, Finucane S, Boardman ND, 3rd, Michener LA. Mechanisms of rotator cuff tendinopathy: intrinsic, extrinsic, or both? *Clin Biomech (Bristol, Avon).* 2011;26(1):1-12.

25. Setton LA, Mow VC, Muller FJ, Pita JC, Howell DS. Mechanical properties of canine articular cartilage are significantly altered following transection of the anterior cruciate ligament. *J Orthop Res.* 1994;12(4):451-463.

26. Solem-Bertoft E, Thuomas KA, Westerberg CE. The influence of scapular retraction and protraction on the width of the subacromial space. An MRI study. *Clin Orthop Relat Res.* 1993(296):99-103.

27. Soslowsky LJ, Carpenter JE, DeBano CM, Banerji I, Moalli MR. Development and use of an animal model for investigations on rotator cuff disease. *J Shoulder Elbow Surg.* 1996;5(5):383-392.

28. Soslowsky LJ, Thomopoulos S, Tun S, et al. Neer Award 1999. Overuse activity injures the supraspinatus tendon in an animal model: a histologic and biomechanical study. *J Shoulder Elbow Surg.* 2000;9(2):79-84.

29. Struyf F, Nijs J, Baeyens JP, Mottram S, Meeusen R. Scapular positioning and movement in unimpaired shoulders, shoulder impingement syndrome, and glenohumeral instability. *Scand J Med Sci Sports.* 2011;21(3):352-358.

30. Suyama H, Moriwaki K, Niida S, Maehara Y, Kawamoto M, Yuge O. Osteoporosis following chronic constriction injury of sciatic nerve in rats. *J Bone Miner Metab.* 2002;20(2):91-97.

31. Thompson WO, Debski RE, Boardman ND, 3rd, et al. A biomechanical analysis of rotator cuff deficiency in a cadaveric model. *Am J Sports Med.* 1996;24(3):286-292.

32. Warner JJ, Micheli LJ, Arslanian LE, Kennedy J, Kennedy R. Scapulothoracic motion in normal shoulders and shoulders with glenohumeral instability and impingement syndrome. A study using Moire topographic analysis. *Clin Orthop Relat Res.* 1992(285):191-199.

33. Weiser WM, Lee TQ, McMaster WC, McMahon PJ. Effects of simulated scapular protraction on anterior glenohumeral stability. *Am J Sports Med.* 1999;27(6):801-805.

34. Whiteside GT, Boulet JM, Sellers R, Bunton TE, Walker K. Neuropathy-induced osteopenia in rats is not due to a reduction in weight born on the affected limb. *Bone.* 2006;38(3):387-393.

35. Wojciak B, Crossan JF. The accumulation of inflammatory cells in synovial sheath and epitenon during adhesion formation in healing rat flexor tendons. *Clin Exp Immunol.* 1993;93(1):108-114.

Chapter 3: Overuse Activity in the Presence of Scapular Dyskinesis Leads to Shoulder Tendon Damage in a Rat Model

A. Introduction

This chapter will investigate the effect of overuse activity on function and mechanical, histological, organizational, and compositional properties of the supraspinatus and biceps tendon in the presence of scapular dyskinesis.

Shoulder injuries including rotator cuff and biceps tendinitis are widespread and debilitating clinical conditions. These injuries are particularly common in individuals who perform repetitive overhead activities due to their occupation or sport.[16] Previous studies have demonstrated that isolated overuse activity, and overuse activity combined with reduced subacromial space, results in the development of rotator cuff tendinopathy.[32] Specifically, overuse activity can lead to chronic tendon injuries characterized by disorganized collagen fibers, increased cellularity, altered cell shape (for example, more rounded), and decreased mechanical properties[33], indicative of degenerative tissue. These changes are likely a result of the repetitive microtrauma and mechanical compression/irritation of the rotator cuff underneath the acromial arch, defined as subacromial impingement.

Individuals who perform repetitive overuse activities (such as athletes and laborers) may also develop abnormal shoulder mechanics. Specifically, altered scapulothoracic joint kinematics, caused by muscular inhibition, adaptation, impaired coordination, or fatigue, is common.[3, 19, 37, 39] These changes may contribute to joint injury, such as subacromial impingement. Specifically, abnormal scapulothoracic joint kinematics, referred to as scapular dyskinesis, may disrupt glenohumeral joint motion, leading to increased joint translations, loosening static restraints, and possibly

predisposing the dynamic stabilizers, such as the rotator cuff and biceps, to injury. Several studies have demonstrated a strong association between scapular dyskinesis and shoulder injuries, such as shoulder impingement and rotator cuff disease.[10, 17] Identification of scapular dyskinesis as a risk factor for shoulder injury in an active population may help guide the development of prevention programs.

In Chapter 2, we demonstrated that scapular dyskinesis can contribute directly to the initiation and progression of rotator cuff and biceps tendon injuries. However, the long term consequences associated with overuse activity in the presence of abnormal scapular kinematics are unknown. The underlying mechanisms and specific relationship by which scapular dyskinesis affects the rotator cuff and biceps can only be elucidated in an animal model where time from injury and post-operative activity levels can be carefully controlled and evaluated over time.

Therefore, the objective of this study was to determine the effect of overuse in combination with scapular dyskinesis on joint mechanics and properties of the rotator cuff and biceps tendon in a rat model. We hypothesized that scapular dyskinesis in combination with repetitive overuse will alter joint function and diminish tendon properties when compared to scapular dyskinesis alone (H1) and when compared to overuse alone (H2).

B. Methods

Study Design. A rat model of scapular dyskinesis was used, as previously described, in this Institutional Animal Care and Use Committee (IACUC) approved study. Ninety male Sprague-Dawley rats (400-450 g) were randomized into 3 groups: nerve transection (SD, N=30), sham nerve transection + overuse activity (OV, N=30), or

nerve transection + overuse activity (SD + OV, N=30). Overuse activity was modeled as stated in our previous publications.[25, 33] Initially, rats in overuse groups underwent a 2-week treadmill training period to acclimate them to running at the desired speed and for the desired duration. All groups then underwent unilateral surgical transection (or sham transection) of the spinal accessory and long thoracic nerves, resulting in denervation of the trapezius and serratus anterior muscles, respectively. Pre- and post-operative analgesics (buprenorphine, 0.05 mg/kg) were administered up to 2 days following surgery. Animals returned to unrestricted cage activity for 5 days and were then subjected to overuse activity or continued unrestricted cage activity. Overuse activity consisted of treadmill running at 17 m/min on a 10° decline for 1 hour per day 5 days per week. Rats were sacrificed 2, 4, and 8 weeks following surgery and either frozen (for mechanical testing, N=10) or fixed in formalin (for histology and immunohistochemistry, N=5).

Quantitative Ambulatory Assessment. Forelimb ground reaction forces (medial/lateral, braking, propulsion, and vertical) and spatio-temporal parameters (step width, stride length, and speed) were quantified using an instrumented walkway, consisting of two 6 degree-of-freedom load/torque cells, as previously described in Chapter 2.[29] Rats were acclimated prior to formal recording of ambulatory data. Data was collected one day prior to surgery (baseline), and at days 5, 7, 14, 28, 42, and 56 days post-surgery. All parameters were normalized to animal body-weight.

Passive Joint Mechanics. Passive shoulder joint range of motion (ROM) and stiffness were quantified using a custom device, as previously described in Chapter 2.[30] Briefly, the animal was placed under anesthesia and the forearm was secured into a

rotating clamp at 90° of elbow flexion and 90° of glenohumeral forward flexion. The scapula was manually stabilizing (to isolate glenohumeral motion) and the arm was rotated through the full range of internal and external rotation three times. Range of motion was calculated using the average of the three maximum values for both internal and external rotation. A bilinear fit was applied to calculate joint stiffness in the toe and linear regions for both internal and external rotation. Data was collected one day prior to surgery (baseline), and at days 14, 28, and 56 days post-surgery. All parameters were normalized to baseline values.

Sample Preparation for Mechanical Testing. Tendon tissue samples were prepared at the time of mechanical testing, as previously described in Chapter 2. Briefly, the animals were thawed and the scapula and humerus were dissected out with the biceps and supraspinatus tendons intact. The tendons were fine dissected under a stereomicroscope to remove surrounding excess tissue. Cross-sectional area of each tendon was measured using a custom laser device.[34]

Tendon Mechanical Testing. Tendon mechanical testing was performed, as previously described in Chapter 2. Briefly, stain lines, for local optical strain measurements, were placed on the biceps and supraspinatus tendons, dividing the insertion and mid-substance regions. The scapula and humerus were embedded using polymethymethacrylate (PMMA) and secured in a custom testing fixture. The proximal end of each tendon was gripped with cyanoacrylate annealed sand paper and secured using custom grips. The specimens were immersed in PBS at 37°C during testing. Uniaxial tensile testing was performed with preconditioning (10 cycles from 0.1 N to 0.5 N), stress relaxation (4% strain for biceps and 5% strain for supraspinatus at a rate of 5

%/sec for 600 sec), and ramp to failure (0.3%/sec). Stress (force divided by cross-sectional area) and strain (determined from stain line displacements that were tracked using custom texture tracking software) were calculated and elastic modulus was determined using a linear regression of the linear region of the stress-strain curve. The viscoelastic parameter, percent relaxation, was calculated through analysis of the stress-relaxation curve and determination of the peak and equilibrium loads.

Tendon Histology. Histologic analysis was performed for the biceps and supraspinatus tendons, as previously described in Chapter 2. Briefly, tissues were harvested immediately following sacrifice and processed using standard paraffin procedures. Sagittal sections (7μm) were collected, stained with Hematoxylin–Eosin (H&E), and imaged at the insertion and mid-substance using traditional and polarized light microscopy at 200X and 100X magnifications, respectively. The mid-substance of the biceps was further subdivided into four regions: insertion site (INS), intra-articular space (INTRA), proximal groove (PROX), and distal groove (DIS), as previously described[22]. Cell density (number of cells/mm^2) and cell shape (aspect ratio; 0–1, with 1 being a circle) were quantified in the traditional light images using a bioquantification software system (Bioquant Osteo II; BIOQUANT Image Analysis Corp, Nashville, TN, USA). Polarized light images were analyzed using custom software to evaluate tendon organization, as previously described.[7] The angular deviation (AD) of the collagen orientation for each specimen, a measure of the collagen fiber alignment, was calculated in each tendon location.

Tendon Immunohistochemistry. Tissue specimens used for histology were also used to localize ECM proteins using previous immunohistochemical techniques.[22]

Specifically, staining for collagens type II and III, the proteoglycan decorin, and the inflammatory marker, IL1-β was performed and the proteins were visualized using DAB (Table 3.1). Staining results were independently graded by three blinded investigators, using a scale of 0-3 (0=undetectable, 1=low, 2= medium, 3=high) and the mode of these values was used as the final specimen score.

Table 3.1. Primary antibodies used for immunohistochemical staining

Protein Target	Antibody	Host	Type	Enzyme pretreatment	Dilution	Incubation period (h)	Source
Collagen II	II-116B3	Mouse	Monoclonal	Hyaluronidase	1:4	16	DSHB, Iowa City, IA, USA
Collagen III	c7805	Mouse	Monoclonal	Hyaluronidase	1:500	38	Sigma, St. Louis, MO, USA
Decorin	LF-113	Rabbit	Polyclonal	Chondroitinase ABC	1:300	38	L. Fisher, Bethesda, MD, USA
IL1-β	AB1832	Rabbit	Polyclonal	Pepsin	1:250	16	Millipore, Billerica, MA, USA

Cartilage Mechanical Testing. Glenoid cartilage properties were examined, as previously described in Chapter 2, to elucidate changes in joint loading in the presence of scapular dyskinesis and overuse. Following completion of biceps testing, the glenoid cartilage was prepared for mechanical testing, as previously described.[24, 25] Briefly, the biceps was sharply detached at its insertion on the superior rim of the glenoid using a scalpel blade. The glenoid was then preserved by wrapping in soft tissue and refreezing (-20°C).

For cartilage thickness measurement[24], each scapula was thawed and immersed in PBS containing a protease inhibitor cocktail (5 mM Benz-HCl, 1mM PMSF, 1 M NEM) at room temperature. Specimens were scanned at 0.25 mm increments using a 55 MHz ultrasound probe (Visualsonics, Inc) in plane with the scapula. Captured B-mode images of each scan were manually segmented (three times and averaged) by selecting the cartilage and bony surfaces of the glenoid. The 3D positions of these surfaces were reconstructed with a custom program (MATLAB, MathWorks, Inc., Natick, Massachusetts) and used to determine cartilage thickness maps. Each thickness map was divided into six regions (center (C), posterior-superior (PS), posterior-inferior (PI), anterior-superior (AS), anterior-inferior (AI), and superior (S)) and an average thickness was computed for each region. Following ultrasound scanning, specimens were again preserved by wrapping in soft tissue and refreezing (-20°C) until mechanical testing.

For cartilage mechanical testing[24], each scapula was thawed and immersed in PBS containing the protease inhibitor cocktail at room temperature. Utilizing a 0.5 mm diameter, non-porous spherical indenter tip, cartilage indentation testing was performed as previously described[24]. Briefly, a preload (0.005 N) was set followed by 8 step-wise

stress relaxation tests (8 μm ramp at 2 μm/s followed by a 300 second hold). The scapula was repositioned for each localized region using angular, rotational, and linear stages such that the indenter tip was perpendicular to the cartilage surface in each region. Cartilage thickness for indentation testing was determined by identifying the indentation location on each cartilage thickness map. Equilibrium elastic modulus was calculated, as described previously[24], at 20% indentation and assuming Poisson's ratio (v=0.30).

Statistical Analysis. For the ambulatory assessment, multiple imputations were conducted using the Markov chain Monte Carlo method for missing data points (~10%). For both ambulatory assessment and passive joint mechanics, significance was assessed using a 2-way ANOVA with repeated measures on time with follow-up t-tests between groups according to our hypotheses (H1: SD vs. SD + OV and H2: OV vs. SD + OV) at each time point. Tissue mechanics and histologic parameters between groups were assessed using a 1-way ANOVA with follow-up t-tests. Immunohistochemistry and cartilage thickness scores were evaluated using a Kruskal Wallis with follow-up Mann-Whitney tests. Significance was set by correcting for the number of comparisons at $p<0.05/2=0.025$, trends at $p<0.1/2=0.05$.

C. Results

Ambulatory Data. Shoulder function was significantly altered in the SD + OV group. Specifically, vertical force was significantly decreased in the SD + OV group compared to OV at 5 days, 2 weeks, and 6 weeks, with a similar trend at 8 weeks (Figure 3.1). However, vertical force for the SD and SD + OV groups was not different at any time point. Propulsion force was significantly increased in the SD + OV group compared to OV at all time-points (Figure 3.2). However, propulsion force for the SD and SD +

OV groups were not different at any time point. Braking force was significantly decreased in the SD + OV group compared to OV at 5 days post-injury (Figure 3.3). No other differences in braking force were observed between groups. Lastly, medial-lateral force was significantly more medial 1 week post-injury in the SD group compared to the SD + OV group (Figure 3.4). No significant differences in spatio-temporal parameters (step width, stride length, or speed) were observed between groups.

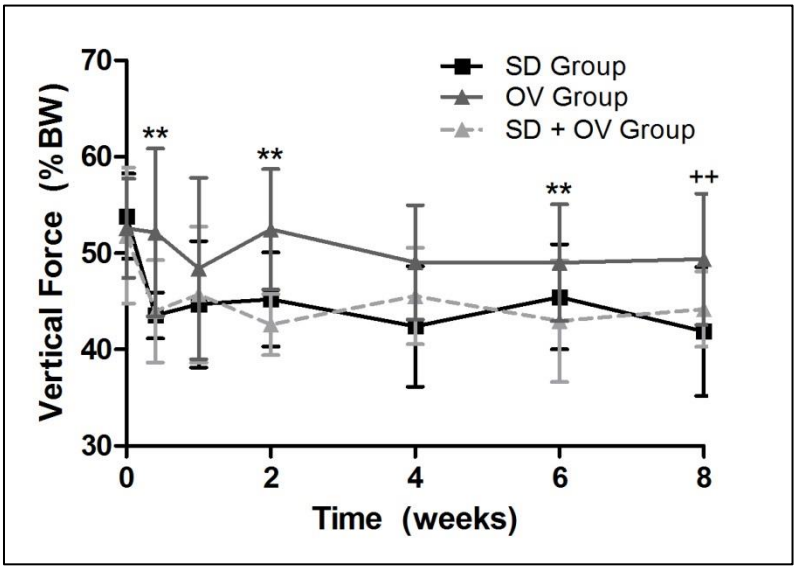

Figure 3.1. The SD + OV group had decreased vertical force compared to OV at most time-points (except 1 and 4 weeks following injury). Data shown as mean ± standard deviation ($p<0.025$ (OV vs. SD + OV**), $p<0.05$ (OV vs. SD + OV^{++})). (SD=scapular dyskinesis, OV=overuse)

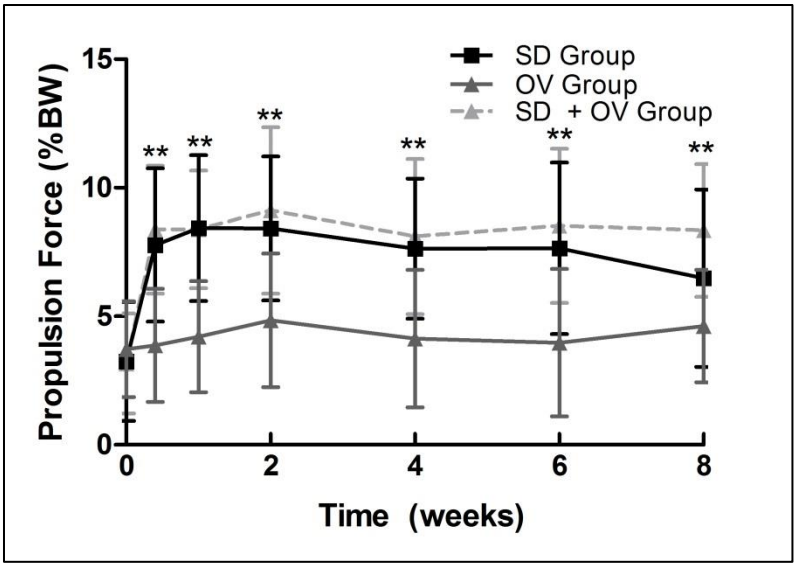

Figure 3.2. The SD + OV group had increased propulsion force compared to OV at all time-points. Data shown as mean ± standard deviation ($p<0.025$(OV vs. SD + OV**)). (SD=scapular dyskinesis, OV=overuse)

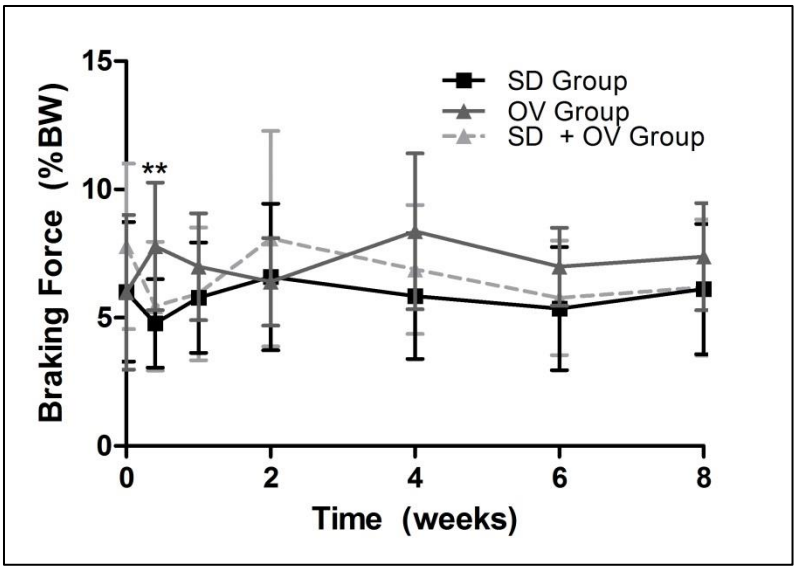

Figure 3.3. The SD + OV group had decreased braking force compared to OV 5 days following injury. Data shown as mean ± standard deviation ($p<0.025$(OV vs. SD + OV**)). (SD=scapular dyskinesis, OV=overuse)

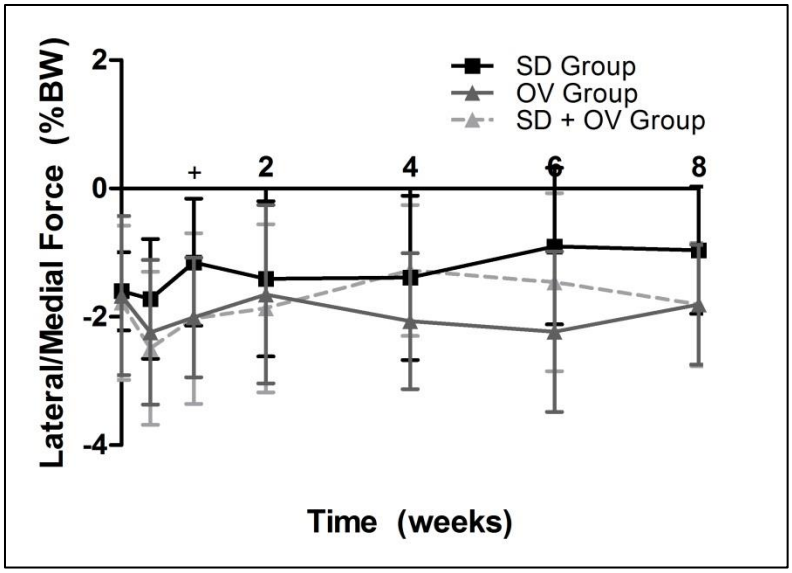

Figure 3.4. No difference in medial/lateral force was observed. Data shown as mean ± standard deviation. (SD=scapular dyskinesis, OV=overuse)

Passive Joint Mechanics. Passive joint mechanics were altered in the SD + OV group (Table 3.2). Specifically, external range of motion was significantly decreased in the SD + OV group compared to the SD group at 2 and 8 weeks post-injury and compared to the OV group 2 weeks post-injury. Data was normalized by baseline values (change from baseline). No other significant differences in passive joint mechanics were observed between groups.

Direction	Measurement	Time (wks)	SD	OV	SD + OV
Internal	ROM (degrees)	2	7.37±18.2	6.52±17.5	9.69±6.33
		4	-0.22±17.3	10.7±12.3	9.02±14.7
		8	1.35±16.3	1.68±23.8	8.64±13.3
	Toe Stiffness (N/mm)	2	-0.03±0.11	-0.02±0.09	-0.10±0.11
		4	0.01±0.11	-0.04±0.10	-0.05±0.12
		8	-0.02±0.12	0.07±0.17	-0.04±0.14
	Linear Stiffness (N/mm)	2	0.16±0.12	0.11±0.18	0.06±0.19
		4	0.13±0.11	0.02±0.15	0.07±0.13
		8	0.24±0.07	0.26±0.14	0.20±0.20
External	ROM (degrees)	2	16.0±7.4	3.49±14.6	-7.24±8.38*,**
		4	-2.58±9.5	8.75±16.7	7.10±19.2
		8	18.21±10.6	8.90±16.6	5.92±15.9*
	Toe Stiffness (N/mm)	2	-0.10±0.14	-0.06±0.10	-0.06±0.18
		4	0.06±0.19	-0.03±0.11	-0.03±0.14
		8	-0.04±0.13	0.01±0.14	-0.06±0.16
	Linear Stiffness (N/mm)	2	0.04±0.20	-0.05±0.16	-0.06±0.19
		4	-0.06±0.16	-0.06±0.15	0.03±0.24
		8	0.13±0.19	0.17±0.20	0.17±0.20

Table 3.2. Results for passive joint mechanics demonstrated decreased external range of motion (ROM) in the SD + OV group compared to the SD group at 2 and 8 weeks and compared to the OV group at 2 weeks. Data is shown as normalized by baseline values (change from baseline) and as mean ± standard deviation ($p<0.025$ (SD vs. SD + OV*, OV vs. SD + OV**)). (SD=scapular dyskinesis, OV=overuse)

Tendon Mechanics. Mechanical parameters were significantly altered in the SD + OV group. Specifically, tendon percent relaxation was significantly increased in the SD + OV group compared to SD for both the supraspinatus (at 4 and 8 weeks post-injury) and the biceps (at 8 weeks post-injury) (Figure 3.5, 3.6). Additionally, supraspinatus tendon insertion modulus was significantly decreased in the SD + OV group compared to SD at 8 weeks post-injury (Figure 3.7). However, no differences were observed at the biceps tendon insertion at either time-point (Figure 3.8). Supraspinatus and biceps

tendon mid-substance modulus were significantly decreased in the SD + OV group compared to the SD group and compared to the OV group at 8 weeks post-injury (Figure 3.9,3.10).

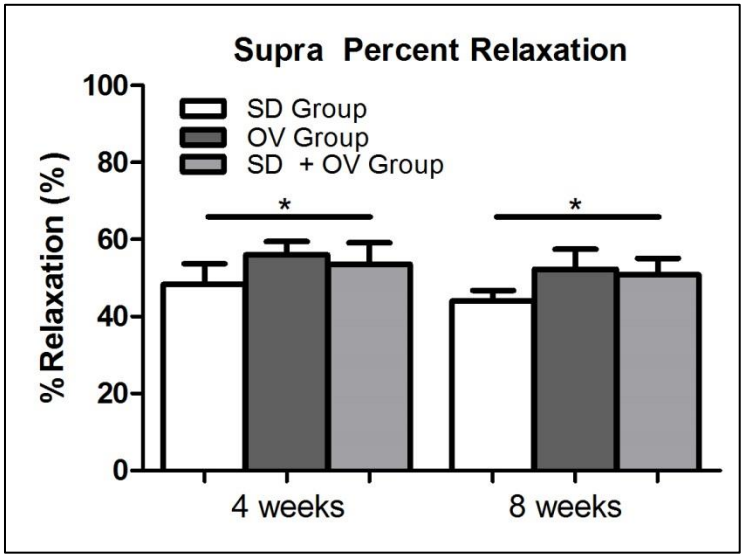

Figure 3.5. The supraspinatus tendon demonstrated increased percent relaxation at 4 and 8 weeks post-injury in the SD + OV group compared to SD. Data shown as mean + standard deviation ($p<0.025$ (SD vs. SD + OV*)). (SD=scapular dyskinesis, OV=overuse)

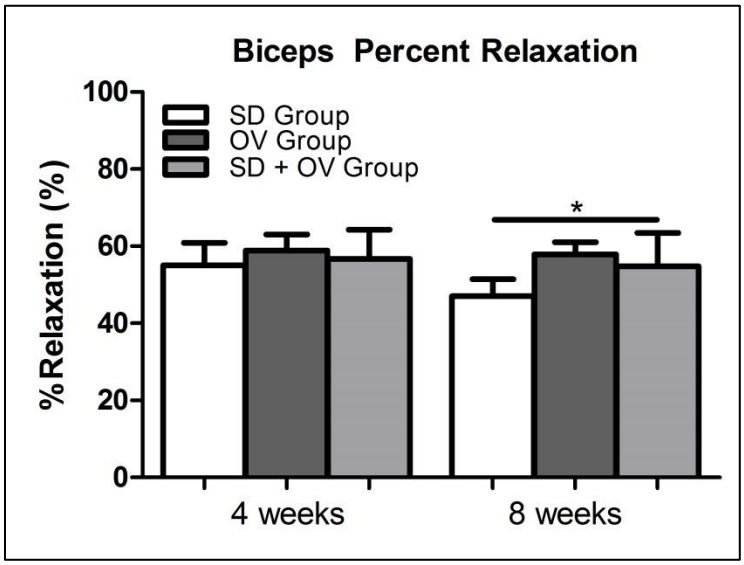

Figure 3.6. The biceps tendon demonstrated increased percent relaxation at 8 weeks post-injury in the SD + OV group compared to SD. Data shown as mean + standard deviation ($p<0.025$ (SD vs. SD + OV*)). (SD=scapular dyskinesis, OV=overuse)

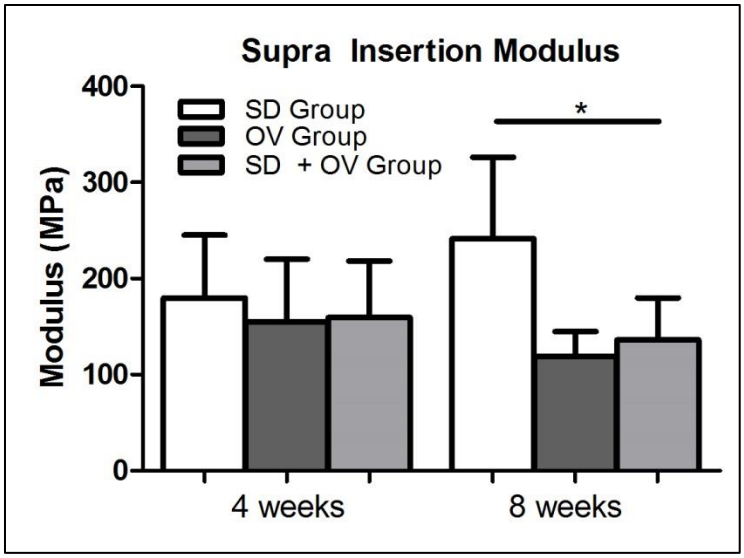

Figure 3.7. Supraspinatus insertion modulus was decreased at 8 weeks post-injury in the SD + OV group compared to SD. Data shown as mean + standard deviation ($p<0.025$ (SD vs. SD + OV*)). (SD=scapular dyskinesis, OV=overuse)

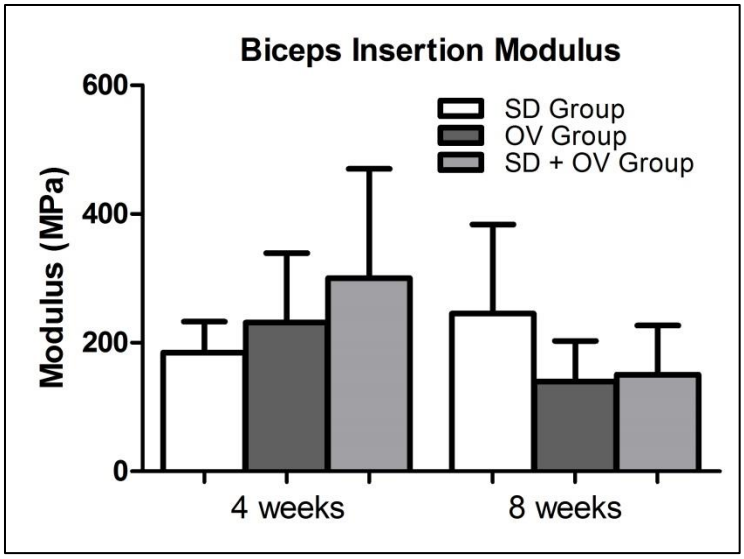

Figure 3.8. No differences in biceps insertion modulus were observed. Data shown as mean + standard deviation. (SD=scapular dyskinesis, OV=overuse)

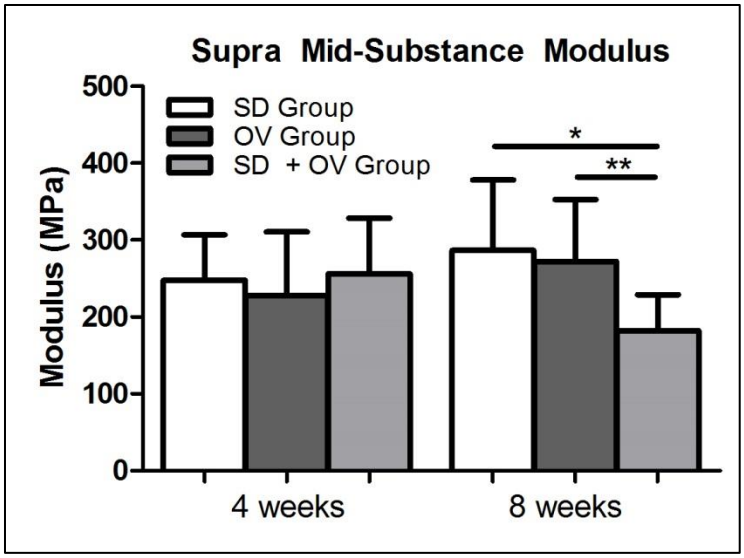

Figure 3.9. Supraspinatus mid-substance modulus was decreased at 8 weeks post-injury in the SD + OV group compared to SD and compared to OV. Data shown as mean + standard deviation ($p<0.025$ (SD vs. SD + OV*, OV vs. SD + OV**)). (SD=scapular dyskinesis, OV=overuse)

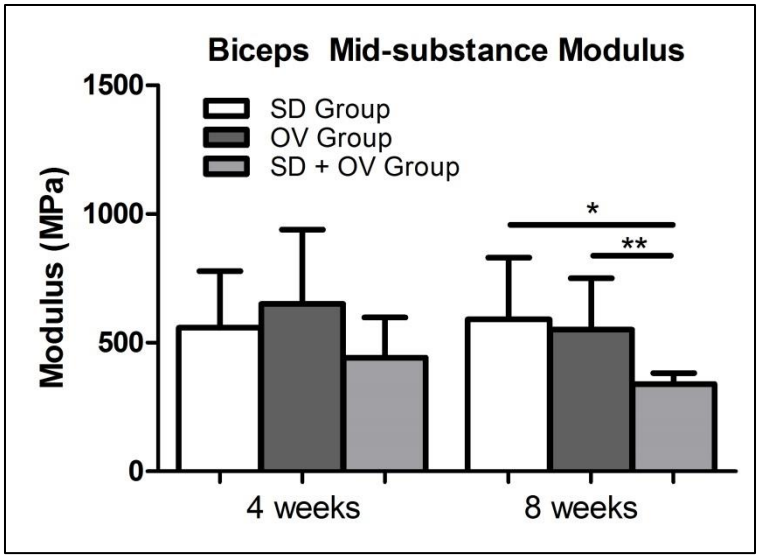

Figure 3.10. Biceps mid-substance modulus was decreased at 8 weeks post-injury in the SD + OV group compared to SD and compared to OV. Data shown as mean + standard deviation ($p<0.025$ (SD vs. SD + OV*, OV vs. SD + OV**)). (SD=scapular dyskinesis, OV=overuse)

Tendon Histology. Tendon histology was significantly altered in the SD + OV group. Specifically, cell shape at the biceps distal groove was significantly less rounded in the SD + OV group compared to both the SD and OV groups at 4 weeks post-injury (Table 3.3). Additionally, cell shape at the supraspinatus mid-substance was significantly more rounded in the SD + OV group compared to the SD group at 8 weeks post-injury. No other differences in cell shape were observed. Cell density was significantly increased at the supraspinatus insertion in the SD + OV group compared to the OV group at 8 weeks post-injury (Table 3.4). No other differences in cell density were observed. Tissue organization was also significantly altered in the SD + OV group. Specifically, angular deviation was significantly increased (indicative of greater collagen disorganization) at the supraspinatus and biceps insertion at 8 weeks in the SD + OV group compared to the SD group (Figure 3.11, 3.12). Additionally, angular deviation was significantly increased at the supraspinatus mid-substance at both 4 and 8 weeks and at the biceps proximal groove at 4 weeks in the SD + OV group compared to SD (Figure 3.13, 3.14).

Tendon	Group	Region	2 weeks (mm/mm)	4 weeks (mm/mm)	8 weeks (mm/mm)
Biceps	SD	INS	0.754 ± 0.09	0.685 ± 0.08	0.623 ± 0.05
	OV		0.752 ± 0.06	0.720 ± 0.05	0.658 ± 0.06
	SD + OV		0.739 ± 0.07	0.689 ± 0.10	0.671 ± 0.07
	SD	INTRA	0.689 ± 0.04	0.689 ± 0.08	0.598 ± 0.10
	OV		0.718 ± 0.06	0.612 ± 0.05	0.601 ± 0.08
	SD + OV		0.698 ± 0.06	0.663 ± 0.05	0.631 ± 0.04
	SD	PROX	0.598 ± 0.04	0.645 ± 0.08	0.609 ± 0.11
	OV		0.638 ± 0.07	0.582 ± 0.06	0.530 ± 0.08
	SD + OV		0.661 ± 0.05	0.558 ± 0.05	0.490 ± 0.03
	SD	DIS	0.494 ± 0.06	0.577 ± 0.04	0.556 ± 0.14
	OV		0.488 ± 0.14	0.520 ± 0.09	0.475 ± 0.13
	SD + OV		0.519 ± 0.14	0.336 ± 0.03*,**	0.410 ± 0.16
Supra	SD	INS	0.695 ± 0.04	0.646 ± 0.09	0.650 ± 0.03
	OV		0.715 ± 0.03	0.702 ± 0.10	0.596 ± 0.08
	SD + OV		0.682 ± 0.02	0.697 ± 0.08	0.640 ± 0.06
	SD	MID	0.662 ± 0.03	0.502 ± 0.06	0.402 ± 0.07
	OV		0.621 ± 0.03	0.487 ± 0.06	0.538 ± 0.04
	SD + OV		0.576 ± 0.06	0.529 ± 0.11	0.579 ± 0.05*

Table 3.3. At 4 weeks, cell shape was significantly less rounded at the biceps distal groove (DIS) in the SD + OV group compared to SD and OV. At 8 weeks, cell shape was significantly more rounded at the supraspinatus mid-substance (MID) in the SD + OV group compared to SD. Data is shown as mean ± standard deviation ($p<0.025$ (SD vs. SD + OV*, OV vs. SD + OV**)). (SD=scapular dyskinesis, OV=overuse)

Tendon	Group	Region	2 weeks (cells/mm^2)	4 weeks (cells/mm^2)	8 weeks (cells/mm^2)
Biceps	SD	INS	300 ± 53	184 ± 94	276 ± 52
	OV		252 ± 37	363 ± 119	437 ± 126
	SD + OV		272 ± 46	262 ± 50	463 ± 305
	SD	INTRA	331 ± 108	328 ± 64	255 ± 27
	OV		309 ± 110	396 ± 114	322 ± 104
	SD + OV		364 ± 89	327 ± 123	306 ± 104
	SD	PROX	426 ± 181	295 ± 65	321 ± 130
	OV		336 ± 99	331 ± 118	352 ± 24
	SD + OV		272 ± 42	440 ± 220	434 ± 126
	SD	DIS	351 ± 199	327 ± 89	334 ± 152
	OV		327 ± 133	474 ± 90	338 ± 131
	SD + OV		402 ± 119	335 ± 42	358 ± 41
Supra	SD	INS	448 ± 306	387 ± 59	461 ± 87
	OV		433 ± 260	308 ± 52	230 ± 83
	SD + OV		597 ± 278	299 ± 74	419 ± 75**
	SD	MID	282 ± 121	431 ± 113	594 ± 23
	OV		393 ± 151	444 ± 181	428 ± 105
	SD + OV		450 ± 81	388 ± 81	806 ± 665

Table 3.4. At 8 weeks, cell density was significantly increased at the supraspinatus insertion (INS) in the SD + OV group compared OV. ($p<0.025$ (OV vs. SD + OV**)) (SD=scapular dyskinesis, OV=overuse)

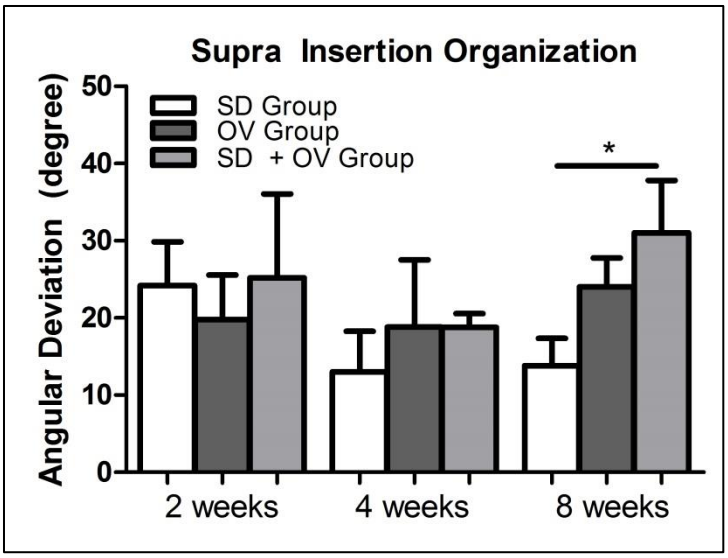

Figure 3.11. Supraspinatus insertion angular deviation was increased at 8 weeks post-injury in the SD + OV group compared to SD. Data shown as mean + standard deviation ($p<0.025$ (SD vs. SD + OV*)). (SD=scapular dyskinesis, OV=overuse)

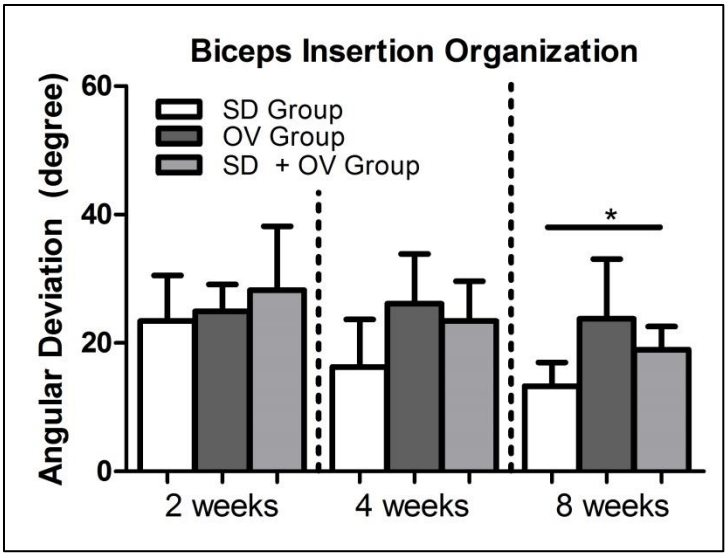

Figure 3.12. Biceps insertion angular deviation was increased at 8 weeks post-injury in the SD + OV group compared to SD. Data shown as mean + standard deviation ($p<0.025$ (SD vs. SD + OV*)). (SD=scapular dyskinesis, OV=overuse)

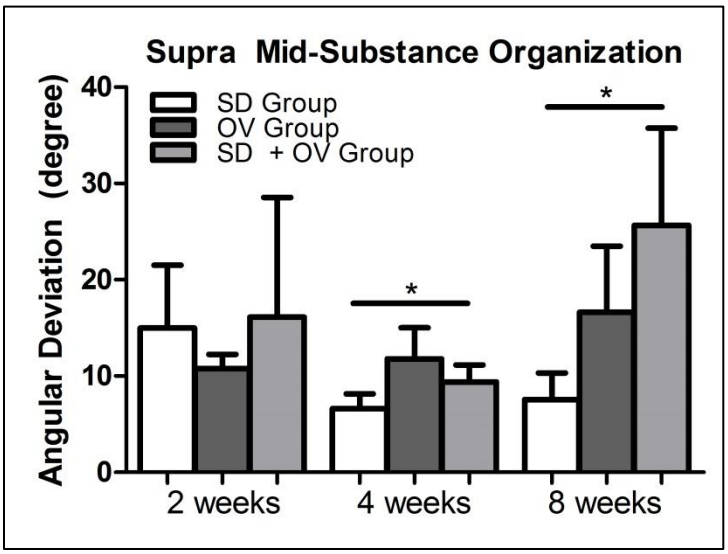

Figure 3.13. Supraspinatus mid-substance angular deviation was increased at 4 and 8 weeks post-injury in the SD + OV group compared to SD. Data shown as mean + standard deviation ($p<0.025$ (SD vs. SD + OV*)). (SD=scapular dyskinesis, OV=overuse)

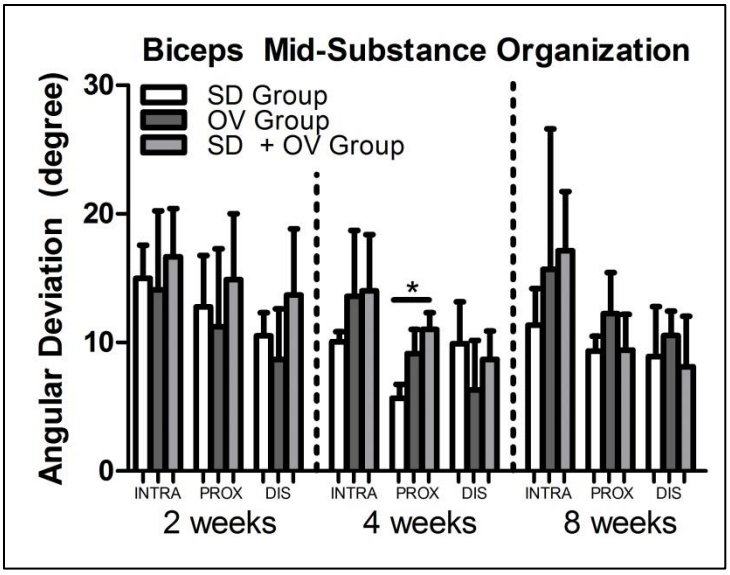

Figure 3.14. Biceps proximal groove (PROX) angular deviation was increased at 4 weeks in the SD + OV group compared to SD. Data is shown as mean + standard deviation ($p<0.025$ (SD vs. SD + OV*)). (SD=scapular dyskinesis, OV=overuse)

Tendon Immunohistochemistry. Tendon protein composition was also significantly altered in the SD + OV group. Specifically, collagen II was significantly increased at the proximal groove of the biceps tendon at 4 weeks in the SD + OV group compared to the SD group (Table 3.5). Collagen III was significantly decreased at the biceps insertion at 2 weeks and supraspinatus insertion and mid-substance at 4 weeks in the SD + OV group compared to the SD group (Table 3.5). Additionally, collagen III was decreased at the proximal groove of the biceps tendon at 8 weeks in the SD + OV group compared to the OV group, with a similar trend compared to the SD group. Decorin was significantly decreased at the supraspinatus mid-substance at 8 weeks in the SD + OV group compared to the SD group (Table 3.6). However, decorin was significantly increased at the biceps tendon insertion, with a trend at the intra-articular space, at 4 weeks in the SD + OV group compared to the SD group. No differences in IL1-β were observed (Table 3.6).

Tendon	Group	Region	Col II			Col III		
			2 weeks	4 weeks	8 weeks	2 weeks	4 weeks	8 weeks
Biceps	SD	INS	2 (1-3)	0(0-0)	0(0-1)	1.5 (1-2)	1(1-2)	2(2-2)
	OV		2 (1.5-2)	1(1-2)	1.5(0.75-2)	0 (0-0.5)	2(1-2)	2(2-2.25)
	SD + OV		1 (1-1)	1(0-1)	0(0-0.25)	0 (0-0.5)*	1(1-1)	2(1-2)
	SD	INTRA	2 (2-3)	0(0-0)	1(0-1)	2 (2-2)	1(1-1)	2(1-2)
	OV		1 (0.5-1.5)	1(1-1.5)	1(0.75-1.25)	0 (0-0.5)	1(1-2)	3(2.75-3)
	SD + OV		1 (0.75-1)	1(1-2)	0(0-1)	0 (0-0)	1(1-1)	2(1-2)
	SD	PROX	1 (1-3)	0(0-0)	1(1-2)	1(1-1.25)	1(1-2)	2(2-2)
	OV		2 (1-2)	1(1-2)	1(0.75-1.5)	1(0.5-1)	0(0-1)	2(2-2.25)
	SD + OV		0.5 (0-1)	1(1-1)*	0(0-1)	0(0-0.5)	1(1-1)	$1(1-1)^{+,}$**
	SD	DIS	1 (1-2)	1(0-1)	1(0-1)	0(0-0)	1(1-2)	1(0.75-1.25)
	OV		1 (1-1)	1(1-1)	0(0-0.5)	0(0-0.5)	0(0-1)	1.5(0.75-2.25)
	SD + OV		1 (0.5-1.5)	1.5(0.75-2)	1(1-1)	0(0-0.5)	1(0-1)	1(1-1)
Supra	SD	INS	1 (1-2)	1(1-2)	2(1-3)	0(0-0)	2(1-2)	2(2-2)
	OV		2 (1.5-2.5)	2(1-3)	1(0.5-1)	0.5(0-1.25)	0(0-0.25)	3(2-3)
	SD + OV		1 (1-1.5)	0(0-1)	1(0-2)	0(0-0)	0(0-1)*	2(2-2)
	SD	MID	1 (1-1)	1(0-1)	1(1-2)	1(0.75-1.25)	1(1-2)	2(2-2)
	OV		1 (1-1)	1(1-1)	1(0.5-1.5)	0.5(0-1)	0(0-1)	1(1-1.5)
	SD + OV		1 (1-1)	0(0-0)	0(0-0.5)	0.5(0.25-0.75)	0(0-0)*	2(1-2)

Table 3.5. At 2 weeks, collagen III staining was decreased at the insertion of the biceps. At 4 weeks, collagen II staining was increased at the biceps proximal groove (PROX) in the SD + OV group compared to SD. Collagen III staining was decreased at the supraspinatus insertion (INS) and mid-substance (MID) in the SD + OV group compared to SD. At 8 weeks, collagen III staining was decreased at the biceps proximal groove in the SD + OV group compared to OV, with a similar trend compared to SD. Data is shown as median and interquartile range ($p<0.025$ (SD vs. SD + OV*), (OV vs. SD + OV**)) ($p<0.05$ (SD vs. SD + OV^{+})). (SD=scapular dyskinesis, OV=overuse)

Tendon	Group	Region	Decorin			IL1-β		
			2 weeks	4 weeks	8 weeks	2 weeks	4 weeks	8 weeks
Biceps	SD	INS	1(0.75-1.25)	1(1-1)	2(2-3)	2(2-2)	1(1-2)	2(2-2)
	OV		1(0.75-1)	3(2-3)	1.5(1-2)	1(1-1.25)	1(1-1.5)	1.5(1-2.25)
	SD + OV		1(0.5-1.5)	2(2-2)*	1(1-2)	1(1-1.25)	1(1-1)	2(1-3)
	SD	INTRA	1(0.5-1.5)	1(1-2)	1(1-2)	2(1-3)	1(1-2)	2(2-2)
	OV		1(1-1)	3(2-3)	1.5(1-2)	1(1-1)	1.5(1-2.25)	2(1.75-2.25)
	SD + OV		1(1-1.5)	2(2-3)$^{+}$	2(1-3)	1(1-1.25)	2(1-2)	2(1.5-2.5)
	SD	PROX	1(0.5-1)	1(1-1)	1(1-1)	1(1-1.5)	1(1-2)	2(2-2)
	OV		1(1-1)	2.5(1.75-3)	2(1.75-2)	1(1-1.5)	1(1-1.5)	1(1-1)
	SD + OV		1(1-1)	2.5(1.75-3)	1(1-1.5)	1.5(1-2)	2(1-2)	1(1-2)
	SD	DIS	1(0.5-1)	1(1-2)	2(2-2)	1.5(1-2.25)	1(1-2)	2.5(2-3)
	OV		1(1-1.5)	3(1.5-3)	2(2-2.5)	1(1-1)	1(1-1.5)	1.5(1-2.25)
	SD + OV		0(0-0.5)	3(2.5-3)	2(2-2)	2(1.5-2.5)	1(1-1.5)	2(2-2.25)
Supra	SD	INS	1(1-1)	3(2-3)	2(2-2)	2(1-2)	2(2-2)	3(3-3)
	OV		1(1-1)	2.5(1.75-3)	3(2.5-3)	3(2-3)	2(1.75-2)	3(2.5-3)
	SD + OV		1.5(1.25-1.75)	2(2-3)	1(1-2)	1(1-2)	2(2-2)	2(2-3)
	SD	MID	1(1-1)	3(2.75-3)	3(3-3)	1(1-1)	1.5(1-2.25)	3(3-3)
	OV		1(1-1)	2(1.5-2)	2(2-2.5)	1(1-1.5)	2(1-2)	2(1.5-2.5)
	SD + OV		1(1-1)	2(1.75-2.25)	1.5(1-2)*	2(2-2.5)	1(1-1)	2(1-2)

Table 3.6. At 4 weeks, decorin staining was increased at the biceps insertion, with a similar trend at the intra-articular space (INTRA), in the SD + OV group compared to SD. At 8 weeks, decorin staining was decreased at the supraspinatus mid-substance in the SD + OV group compared to SD. No differences in IL1-β were observed. Data is shown as median and interquartile range ($p<0.025$ (SD vs. SD + OV*)) ($p<0.05$ (SD vs. SD + OV^{+})). (SD=scapular dyskinesis, OV=overuse)

Cartilage Mechanics and Thickness. No differences in cartilage equilibrium elastic modulus were observed in any region and any time point, except a small but significant increase in the posterior-superior region at 8 weeks in the SD + OV group compared to the OV group (Figure 2.16). Cartilage thickness was decreased in the anterior-inferior, center, posterior-inferior, and superior regions at 4 weeks and increased in the anterior-inferior, center, posterior-superior, and superior regions at 8 weeks in the SD + OV group compared to SD (Figure 2.17).

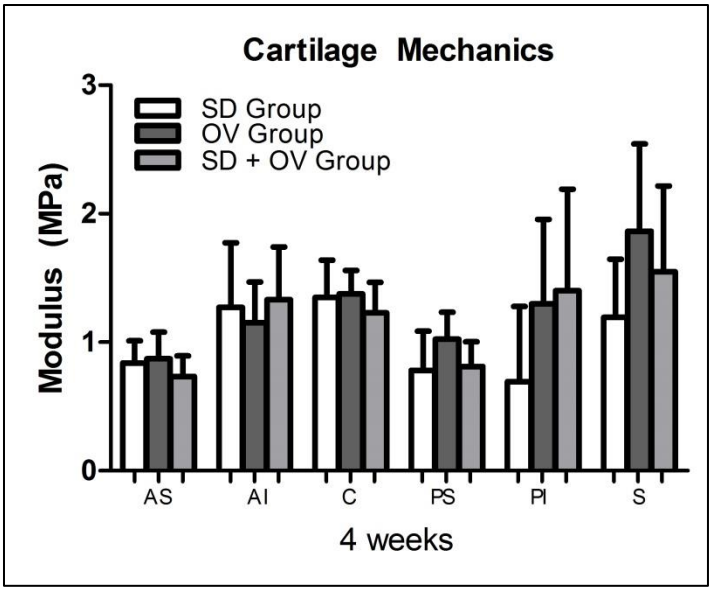

Figure 3.15. No differences in equilibrium elastic modulus were observed at 4 weeks. Data is shown as mean + standard deviation. (SD=scapular dyskinesis, OV=overuse)

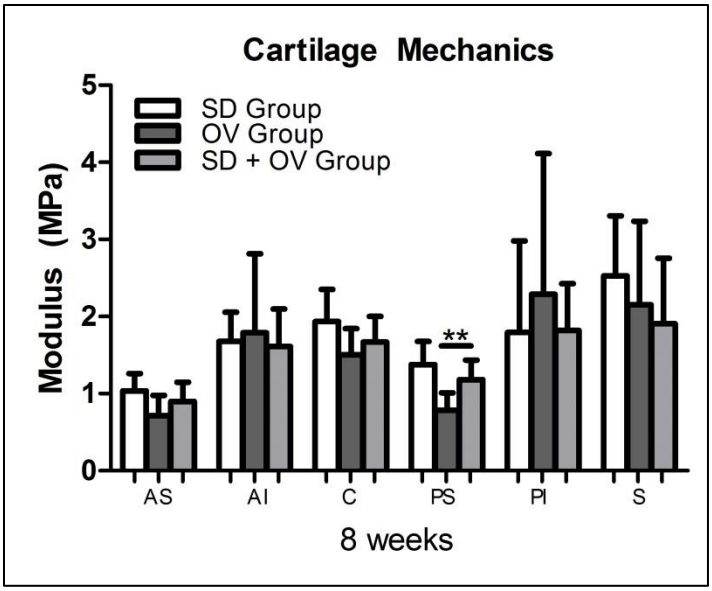

Figure 3.16. A significant increase in equilibrium elastic modulus was observed in posterior-superior region in the SD + OV group compared to OV at 8 weeks. Data shown as mean + standard deviation ($p<0.025$(OV vs. SD + OV**)). (SD=scapular dyskinesis, OV=overuse)

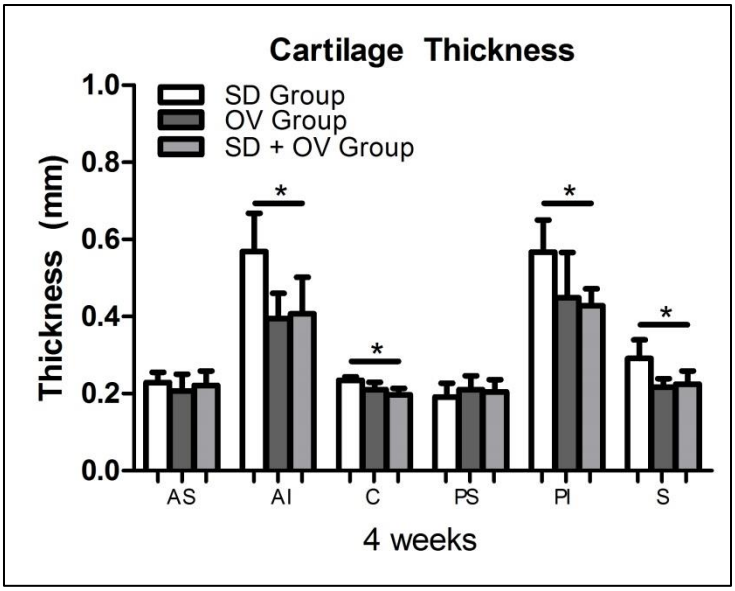

Figure 3.17. A significant decrease in cartilage thickness was observed in the anterior-inferior, center, posterior-inferior, and superior regions in the SD + OV group compared to SD at 4 weeks. Data shown as mean + standard deviation ($p<0.025$(SD vs. SD + OV*)). (SD=scapular dyskinesis, OV=overuse)

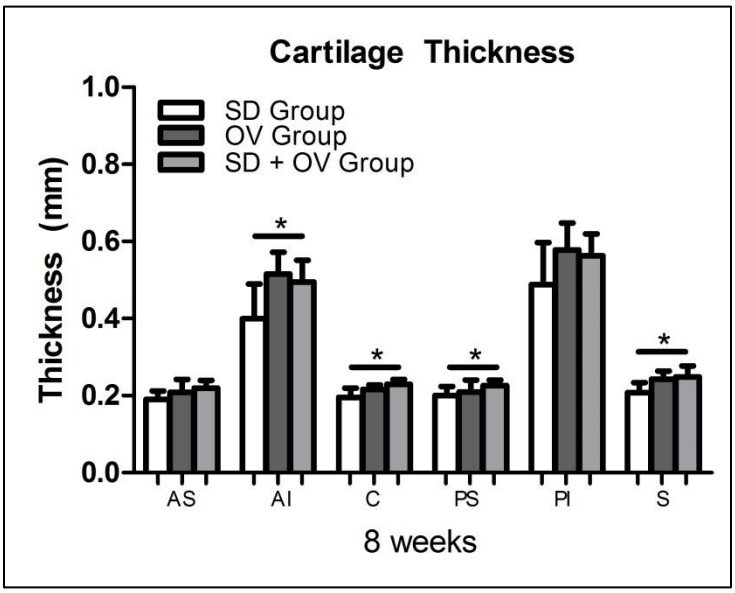

Figure 3.18. A significant increase in cartilage thickness was observed in the anterior-inferior, center, posterior-superior, and superior regions in the SD + OV group compared to SD at 8 weeks. Data shown as mean + standard deviation ($p<0.025$(OV vs. SD + OV**)). (SD=scapular dyskinesis, OV=overuse)

D. Discussion

Overhead athletes and manual laborers commonly develop scapular dyskinesis and continue performing overuse activity, potentially placing their shoulders at increased risk of injury. However, the long term consequences of continuing overuse activity in the presence of abnormal scapulothoracic joint kinematics have not been fully elucidated. Using a variety of measurements, results from this study demonstrate that overuse activity in the presence of scapular dyskinesis is detrimental to shoulder properties and that overuse activity alone has a greater effect (more parameters altered) on shoulder properties than scapular dyskinesis alone (Table 3.7). These results suggest that overuse activity in the presence of scapular dyskinesis contributes to shoulder injury.

Parameter	SD + Overuse vs.	
	SD (H1): Effect of Overuse	**Overuse (H2): Effect of SD**
Kinetic Variables		
↓Vertical force	NS	Day 5, 14, 48
↑Propulsion force	NS	All time points
↓Braking force	NS	Day 5
Medial/lateral force	NS	NS
Passive Joint Mechanics		
↓Range of Motion	Day 14, 64 (External)	Day 14 (External)
Toe Stiffness	NS	NS
Linear Stiffness	NS	NS
Tendon Mechanics		
↑Percent Relaxation	All time points (S) and at day 56 (B)	NS
↓Insertion Modulus	Day 56 (S)	NS
↓Mid Modulus	Day 56 (S+B)	Day 56 (S+B)
Tendon Histology		
↓Aspect Ratio	Day 28 (B)	Day 28 (B)
↑Aspect Ratio	Day 56 (S)	NS
↑Cell Density	NS	Day 56 (S)
↓Insertion Organization	Day 56 (S+B)	NS
↓Mid Organization	All time points (S) and at day 28 (B)	NS
Tendon Immunohistochemistry		
↑Col II	Day 28 (B)	NS
↓Col III	Day 28 (S) and at day 14 (B)	Day 56 (B)
↑Decorin	Day 28 (B)	NS
↓Decorin	Day 56 (S)	NS
↑IL1-β	NS	NS
Cartilage Properties		
↑Modulus	NS	Day 56 (1 region)
↓Thickness	Day 28 (4 regions)	NS
↑Thickness	Day 56 (4 regions)	NS

Table 3.7. Comparison of all parameters between groups (SD=scapular dyskinesis, NS=no significance, S=supraspinatus, B=biceps)

Results of this study demonstrated that overuse activity does not alter joint function (opposite H1) while scapular dyskinesis significantly alters shoulder function (consistent with H2). Specifically, no differences were observed with the addition of overuse (SD vs. SD + OV) while vertical and braking force decreased and propulsion force increased with scapular dyskinesis (OV vs. SD + OV). Propulsion and braking, which are measured in the forward flexion plane in the rat, correlate to human abduction,

which is often used as an objective measure of shoulder function. The changes in these forces are likely present due to the induced paralysis of the scapular rotators in this model (i.e., the trapezius and serratus anterior), which are particularly important in abduction, acting in coordination with the humerus, to upwardly rotate the scapula in order to achieve proper clearance of the rotator cuff under the acromion, preventing subacromial impingement. Additionally, vertical force has been used as an objective assessment of weight-bearing and pain.[8, 27] The altered loading profile placed on the shoulder joint in the presence of scapular dyskinesis may relate to functional deficits and associated pain and could have a significant effect on tendon properties. The changes due to scapular dyskinesis are similar to those previously described in Chapter 2. Alternatively, overuse activity did not diminish joint function. Therefore, we can conclude that the mechanical mechanism by which overuse activity alters tendon properties and by which scapular dyskinesis alters tendon properties are distinct.

Passive joint mechanics were significantly altered with the addition of overuse (SD vs. SD + OV). Specifically, the addition of overuse activity in the SD + OV group resulted in decreased external range of motion compared to SD alone (at two time points) and compared to OV alone (at one time point). Passive motion is often used as a clinical measure of shoulder range of motion and stiffness. Several factors can contribute to shoulder stiffness including tightening of the capsuloligamentous structures and/or surrounding musculature, rotator cuff tears, arthritis, adhesion formation, and inflammation. Shoulder range of motion in overhead athletes is typically characterized by increased external range of motion and limited internal range of motion due to stretching of the anterior capsule and tightening of the posterior capsule.[4] Surprisingly, in this

study, we observed decreased external range of motion, indicative of tightening in the anterior structures. In the presence of scapular dyskinesis, overuse activity may make it difficult for the rotator cuff to effectively maintain concavity compression of the humeral head on the glenoid fossa, leading to excessive humeral head migration and increased stress on the surrounding tendons and joint capsule. These increased stresses could result in structural adaptations in the shoulder joint, such as tightening of the tendons and capsule. The changes observed in this study could also be related to increased reliance on the surrounding muscles, such as the subscapularis, pectoralis major, teres major, or the latissimus dorsi, in response to eccentric overload and overuse of these muscles and leading to subsequent tightening. Eccentric loading has been associated with increased risk for tendon injury and muscle damage.[14] Specifically, the elastic properties of the tendon and muscle may both be diminished in response to the increased loading due to overuse. Alternatively, the addition of scapular dyskinesis in the presence of overuse (OV vs. SD + OV) had less of an effect on passive joint mechanics, except at 2 weeks post-injury. The initial insult of scapular dyskinesis may have had a significant effect on the secondary joint stabilizers, such as the joint capsule and surrounding musculature, leading to decreased range of motion. However, as both groups continued repetitive overuse activity, these changes were no longer apparent, suggesting that the effect of overuse may mask any underlying deficits due to scapular dyskinesis.

Consistent with our first hypothesis, overuse activity in the presence of scapular dyskinesis led to compromised tendon properties when compared to scapular dyskinesis alone (SD vs. SD + OV). Specifically, tendon percent relaxation was increased for both the supraspinatus and biceps tendons with the addition of overuse, consistent with

previous findings for injured tendon.[5] Additionally, supraspinatus insertion and mid-substance modulus and biceps mid-substance modulus were significantly diminished. Results for tendon organization support the mechanical changes observed. Specifically, the supraspinatus and biceps insertion and mid-substance regions were more disorganized with the addition of overuse activity. In healthy tendon, collagen fibers, the main structural component of tendon, typically align with the axis of loading. Alterations in loading (e.g. tensile, shear, compressive) could lead to a more random orientation of collagen fibers and diminish the mechanical integrity of the tendon as observed in this study (decreased viscoelastic and elastic properties). Additionally, the changes in collagen alignment may be related to microtrauma caused by mechanical compression and shear of the tendons due to repetitive excursion of the tendons under the acromion during overuse activity. Histologic changes in the tendon also supported the mechanical changes observed. Specifically, a more rounded cell shape was observed in the supraspinatus mid-substance, consistent with a tendinopathic condition and compressive and shear loading due to overuse. Cell shape is strongly associated with cellular function (e.g., maintenance, repair, and remodeling of tendon matrix) and it has been demonstrated that more elongated cells express higher collagen I (major fibrillar component in normal tendon) than rounded cells.[15] Additionally, elongated cells, which produce traction forces along their axis of loading, tend to produce more aligned collagen matrix.[38] Alternatively, more rounded chondrocyte-like cells tend to produce higher levels of collagen type II and likely deposit more disorganized collagen, as observed in this study. Cell shape was less rounded in the biceps tendon distal groove, which may

indicate increased eccentric stretching and tensile loading in this region, which does not pass under the acromial arch, with overuse.

In order to further elucidate the mechanical changes observed with overuse, protein expression was evaluated. Overuse activity resulted in increased collagen II in the biceps tendon, decreased collagen III in both the supraspinatus and biceps tendons, and decreased and increased decorin in the supraspinatus and biceps. The increased presence of collagen II in tendon may be related to changes in the mechanical loading environment observed by the tendon, leading to abnormal collagen metabolism. and resulting in the subsequent mechanical changes in the tendon at later time points. The reduction in collagen III with overuse is surprising, as the presence of collagen III in tendon has been associated with tendon microtrauma and decreased mechanical strength.[2, 6] However, in the supraspinatus and biceps, these findings were only observed early (at 4 weeks and 2 weeks, respectively) and were not present later (at 8 weeks). This alteration in collagen III is indicative of abnormal collagen metabolism. The ratio of collagen I to collagen III deposition is important in tendon and the initial decrease in collagen III may be a compensatory strategy to maintain proper coordination and synthesis of the collagen matrix. The increased decorin observed in the biceps tendon at 4 weeks may be related to the tendon's initial response to changes in the mechanical loading environment and is consistent with the increased proteoglycan content observed with tendinopathy.[9] Additionally, some in vitro studies have suggested that decorin inhibits type I collagen fibrillogenesis[23, 36] (i.e., the organization of collagen into fibrillar structures), which is important for proper tendon function and force transmission. Therefore, we can speculate that the increase in decorin which occurred at 4 weeks post-

injury may alter type I collagen fibrillogenesis, which could explain the mechanical deficits which followed at 8 weeks. The decreased decorin observed in the supraspinatus tendon at 8 weeks is consistent with mechanical changes (increased percent relaxation and decreased modulus) observed at the same time point and with previous studies that have demonstrated downregulation of decorin following tendon injury.[2, 35]

Consistent with our second hypothesis, scapular dyskinesis did further diminish tendon properties (OV vs. SD + OV). Specifically, supraspinatus and biceps mid-substance modulus were both diminished with the addition of scapular dyskinesis. However, the tendon changes due to scapular dyskinesis were not as prominent (only one mechanical parameter) as changes due to overuse (several mechanical parameters). Additionally, no differences in organization were observed with the addition of scapular dyskinesis. However, a few changes in histologic parameters (cell shape and cell density) were observed, with less rounded cell shape in the biceps distal groove and increased cell density at the supraspinatus insertion. Changes in protein were also observed with the addition of scapular dyskinesis. Specifically, decreased Collagen III was observed in the biceps tendon (OV vs. SD + OV), as similarly observed due to overuse. However, consistent with our mechanical and histological findings, immunohistochemical changes due to the addition of scapular dyskinesis were not as prominent as changes due to overuse alone. These findings indicate that overuse activity alone may have a greater effect on tendon properties than scapular dyskinesis alone.

Previous studies have demonstrated that tendon damage can be explained by two mechanically-based mechanisms: 1) tendon overuse and 2) tendon overload (i.e. abnormal joint mechanics).[26, 33] However, the association between injury due to overuse

and injury due to abnormal joint mechanics is unclear. Results from this study demonstrate that overuse activity and abnormal joint mechanics can each independently lead to tendon mechanical damage. However, the effect of overuse activity seems to be more substantial, with more parameters altered, then the effect of abnormal joint mechanics (scapular dyskinesis). It is clear that the loading profile in each of these scenarios is different, as evidenced by differences in kinetic variables, which may explain why the effect on tendon properties is different. Specifically, scapular dyskinesis significantly altered joint mechanics while overuse activity did not. However, overuse activity resulted in significantly more structural and biological adaptations (such as decreased range of motion, diminished tendon properties, and altered matrix synthesis) than scapular dyskinesis alone. Overuse activity in the presence of scapular dyskinesis may be a more significant injury due to the extreme physiological demands placed on the joint. Clinically, asymmetric scapular motion is often present in healthy subjects (absent of symptoms),[18, 20] suggesting that while scapular dyskinesis may be a risk factor, not everyone will develop significant shoulder injuries. Taken together, results from this study suggest that the risk for shoulder injury in patients with scapular dyskinesis may be higher in an active population.

Mechanical properties and geometry of the glenoid cartilage in the presence of scapular dyskinesis and overuse activity were also examined. These measurements were used to elucidate differences in loading and contact patterns. Results from this study suggest that the addition of overuse activity in the presence of scapular dyskinesis may alter joint loading, leading to differences in cartilage thickness compared to scapular dyskinesis alone. At 4 weeks, cartilage thickness was significantly decreased in several

regions, which may be indicative of cartilage wear due to overuse. However, at 8 weeks, increased cartilage thickness was observed in several regions. Some previous studies have demonstrated increased cartilage remodeling and increased cartilage thickness in response to dynamic loading.[11-13, 21, 28] We can speculate that the increased cartilage thickness may be indicative of an adaptive response due to overuse. Surprisingly, no differences were observed in cartilage equilibrium modulus (except in one region for OV vs. SD + OV), indicating that the mechanical integrity of the cartilage is maintained, despite overuse activity.

This study has several limitations. First, we acknowledge that the use of an animal model does not exactly replicate the human condition. However, the rat shoulder has been well-established as an appropriate model for rotator cuff disease.[31] Additionally, this model has been shown to reproducibly develop tendinopathy following repetitive overuse activity.[33] Second, acute transection of the spinal accessory and long thoracic nerves to induce scapular dyskinesis does not exactly mimic the clinical scenario. However, this model successfully and consistently creates scapular dyskinesis. The cause and effect relationships addressed in this clinical scenario can only be studied in an animal model where time from injury and activity level can be controlled and tissues rigorously evaluated. Finally, for this study, overuse was modeled using a well-established treadmill running protocol.[33] However, additional models of overuse, such as models of work-related tasks such as repetitive reaching[1], should be considered for future studies in order to elucidate the role of scapular dyskinesis in occupational shoulder tendon pathology. Despite these limitations, results clearly and consistently demonstrate

that overuse activity and scapular dyskinesis are detrimental to shoulder tendon properties.

Identification of overuse activity as a risk factor for shoulder injury in individuals with scapular dyskinesis will help inform and guide clinicians in developing prevention and treatment programs. Specifically, activity levels of athletes and laborers could be monitored in order to prevent permanent shoulder injury. Additionally, early detection and intervention programs can be developed, such as preventative neuromuscular training and scapular movement screens, which could assist in prevention of further detrimental changes due to scapular dyskinesis. The next chapter will examine the effect of scapular dyskinesis following rotator cuff injury and repair in order to further elucidate the mechanical processes that compromise tendon healing potential following repair.

E. References

1. Barbe MF, Barr AE, Gorzelany I, Amin M, Gaughan JP, Safadi FF. Chronic repetitive reaching and grasping results in decreased motor performance and widespread tissue responses in a rat model of MSD. *J Orthop Res.* 2003;21(1):167-176.

2. Berglund M, Reno C, Hart DA, Wiig M. Patterns of mRNA Expression for Matrix Molecules and Growth Factors in Flexor Tendon Injury: Differences in the Regulation Between Tendon and Tendon Sheath. *The Journal of Hand Surgery.* 2006;31(8):1279-1287.

3. Clarsen B, Bahr R, Andersson S, Kristensen R, Myklebust G. Risk factors for overuse shoulder injuries among male professional handball players. *Br J Sports Med.* 2014;48(7):579.

4. Crockett HC, Gross LB, Wilk KE, et al. Osseous adaptation and range of motion at the glenohumeral joint in professional baseball pitchers. *Am J Sports Med.* 2002;30(1):20-26.

5. Dourte LM, Perry SM, Getz CL, Soslowsky LJ. Tendon properties remain altered in a chronic rat rotator cuff model. *Clin Orthop Relat Res.* 2010;468(6):1485-1492.

6. Eriksen HA, Pajala A, Leppilahti J, Risteli J. Increased content of type III collagen at the rupture site of human Achilles tendon. *Journal of Orthopaedic Research.* 2002;20(6):1352-1357.

7. Gimbel JA, Van Kleunen JP, Mehta S, Perry SM, Williams GR, Soslowsky LJ. Supraspinatus tendon organizational and mechanical properties in a chronic rotator cuff tear animal model. *J Biomech.* 2004;37(5):739-749.

8. Hazewinkel HA, van den Brom WE, Theijse LF, Pollmeier M, Hanson PD. Reduced dosage of ketoprofen for the short-term and long-term treatment of joint pain in dogs. *Vet Rec.* 2003;152(1):11-14.

9. Joseph M, Maresh CM, McCarthy MB, et al. Histological and molecular analysis of the biceps tendon long head post-tenotomy. *Journal of Orthopaedic Research.* 2009;27(10):1379-1385.

10. Kibler WB, McMullen J. Scapular dyskinesis and its relation to shoulder pain. *J Am Acad Orthop Surg.* 2003;11(2):142-151.

11. Kiviranta I, Jurvelin J, Tammi M, Saamanen AM, Helminen HJ. Weight bearing controls glycosaminoglycan concentration and articular cartilage thickness in the knee joints of young beagle dogs. *Arthritis Rheum.* 1987;30(7):801-809.

12. Kiviranta I, Tammi M, Jurvelin J, Arokoski J, Saamanen AM, Helminen HJ. Articular cartilage thickness and glycosaminoglycan distribution in the canine knee joint after strenuous running exercise. *Clin Orthop Relat Res.* 1992(283):302-308.

13. Kiviranta I, Tammi M, Jurvelin J, Saamanen AM, Helminen HJ. Moderate running exercise augments glycosaminoglycans and thickness of articular cartilage in the knee joint of young beagle dogs. *J Orthop Res.* 1988;6(2):188-195.

14. LaStayo PC, Woolf JM, Lewek MD, Snyder-Mackler L, Reich T, Lindstedt SL. Eccentric muscle contractions: their contribution to injury, prevention, rehabilitation, and sport. *J Orthop Sports Phys Ther.* 2003;33(10):557-571.

15. Li F, Li B, Wang QM, Wang JH. Cell shape regulates collagen type I expression in human tendon fibroblasts. *Cell Motil Cytoskeleton.* 2008;65(4):332-341.

16. Lo YP, Hsu YC, Chan KM. Epidemiology of shoulder impingement in upper arm sports events. *Br J Sports Med.* 1990;24(3):173-177.

17. Ludewig PM, Reynolds JF. The association of scapular kinematics and glenohumeral joint pathologies. *J Orthop Sports Phys Ther.* 2009;39(2):90-104.

18. Morais NV, Pascoal AG. Scapular positioning assessment: is side-to-side comparison clinically acceptable? *Man Ther.* 2013;18(1):46-53.

19. Myers JB, Laudner KG, Pasquale MR, Bradley JP, Lephart SM. Scapular position and orientation in throwing athletes. *Am J Sports Med.* 2005;33(2):263-271.

20. Oyama S, Myers JB, Wassinger CA, Daniel Ricci R, Lephart SM. Asymmetric resting scapular posture in healthy overhead athletes. *J Athl Train.* 2008;43(6):565-570.

21. Panula HE, Hyttinen MM, Arokoski JP, et al. Articular cartilage superficial zone collagen birefringence reduced and cartilage thickness increased before surface fibrillation in experimental osteoarthritis. *Ann Rheum Dis.* 1998;57(4):237-245.

22. Peltz CD, Hsu JE, Zgonis MH, Trasolini NA, Glaser DL, Soslowsky LJ. Intra-articular changes precede extra-articular changes in the biceps tendon after rotator cuff tears in a rat model. *J Shoulder Elbow Surg.*21(7):873-881.

23. Reese SP, Underwood CJ, Weiss JA. Effects of decorin proteoglycan on fibrillogenesis, ultrastructure, and mechanics of type I collagen gels. *Matrix Biol.* 2013;32(7-8):414-423.

24. Reuther KE, Sarver JJ, Schultz SM, et al. Glenoid cartilage mechanical properties decrease after rotator cuff tears in a rat model. *J Orthop Res.* 2012;30(9):1435-1439.

25. Reuther KE, Thomas SJ, Sarver JJ, et al. Effect of return to overuse activity following an isolated supraspinatus tendon tear on adjacent intact tendons and glenoid cartilage in a rat model. *J Orthop Res.*

26. Reuther KE, Thomas SJ, Tucker JJ, et al. Disruption of the anterior-posterior rotator cuff force balance alters joint function and leads to joint damage in a rat model. *J Orthop Res.* 2014;32(5):638-644.

27. Rumph PF, Kincaid SA, Baird DK, Kammermann JR, Visco DM, Goetze LF. Vertical ground reaction force distribution during experimentally induced acute synovitis in dogs. *Am J Vet Res.* 1993;54(3):365-369.

28. Sah RL, Kim YJ, Doong JY, Grodzinsky AJ, Plaas AH, Sandy JD. Biosynthetic response of cartilage explants to dynamic compression. *J Orthop Res.* 1989;7(5):619-636.

29. Sarver JJ, Dishowitz MI, Kim SY, Soslowsky LJ. Transient decreases in forelimb gait and ground reaction forces following rotator cuff injury and repair in a rat model. *J Biomech.*43(4):778-782.

30. Sarver JJ, Peltz CD, Dourte L, Reddy S, Williams GR, Soslowsky LJ. After rotator cuff repair, stiffness--but not the loss in range of motion--increased

transiently for immobilized shoulders in a rat model. *J Shoulder Elbow Surg.* 2008;17(1 Suppl):108S-113S.

31. Soslowsky LJ, Carpenter JE, DeBano CM, Banerji I, Moalli MR. Development and use of an animal model for investigations on rotator cuff disease. *J Shoulder Elbow Surg.* 1996;5(5):383-392.

32. Soslowsky LJ, Thomopoulos S, Esmail A, et al. Rotator cuff tendinosis in an animal model: role of extrinsic and overuse factors. *Ann Biomed Eng.* 2002;30(8):1057-1063.

33. Soslowsky LJ, Thomopoulos S, Tun S, et al. Neer Award 1999. Overuse activity injures the supraspinatus tendon in an animal model: a histologic and biomechanical study. *J Shoulder Elbow Surg.* 2000;9(2):79-84.

34. Struyf F, Nijs J, Baeyens JP, Mottram S, Meeusen R. Scapular positioning and movement in unimpaired shoulders, shoulder impingement syndrome, and glenohumeral instability. *Scand J Med Sci Sports.* 2011;21(3):352-358.

35. Thomopoulos S, Hattersley G, Rosen V, et al. The localized expression of extracellular matrix components in healing tendon insertion sites: an in situ hybridization study. *J Orthop Res.* 2002;20(3):454-463.

36. Vogel KG, Paulsson M, Heinegard D. Specific inhibition of type I and type II collagen fibrillogenesis by the small proteoglycan of tendon. *Biochem J.* 1984;223(3):587-597.

37. Wadsworth DJ, Bullock-Saxton JE. Recruitment patterns of the scapular rotator muscles in freestyle swimmers with subacromial impingement. *Int J Sports Med.* 1997;18(8):618-624.

38. Wang JH, Jia F, Gilbert TW, Woo SL. Cell orientation determines the alignment of cell-produced collagenous matrix. *J Biomech.* 2003;36(1):97-102.

39. Weldon EJ, 3rd, Richardson AB. Upper extremity overuse injuries in swimming. A discussion of swimmer's shoulder. *Clin Sports Med.* 2001;20(3):423-438.

Chapter 4: Effect of Scapular Dyskinesis on Supraspinatus Tendon Healing in a Rat Model

A. Introduction

Rotator cuff tears are common conditions that often require surgical repair in order to improve function and relieve pain. Unfortunately, despite successes in relieving pain, the success associated with repair integrity has shown to be mixed, with 5-95% of patients having recurrent tears[2, 8, 10, 11, 14], and resulting in decreased strength.[25] Several factors may contribute to repair failure including age, tear size, and time from injury; however, the mechanical mechanisms behind repair failure are not well-established, making clinical management difficult. Identifying modifiable mechanical and biologic mechanisms that lead to compromised tendon healing will help improve outcomes following repair.

Tendon healing following repair does not regenerate the normal tendon-bone interface and instead creates a fibrovascular scar.[9, 21] This scar tissue is mechanically inferior to native tendon and is therefore prone to re-rupture. Several augmentation (conservative and surgical) strategies have been developed to improve healing rates and re-establish insertion architecture. Conservatively, rehabilitation protocols are typically implemented pre-operatively in an attempt to correct deficits and post-operatively in an attempt to improve healing and outcomes.[18] Surgically, biologics, such as growth factors, cytokines, and stem cells, and tissue grafting approaches have been introduced at the repair sites in an attempt to promote healing and strengthen the repair site.

Mechanical loading plays an important role in tendon-to-bone healing following repair.[29] However, the optimal loading conditions in the treatment of healing repair tissues are not well-defined. Specifically, previous studies have shown conflicting

results, regarding immobilization, passive motion, and increased loading.[3, 5, 13, 15, 16, 24] In general, low loading regimens and immobilization seems to promote healing while excessive or abnormal joint loading may have detrimental effects. The goal of pre- and post-operative rehabilitation protocols is to optimize the mechanical loading environment of the tendon and improve healing potential.

At the shoulder, abnormal scapulothoracic joint kinematics (termed scapular dyskinesis) contributes to tendon injury.[20, 22] Specifically, the abnormal loading environment in the presence of scapular dyskinesis alters the tendon composition and diminishes its mechanical properties, as observed in Chapter 2. It is likely that scapular dyskinesis is also detrimental to the supraspinatus tendon following surgical repair, compromising healing. Specifically, in the presence of scapular dyskinesis, the mechanical loading environment of the tendon is likely abnormal in both amount (i.e., overload) and type (i.e., compressive and shear) of loading, which may diminish tendon-to-bone healing potential. Abnormal joint mechanics may be one mechanical mechanism by which failed healing following cuff repair occurs.

Previous studies in the knee have demonstrated that deficits in strength and function may have negative consequences on the long term outcomes following ACL reconstruction.[7, 23] However, in the shoulder, the consequences on rotator cuff tendon healing and functional outcomes following rotator cuff repair in the presence of scapular dyskinesis have never been evaluated. Current treatment options for managing scapular dyskinesis include rehabilitation strategies[4, 18, 19] to re-educate and establish proper neuromuscular control of the scapular muscles and correct positional abnormalities. Successful pre-operative scapular rehabilitation may be necessary in order to achieve

successful outcomes post-operatively. However, the benefits of correcting scapular deficits prior to rotator cuff repair are unknown.

Therefore, the objective of this study was to determine the effect of scapular dyskinesis on supraspinatus tendon to bone healing following tendon repair. We hypothesized that scapular dyskinesis will result in H1) diminished joint function and passive joint mechanics and H2) decreased supraspinatus tendon to bone healing following tendon repair due to the compromised mechanical environment present during healing.

B. Methods

Study Design. A rat model was used in this Institutional Animal Care and Use Committee (IACUC) approved study. Seventy male Sprague Dawley rats (400-450 g) were randomized into 2 groups: nerve transection to create scapular dyskinesis (SD, N=35) or sham nerve transection (Control, N=35). For the nerve transection surgery, the spinal accessory and long thoracic nerves were visualized and transected, as previously described. For the sham nerve transection surgery, the nerves were visualized but were not transected. Following this procedure, all rats underwent unilateral detachment and repair of the supraspinatus tendon, as previously described. Pre- and post-operative analgesics (buprenorphine, 0.05 mg/kg) were administered up to 2 days following surgery. Animals then returned to unrestricted cage activity and were sacrificed 2, 4, and 8 weeks following surgery and either frozen (for mechanical testing at 4 and 8 weeks, N=10) or fixed in formalin (for histology and immunohistochemistry at each time point, N=5)

Detachment and Repair Surgery. For the detachment and repair surgery, surgical exposure of the tendon was achieved as follows. A 2 cm skin incision was made over the craniolateral aspect of the scapulohumeral joint, followed by dissection, through the deltoid, down to the rotator cuff musculature. The rotator cuff tendons were identified as the subscapularis (the most anterior and broadest rotator cuff tendon), the supraspinatus (the tendon that passes under the bony arch created by the acromion, coracoid, and clavicle), and the infraspinatus (posterior to the other tendons with a similar insertion to the supraspinatus). After the tendons were identified, the supraspinatus was grasped using a 5-0 polypropylene suture (Surgipro II, Covidien, Mansfield, MA) using a grasping suture technique and detached at its insertion point on the humerus using a sharp blade and allowed to freely retract. For repair, a 5mm diameter high speed burr (Multipro 395, Dremel, Mt. Prospect, IL) was then used to remove any remaining fibrocartilage at the insertion site. A 0.5 mm anterior/posterior hole is drilled through the humerus just below the insertion site. Suture was then secured through the bone tunnel and the tendon was then reapposed to the insertion site. Closure was achieved by suturing the deltoid muscle and the skin was closed using staples.

Quantitative Ambulatory Assessment. Forelimb ground reaction forces (medial/lateral, braking, propulsion, and vertical) and spatio-temporal parameters (step width, stride length, speed) were quantified using an instrumented walkway, as described previously.[26] The system consists of two 6 degree-of-freedom load cells incorporated into a walkway. Rats were acclimated to walk freely along the instrumented walkway over a period of 1 week prior to formal recording of ambulatory data. Data was collected one

day prior to surgery to obtain baseline, uninjured values and then collected at days 5, 7, 14, 28, 42, and 56 following surgery. All data was normalized by body-weight.

Passive Joint Mechanics. Passive range of motion measurements were performed utilizing the instruments and methodology, as previously described.[27] Data was collected one day prior to surgery to obtain baseline, uninjured values and then at 2, 4, and 8 weeks following surgery. Under anesthesia, the forelimb was secured into the rotating clamp at 90° of elbow flexion and 90° of glenohumeral forward flexion. The scapula was manually stabilized to isolate glenohumeral motion and prevent scapulothoracic motion. The forelimb was then rotated through full range of internal and external rotation three times. The ROM was calculated as the difference in the average of three measures of maximal internal and external rotation. A bilinear fit utilizing least-squares optimization was applied to calculate joint stiffness in the toe and linear regions in both directions. All data was normalized to baseline values.

Sample Preparation for Mechanical Testing. At the time of testing, the animals were thawed and the humerus was dissected out with the supraspinatus tendon intact. The tendon was fine dissected under a microscope to remove muscle and any excess, non-loadbearing tissue near the repaired insertion site. Cross-sectional area was measured using a custom laser device.[28]

Tendon Mechanical Testing. Elastic and viscoelastic mechanical properties of the supraspinatus tendon were determined using uniaxial tensile testing, as previously described.[12] Verhoeff stain lines were placed along the length of each tendon to divide the insertion and mid-substance regions for local optical strain measurements. The humerus were embedded in a holding fixture using polymethylmethacrylate (PMMA) and

inserted into a custom testing fixture. The proximal end of the tendon was gripped with cyanocrylate annealed sand paper in custom grips. The specimen was immersed in PBS at 37°C during testing. Tensile testing of the tendon was performed as follows: preconditioning for 10 cycles from 0.1 N to 0.5 N, stress relaxation to 5% strain at a rate of 5 %/sec for 600 sec, and ramp to failure at 0.3%/sec. Stress was calculated as force divided by initial area and 2D Lagrangian strain was determined from the stain line displacements, using custom texture tracking software. Elastic properties were calculated using a linear regression from the linear region of the stress-strain curves. For viscoelastic parameters, percent relaxation was determined using the peak and equilibrium loads.

Tendon Histology. Histologic analysis was performed to examine cellular and organizational changes in the supraspinatus tendon. Tissues were harvested immediately after sacrifice and processed using standard paraffin procedures. Sagittal sections (7 um) were collected, and stained with Hematoxylin–Eosin (H&E). Stained supraspinatus tendon sections were imaged at the insertion site and mid-substance using a microscope at 200X and 100X magnification using traditional and polarized light, respectively. Cell density and cell shape were independently graded by three blinded investigators, who were provided with previously prepared standard images, using a scale of 1-3 (1=low, 2= moderate, 3=high) for cellularity and 1-3 (1=spindle shaped, 2= mixed, 3= rounded) for cell shape. Polarized light images were analyzed using custom software to evaluate tendon organization, as previously described.[12] The angular deviation (AD) of the collagen orientation for each specimen (a measure of the fiber distribution spread) was calculated in each tendon location.

Tendon Immunohistochemistry. The distribution of ECM proteins was localized using immunohistochemical techniques. The same tissue specimens from histology were used and stained for collagens type II and III, the proteoglycan decorin, and the inflammatory marker, IL1-β (Table 4.1). The proteins were visualized using DAB, making the antibody-protein conjugate turn brown. The insertion site and mid-substance of each tendon were evaluated separately. Staining results were independently graded by three blinded investigators, who were provided with previously prepared standard images, using a scale of 0-3 (0=undetectable, 1=low, 2=medium, 3=high), and the mode was used as the final score.

Table 4.1. Antibodies used for immunohistochemical staining

Protein Target	Antibody	Host	Type	Enzyme pretreatment	Dilution	Incubation period (h)	Source
Collagen II	II-116B3	Mouse	Monoclonal	Hyaluronidase	1:4	16	DSHB, Iowa City, IA, USA
Collagen III	c7805	Mouse	Monoclonal	Hyaluronidase	1:500	38	Sigma, St. Louis, MO, USA
Decorin	LF-113	Rabbit	Polyclonal	Chondroitinase ABC	1:300	38	L. Fisher, Bethesda, MD, USA
IL1-β	AB1832	Rabbit	Polyclonal	Pepsin	1:250	16	Millipore, Billerica, MA, USA

Statistical Analysis. For the ambulatory assessment, multiple imputations were conducted using the Markov chain Monte Carlo method for missing data points (~10%). For both ambulatory assessment and passive joint mechanics, significance was assessed using a 2-way ANOVA with repeated measures on time with follow-up t-tests between groups at each time point. Tissue mechanics between groups were assessed using a t-test. Histology and immunohistochemistry scores were evaluated using a Mann-Whitney test. Significance was set at $p<0.05$, trends at $p<0.1$.

C. Results

Ambulatory Data. Shoulder joint function was significantly altered in the SD group compared to control. Specifically, propulsion force was significantly increased in the SD group compared to control at nearly every time point, except 5 days post-injury (Figure 4.1). Braking force was significantly decreased in the SD group compared to control at 6 and 8 weeks post-injury (Figure 4.2). No differences in vertical or medial/lateral forces were observed between groups (Figure 4.3, 4.4). No significant differences in spatio-temporal parameters (step width, stride length, or speed) were observed between groups.

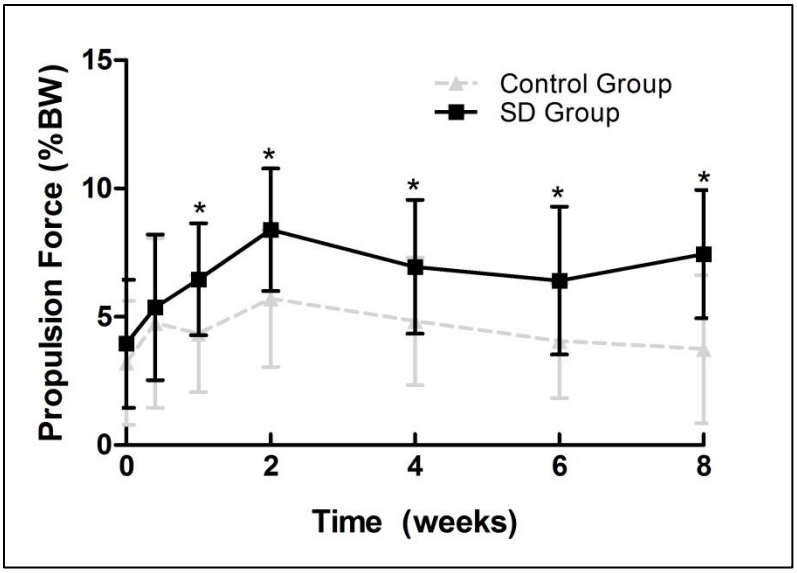

Figure 4.1. Propulsion force was significantly increased in the SD group compared to control. Data shown as mean ± standard deviation (*p<0.05). (SD=scapular dyskinesis)

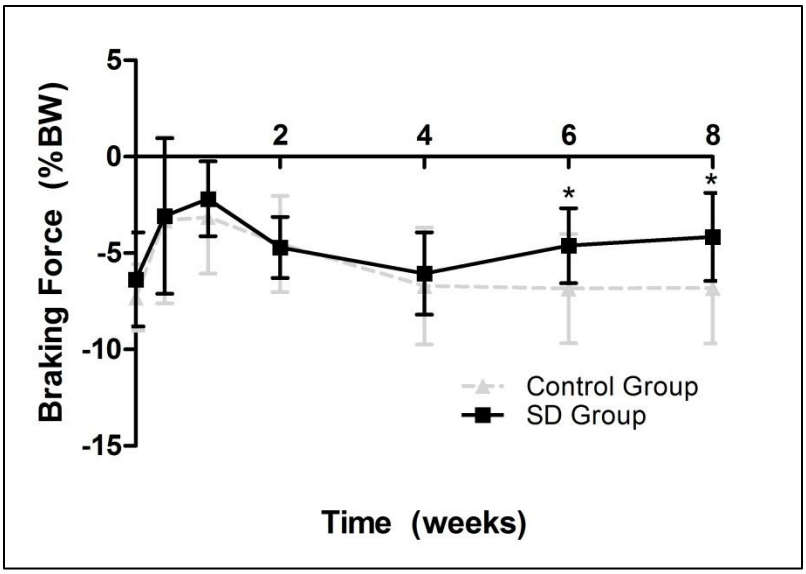

Figure 4.2. Braking force was significantly decreased in the SD group compared to control at 6 and 8 weeks. Data shown as mean ± standard deviation (*p<0.05). (SD=scapular dyskinesis)

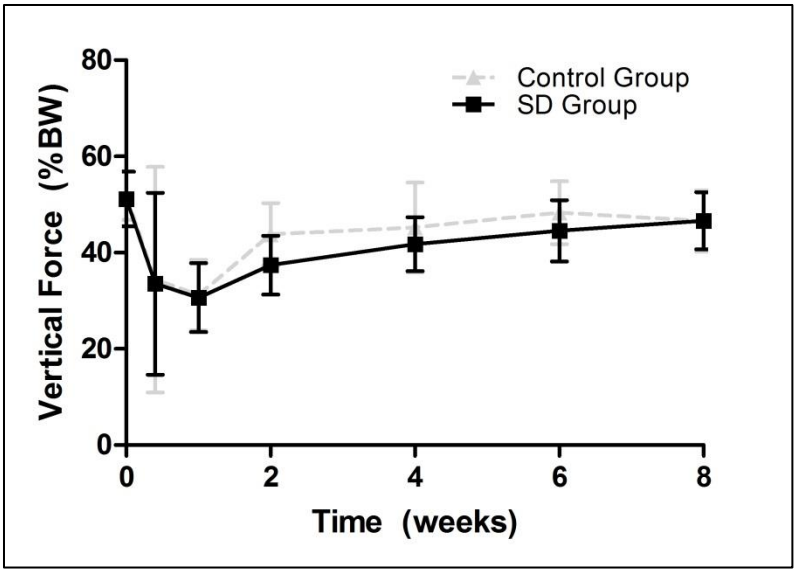

Figure 4.3. No differences in vertical ground reaction force was observed between groups. Data shown as mean ± standard deviation. (SD=scapular dyskinesis)

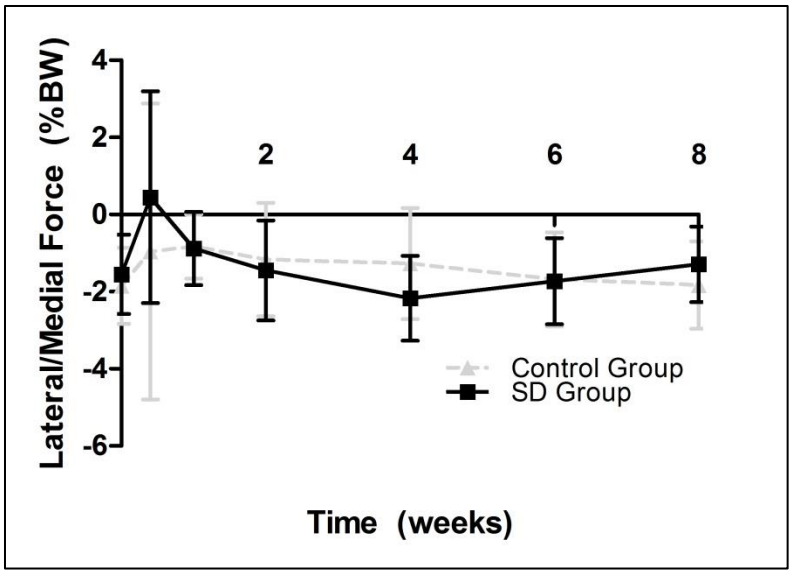

Figure 4.4. No differences in medial-lateral ground reaction force was observed between groups. Data shown as mean ± standard deviation. (SD=scapular dyskinesis)

Passive Joint Mechanics. No differences in passive joint mechanics were observed between groups at any time point (Table 4.2).

Direction	Measurement	Time (wks)	Control	SD
Internal	ROM (degrees)	2	-15.09 ±20.77	-9.46 ±15.79
		4	-16.19 ±12.46	-10.30 ±11.51
		8	-13.55 ±14.71	-10.93 ±17.84
	Toe Stiffness (N/mm)	2	0.07±0.10	0.07±0.16
		4	0.10±0.14	0.10±0.12
		8	0.10±0.16	0.12±0.14
	Linear Stiffness (N/mm)	2	0.35±0.14	0.30±0.43
		4	0.43±0.25	0.43±0.20
		8	0.57±0.39	0.58±0.38
External	ROM (degrees)	2	-15.33 ±16.73	-14.41 ±20.01
		4	-18.59 ±17.69	-18.63 ±16.43
		8	-25.99 ±16.36	-27.93 ±27.79
	Toe Stiffness (N/mm)	2	0.08±0.24	0.07±0.22
		4	0.03±0.22	0.01±0.13
		8	0.06±0.19	0.07±0.18
	Linear Stiffness (N/mm)	2	0.10±0.15	0.01±0.17
		4	0.19±0.21	0.14±0.22
		8	0.26±0.34	0.18±0.29

Table 4.2. No differences in passive joint mechanics were observed between groups at any time point. Data shown as mean ± standard deviation and normalized from baseline (change from baseline). (SD=scapular dyskinesis)

Tendon Mechanics. Mechanical properties were altered in the SD group compared to control for some parameters. Specifically, insertion cross-sectional area was significantly decreased in the SD group compared to control at 4 weeks, with a similar trend at the tendon mid-substance (Figure 4.5, 4.6). No differences in insertion elastic modulus or stiffness were observed between groups (Figure 4.7, 4.8). Mid-substance elastic modulus and stiffness were significantly decreased in the SD group compared to control at 4 weeks (Figure 4.9). However, a trend toward increased stiffness was observed at the mid-substance in the SD group compared to control at 8 weeks (Figure

4.10). No differences in maximal load were observed (Figure 4.11). For viscoelastic properties, a trend toward increased percent relaxation in the SD group compared to control was observed at 8 weeks post-injury (Figure 4.12).

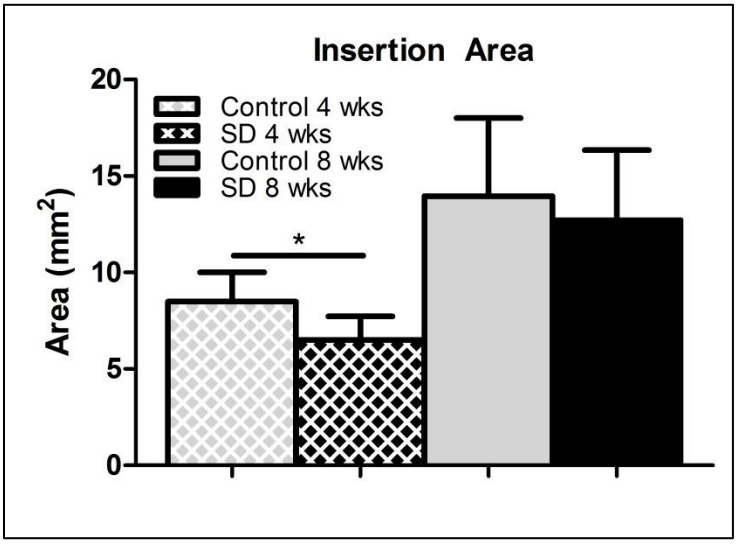

Figure 4.5. Insertion cross-sectional area was significantly decreased in the SD group compared to control at 4 weeks. Data shown as mean + standard deviation (*$p<0.05$). (SD=scapular dyskinesis)

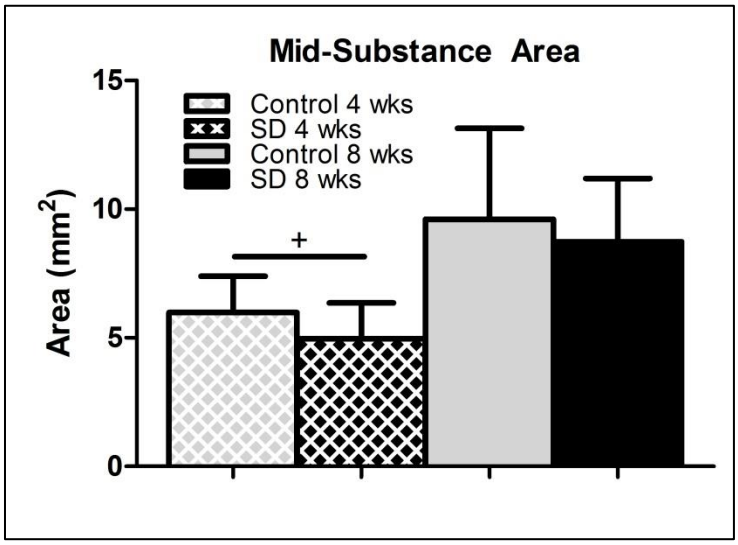

Figure 4.6. A trend toward decreased mid-substance cross-sectional area was observed in the SD group compared to control at 4 weeks. Data shown as mean + standard deviation ($^{+}p<0.1$). (SD=scapular dyskinesis)

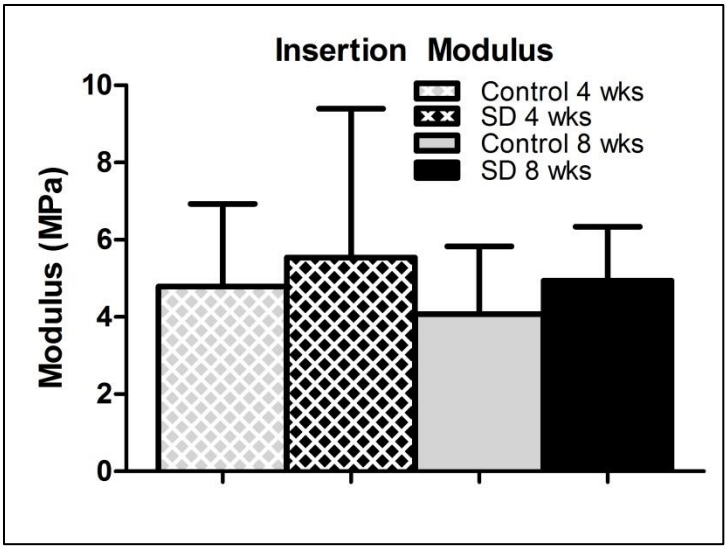

Figure 4.7. No differences in insertion elastic modulus were observed between groups. Data shown as mean + standard deviation. (SD=scapular dyskinesis)

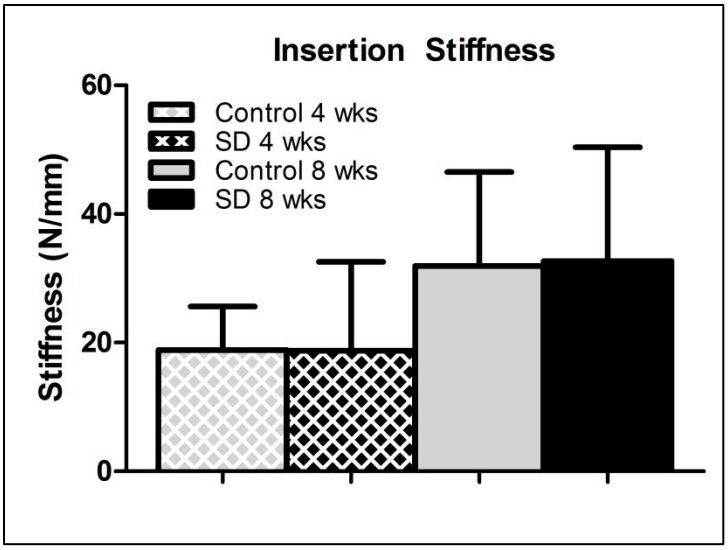

Figure 4.8. No differences in insertion stiffness were observed between groups. Data shown as mean + standard deviation. (SD=scapular dyskinesis)

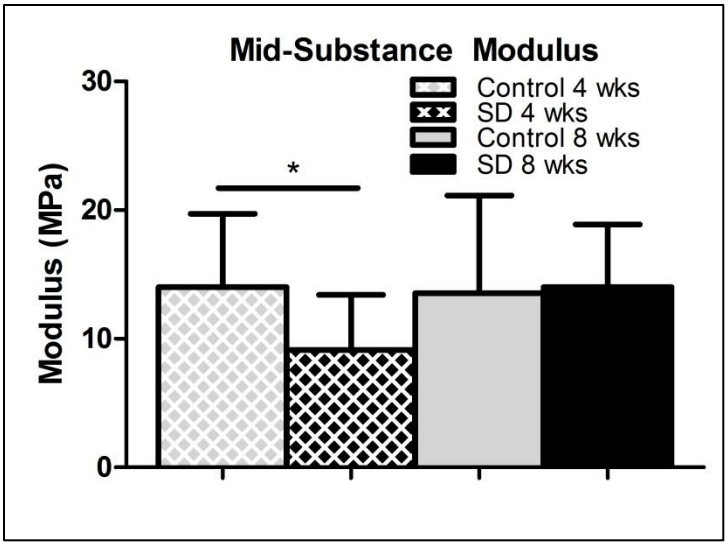

Figure 4.9. Mid-substance modulus was significantly decreased in the SD group compared to control at 4 weeks. Data shown as mean + standard deviation (*$p<0.05$). (SD=scapular dyskinesis)

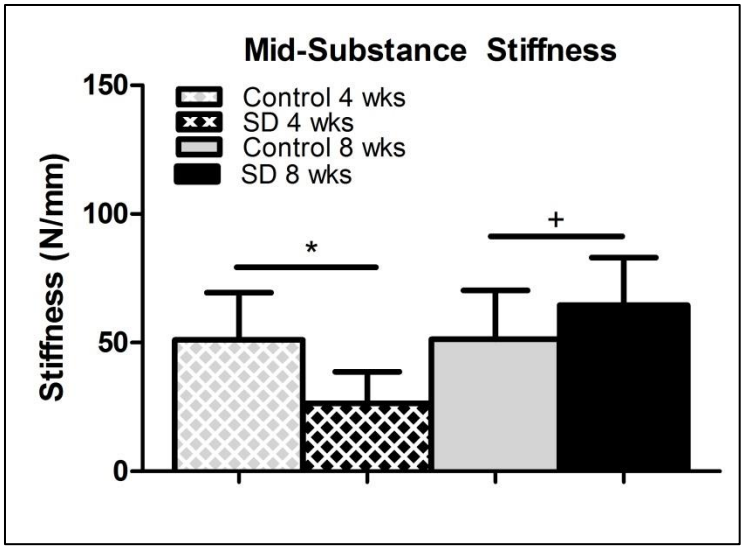

Figure 4.10. Mid-substance stiffness was significantly decreased in the SD group compared to control at 4 weeks, with an opposite trend at 8 weeks. Data shown as mean + standard deviation (*$p<0.05$, $^{+}p<0.1$). (SD=scapular dyskinesis)

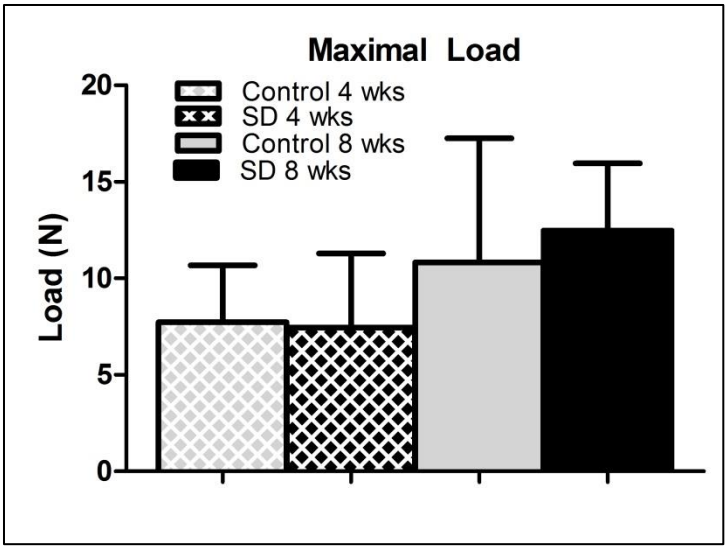

Figure 4.11. No differences in maximal load were observed between groups. Data shown as mean + standard deviation. (SD=scapular dyskinesis)

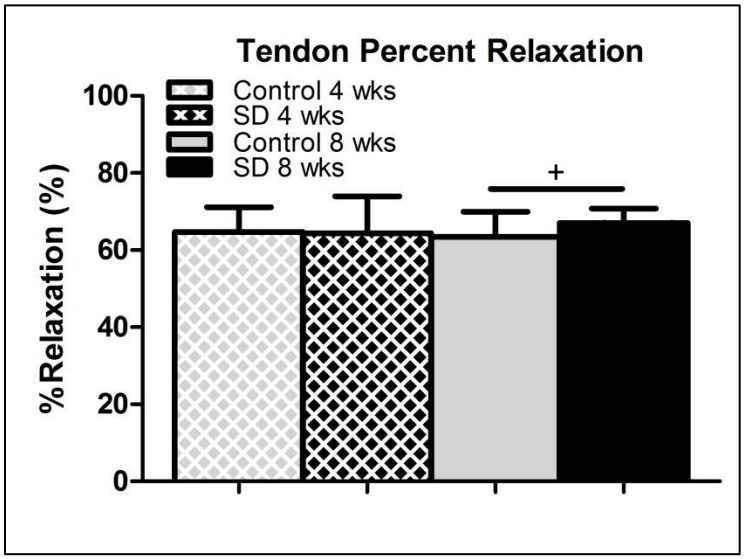

Figure 4.12. A trend toward increased percent relaxation was observed in the SD group compared to control. Data shown as mean + standard deviation ($^{+}p<0.1$). (SD=scapular dyskinesis)

Tendon Histology. No differences in cellularity were observed between groups (Table 4.3). A trend toward a more rounded cell shape was observed at the supraspinatus insertion in the SD group compared to control at 4 weeks. No differences in organization were observed at the supraspinatus insertion (Figure 4.13). A trend toward increased

angular deviation (greater disorganization) was observed at the supraspinatus mid-substance in the SD group compared to control at 2 weeks (Figure 4.14)

Histology	Group	Region	2 weeks	4 weeks	8 weeks
Cell Shape	SD	INS	1 (1-2)	2 (2-2) +	2 (2-2)
	Control		2(2-2)	1 (1-1)	2 (1.75-2)
	SD	MID	2 (1.75-2)	2 (2-2)	3 (2-3)
	Control		2 (1-2)	2 (2-2)	2 (2-3)
Cell Density	SD	INS	2 (2-3)	3 (2-3)	2 (1-2)
	Control		2 (2-3)	3 (2-3)	2 (1-3)
	SD	MID	3 (3-3)	3(3-3)	2 (2-2)
	Control		3(3-3)	3(2-3)	2 (2-3)

Table 4.3. A trend toward more rounded cell shape was observed in the SD group compared to control at 4 weeks. Data shown as median and interquartile range ($^{+}p<0.1$). (SD=scapular dyskinesis)

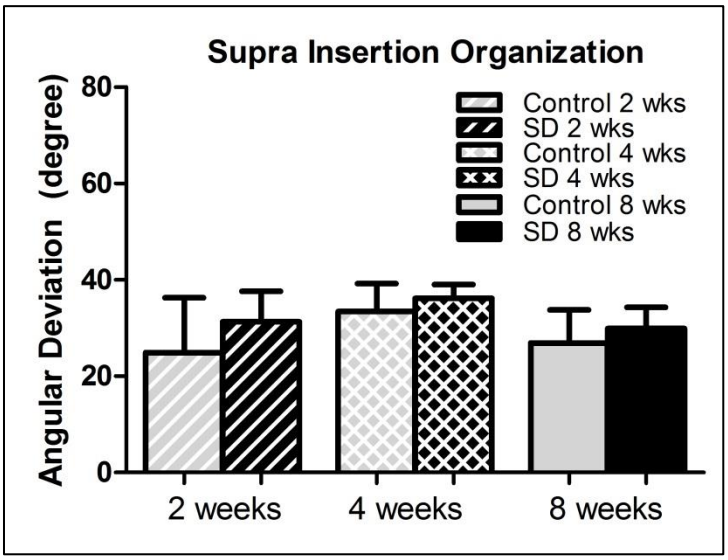

Figure 4.13. No differences in supraspinatus insertion organization were observed at any time point. Data shown as mean + standard deviation. (SD=scapular dyskinesis)

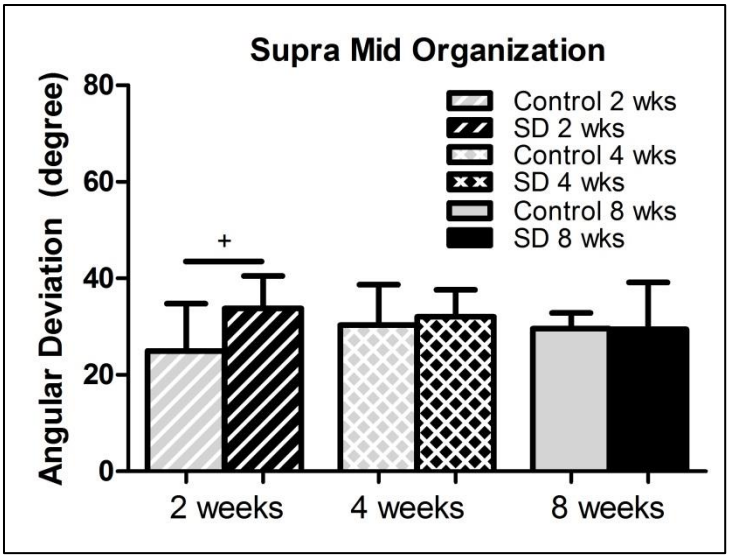

Figure 4.14. A trend toward increased angular deviation was observed in the supraspinatus mid-substance at 2 weeks. Data shown as mean + standard deviation ($^{+}p<0.1$). (SD=scapular dyskinesis)

Tendon Immunohistochemistry. No differences were observed at any time point or in any region (Table 4.4).

Tendon	Group	Region	Col II			Col III			Decorin			IL1-β		
			2 weeks	4 weeks	8 weeks	2 weeks	4 weeks	8 weeks	2 weeks	4 weeks	8 weeks	2 weeks	4 weeks	8 weeks
Supra	SD	INS	3(2-3)	1(1-1)	1(0-1)	3 (1-3)	1 (0-2)	1 (1-2)	1 (0-1)	2 (2-2)	2 (1-2)	2 (1.5-2)	2 (1-3)	1 (1-2)
	Control		2(2-2)	0(0-1)	0(0-2)	3 (2-3)	2.5 (1.5-3)	1 (1-2)	1 (0-1)	2 (2-3)	2 (1.75-2)	2 (2-2)	3 (3-3)	2 (1.75-2.25)
	SD	MID	1(1-3)	0(0-0)	1(0-1)	1 (1-2)	1 (0-2)	1 (1-2)	0 (0-1)	2 (1-2)	1 (1-2)	2 (1.5-2)	2 (2-3)	2 (2-2)
	Control		1(1-1)	0(0-0)	1(1-1)	2 (2-3)	1 (1-2)	2 (2-3)	0 (0-1)	1 (1-2)	1.5 (1-2.25)	1 (1-2)	3 (3-3)	2 (1.75-2.25)

Table 4.4 No differences were observed at any time point or in any region.
(SD=scapular dyskinesis)

D. Discussion

While the prevalence of rotator cuff repair failures is well-documented, the mechanical mechanisms by which failure occurs are not well-established, making clinical management difficult. Previous studies have also demonstrated a strong association between abnormal scapulothoracic joint kinematics (termed scapular dyskinesis) and shoulder injury. Using this animal model, we were able to prescribe scapular dyskinesis and rigorously evaluate the effect on supraspinatus tendon healing following cuff repair.

Consistent with our first hypothesis, scapular dyskinesis significantly altered joint function. Specifically, propulsion force was significantly increased in the SD group compared to control while braking force was significantly decreased at later time points. These changes indicate an alteration in the loading environment at the shoulder due to scapular dyskinesis and may place the healing supraspinatus tendon at risk for injury. These findings are consistent with but less dramatic than our previous findings that have also identified significant changes in joint function in propulsion force and in additional parameters (i.e., vertical ground reaction force) due to scapular dyskinesis. A higher propulsion force may place increased stresses on the healing supraspinatus, compromising the mechanical integrity of the repair. Decreased braking force, which was observed only at later time points, may be indicative of a functional adaptation to prevent further damage. As stated in Chapter 3, propulsion and braking, correlate to human abduction, which is often used as an objective measure of shoulder function. During forward locomotion, the rat undergoes large amounts of forward flexion (which correlates with human abduction), requiring large amounts of rotation by both the humerus and scapula at the shoulder joint. In this scapular dyskinesis model, the scapular

rotators (i.e., trapezius and serratus anterior) are not functioning and the scapula is unable to rotate, which likely led to these alterations in braking and propulsion forces. Changes in medial/lateral forces, which correlate to internal and external rotation, were not observed, indicating that the serratus anterior and trapezius are not involved in these motions in this animal model. Interestingly, no changes in vertical forces were observed, as in Chapter 2 and 3. This is likely because vertical force corresponds to weight-bearing and pain and it is likely that the effect of the repair surgery on pain was greater than the effect of scapular dyskinesis on function, masking any underlying alterations due to scapular dyskinesis. Loading environment is important in healing tissues and can differ in amount/magnitude (i.e., immobilization, exercise, overuse) and type (i.e., tensile, compressive, shear). In this study, scapular dyskinesis likely alters the type of loading the tendon experiences, thus altering the mechanical integrity of the healing tendon.

Contrary to our first hypothesis, scapular dyskinesis had no effect on passive joint mechanics. Previous studies have demonstrated that increased stiffness and decreased range of motion is observed following cuff repair.[27] This may be attributed to scar formation in the healing tissue and joint capsule or muscular adaptations in response to the repair surgery. While tendon stiffening, capsular tightening, and muscular dysfunction are likely to contribute to changes in glenohumeral joint stiffness and range of motion, the excessive scar formation present following repair surgery may mask these underlying issues and therefore changes in passive joint mechanics between groups were not identified. It is likely that the surgical repair has a greater effect on passive joint mechanics than the effect of scapular dyskinesis. If followed at later time points, the

groups would likely deviate, in response to changes in joint function as observed at later time points.

Consistent with our second hypothesis, scapular dyskinesis was detrimental to supraspinatus tendon mechanical properties for some parameters. Specifically, mid-substance modulus was significantly diminished at 4 weeks in the SD group compared to control. However, this change did not persist at 8 weeks. Additionally, a trend toward a more rounded cell shape was observed in the supraspinatus mid-substance at 4 weeks, which may be indicative of compressive loading and is consistent with the mechanical changes observed at this time point. In this region, tendon organization was also more disorganized in the SD group compared to control at 2 weeks. The location specific tendon changes (mid-substance region) are similar to findings observed previously in the supraspinatus tendon in the presence of scapular dyskinesis (Chapter 2) and may be due to its anatomic location under the acromial arch during forward flexion, resulting in impingement and an altered loading environment. Surprisingly, decreased cross-sectional area was observed in the SD group compared to control at 4 weeks. This finding may be related to the reduced subacromial space present in the SD group due to the diminished upward rotation of the scapula, allowing less space for tissue proliferation and matrix production. This finding did not persist at 8 weeks and an improvement in tissue elasticity is apparent (no difference in elastic modulus). This may be related to the compensatory decrease in braking force observed at later time points (6 and 8 weeks), reducing stress on the repair site and preserving mechanical properties. However, a trend toward increased percent relaxation (a viscoelastic parameter) was observed in the SD group compared to control at 8 weeks post-injury. Previous studies have found increased

percent relaxation in injured tendon, indicative of inferior tissue properties and poor healing.[1, 6] Specifically, increased percent relaxation is associated with increased water content and altered proteoglycan composition. Contrary to our first hypothesis, no differences were observed in insertion modulus or maximal load. While insertion modulus may be an indicator of tendon healing, we have observed previously that scapular dyskinesis has no effect on insertion site properties (Chapter 2). Additionally, while maximal load is an important indicator of repair strength, the typical loads at which the supraspinatus operates is not near this threshold. Material properties, such as elastic modulus and percent relaxation, which highlight the quality of the tissue, may be a better indicator of repair integrity and functionality then maximal load at failure. In general, these findings indicate that there may be mechanical consequences associated with poor scapulothoracic joint kinematics for the healing supraspinatus tendon following repair.

Interestingly, no differences in tendon composition were identified. Tendon healing is characterized by a reactive scar formation and involves excessive inflammation, cell proliferation, and increased matrix synthesis characterized by increased deposition of type III collagen.[17] This heightened response to tendon injury and repair may mask any effect of scapular dyskinesis in this study. As observed with passive joint mechanics, surgical repair may have a greater effect on tendon composition than the effect of scapular dyskinesis.

This study has several limitations. First, the use of a quadruped animal does not exactly replicate the human shoulder. However, the presence of the acromial arch and its position over the rotator cuff is similar to the human shoulder and is essential in our model to evaluate the effect of scapular dyskinesis on the supraspinatus as it passes

underneath it. Secondly, in this study, we examined 4 proteins, collagens type II and III, decorin, and IL1-β, and did not identify any differences. However, additional proteins, such as collagen I, aggrecan, and TNF-α, should be evaluated in order to more fully characterize changes in composition due to scapular dyskinesis. In particular, the ratio of collagen III to collagen I, may be elevated in the group with scapular dyskinesis, implying poor matrix synthesis and compromised tendon healing. Thirdly, acute transection of the supraspinatus tendon and immediate repair does not exactly replicate the human condition. Specifically, rotator cuff tears are typically chronic in nature. However, using an acute transection and repair allows us to examine the mechanical and biologic healing response in a more controlled manner.

In summary, results from this study suggest the functional consequences associated with scapular dyskinesis may compromise supraspinatus tendon healing following repair by diminishing tendon mechanical properties. Identification of abnormal joint mechanics as a potential mechanical mechanism of failed rotator cuff healing will help guide clinicians in prescribing treatment strategies for patients with cuff tears. This study supports the need to evaluate joint kinematics prior to rotator cuff repair and possibly correct any abnormalities prior to surgical repair. This may allow for optimization of the mechanical loading environment and improve tendon healing rates.

E. References

1. Abramowitch SD, Woo SL, Clineff TD, Debski RE. An evaluation of the quasi-linear viscoelastic properties of the healing medial collateral ligament in a goat model. *Ann Biomed Eng.* 2004;32(3):329-335.

2. Bigliani LU, Cordasco FA, McIlveen SJ, Musso ES. Operative treatment of failed repairs of the rotator cuff. *J Bone Joint Surg Am.* 1992;74(10):1505-1515.

3. Brophy RH, Kovacevic D, Imhauser CW, et al. Effect of short-duration low-magnitude cyclic loading versus immobilization on tendon-bone healing after ACL reconstruction in a rat model. *J Bone Joint Surg Am.* 2011;93(4):381-393.

4. Burkhart SS, Morgan CD, Kibler WB. The disabled throwing shoulder: spectrum of pathology Part III: The SICK scapula, scapular dyskinesis, the kinetic chain, and rehabilitation. *Arthroscopy.* 2003;19(6):641-661.

5. Dagher E, Hays PL, Kawamura S, Godin J, Deng XH, Rodeo SA. Immobilization modulates macrophage accumulation in tendon-bone healing. *Clin Orthop Relat Res.* 2009;467(1):281-287.

6. Dourte LM, Perry SM, Getz CL, Soslowsky LJ. Tendon properties remain altered in a chronic rat rotator cuff model. *Clin Orthop Relat Res.* 2010;468(6):1485-1492.

7. Eitzen I, Holm I, Risberg MA. Preoperative quadriceps strength is a significant predictor of knee function two years after anterior cruciate ligament reconstruction. *Br J Sports Med.* 2009;43(5):371-376.

8. Galatz LM, Ball CM, Teefey SA, Middleton WD, Yamaguchi K. The outcome and repair integrity of completely arthroscopically repaired large and massive rotator cuff tears. *J Bone Joint Surg Am.* 2004;86-A(2):219-224.

9. Galatz LM, Sandell LJ, Rothermich SY, et al. Characteristics of the rat supraspinatus tendon during tendon-to-bone healing after acute injury. *J Orthop Res.* 2006;24(3):541-550.

10. Gazielly DF, Gleyze P, Montagnon C. Functional and anatomical results after rotator cuff repair. *Clin Orthop Relat Res.* 1994(304):43-53.

11. Gerber C, Fuchs B, Hodler J. The results of repair of massive tears of the rotator cuff. *J Bone Joint Surg Am.* 2000;82(4):505-515.

12. Gimbel JA, Van Kleunen JP, Mehta S, Perry SM, Williams GR, Soslowsky LJ. Supraspinatus tendon organizational and mechanical properties in a chronic rotator cuff tear animal model. *J Biomech.* 2004;37(5):739-749.

13. Gimbel JA, Van Kleunen JP, Williams GR, Thomopoulos S, Soslowsky LJ. Long durations of immobilization in the rat result in enhanced mechanical properties of the healing supraspinatus tendon insertion site. *J Biomech Eng.* 2007;129(3):400-404.

14. Harryman DT, 2nd, Mack LA, Wang KY, Jackins SE, Richardson ML, Matsen FA, 3rd. Repairs of the rotator cuff. Correlation of functional results with integrity of the cuff. *J Bone Joint Surg Am.* 1991;73(7):982-989.

15. Hettrich CM, Gasinu S, Beamer BS, et al. The effect of immobilization on the native and repaired tendon-to-bone interface. *J Bone Joint Surg Am.* 2013;95(10):925-930.

16. Hettrich CM, Gasinu S, Beamer BS, et al. The Effect of Mechanical Load on Tendon-to-Bone Healing in a Rat Model. *Am J Sports Med.* 2014.

17. James R, Kesturu G, Balian G, Chhabra AB. Tendon: biology, biomechanics, repair, growth factors, and evolving treatment options. *J Hand Surg Am.* 2008;33(1):102-112.

18. Kibler WB. The role of the scapula in athletic shoulder function. *Am J Sports Med.* 1998;26(2):325-337.

19. Kibler WB, McMullen J. Scapular dyskinesis and its relation to shoulder pain. *J Am Acad Orthop Surg.* 2003;11(2):142-151.

20. Kibler WB, Sciascia A, Wilkes T. Scapular dyskinesis and its relation to shoulder injury. *J Am Acad Orthop Surg.*20(6):364-372.

21. Killian ML, Cavinatto L, Galatz LM, Thomopoulos S. The role of mechanobiology in tendon healing. *J Shoulder Elbow Surg.* 2012;21(2):228-237.

22. Ludewig PM, Reynolds JF. The association of scapular kinematics and glenohumeral joint pathologies. *J Orthop Sports Phys Ther.* 2009;39(2):90-104.

23. McHugh MP, Tyler TF, Gleim GW, Nicholas SJ. Preoperative indicators of motion loss and weakness following anterior cruciate ligament reconstruction. *J Orthop Sports Phys Ther.* 1998;27(6):407-411.

24. Peltz CD, Sarver JJ, Dourte LM, Wurgler-Hauri CC, Williams GR, Soslowsky LJ. Exercise following a short immobilization period is detrimental to tendon properties and joint mechanics in a rat rotator cuff injury model. *J Orthop Res.* 2010;28(7):841-845.

25. Russell RD, Knight JR, Mulligan E, Khazzam MS. Structural integrity after rotator cuff repair does not correlate with patient function and pain: a meta-analysis. *J Bone Joint Surg Am.* 2014;96(4):265-271.

26. Sarver JJ, Dishowitz MI, Kim SY, Soslowsky LJ. Transient decreases in forelimb gait and ground reaction forces following rotator cuff injury and repair in a rat model. *J Biomech.*43(4):778-782.

27. Sarver JJ, Peltz CD, Dourte L, Reddy S, Williams GR, Soslowsky LJ. After rotator cuff repair, stiffness--but not the loss in range of motion--increased transiently for immobilized shoulders in a rat model. *J Shoulder Elbow Surg.* 2008;17(1 Suppl):108S-113S.

28. Struyf F, Nijs J, Baeyens JP, Mottram S, Meeusen R. Scapular positioning and movement in unimpaired shoulders, shoulder impingement syndrome, and glenohumeral instability. *Scand J Med Sci Sports.* 2011;21(3):352-358.

29. Thomopoulos S, Williams GR, Soslowsky LJ. Tendon to bone healing: differences in biomechanical, structural, and compositional properties due to a range of activity levels. *J Biomech Eng.* 2003;125(1):106-113.

Chapter 5: Conclusion and Future Directions

A. Introduction

The established rat rotator cuff and biceps model was used to develop an animal model of scapular dyskinesis and characterize the functional consequences and mechanical, histological, organizational, and compositional changes to the supraspinatus and biceps tendons (Chapter 2). This model was then used to investigate the effect of overuse activity in the presence of scapular dyskinesis on function and mechanical, histological, organizational, and compositional properties of the supraspinatus and biceps tendons (Chapter 3). Additionally, this model was used to investigate the effect of scapular dyskinesis on supraspinatus tendon healing following repair as characterized by function and mechanical, histological, organizational, and compositional properties of the supraspinatus tendon (Chapter 4). The main findings and conclusions from these chapters and potential future directions are included in this chapter.

B. Scapular Dyskinesis is Detrimental to Shoulder Tendon Properties and Joint Mechanics in a Rat Model

Shoulder tendon injuries are frequently seen in the presence of abnormal scapular motion, termed scapular dyskinesis. The cause and effect relationship between scapular dyskinesis and shoulder injury has not been directly defined. The underlying mechanisms and relationships can only be addressed in an animal model where time from injury can be controlled and evaluated over time. Therefore, the objective of this study was to develop and use an animal model to examine the initiation and progression of pathological changes in the rotator cuff and biceps tendon.

We utilized an established rat shoulder model and extended it to include the induction of scapular dyskinesis. This was achieved through denervation of the trapezius and serratus anterior muscles through surgical transection of the accessory and long-thoracic nerve, respectively. We hypothesized that scapular dyskinesis would: H1) diminish shoulder function and passive joint mechanics and H2) diminish supraspinatus and biceps tendon histological, compositional, and mechanical properties.

Consistent with the first hypothesis, gross observation demonstrated clear alterations in scapular motion, consistent with scapular "winging". Quantitatively, we found that joint function (vertical and propulsion force) was significantly altered in the presence of scapular dyskinesis compared to control at all time-points. Specifically, vertical force was significantly decreased while propulsion force was significantly increased. Due to the orientation of the scapula, propulsion force correlates with human abduction, which is often used as an objective measure of shoulder function. An increased propulsion force due to scapular dyskinesis may place high stresses on the supraspinatus and biceps tendon, placing them at increased risk for injury. Decreased vertical force, which provides a measure of weight-bearing and pain, suggest that scapular dyskinesis may increase pain at the shoulder joint, as observed in the clinical scenario due to impingement. Additionally, passive internal range of motion was significantly increased compared to control at all time-points. Scapular dyskinesis compromises the dynamic stability of the shoulder joint, requiring increased reliance on the static structures, such as the joint capsule, for stability. It is likely that the increased stresses placed on the posterior joint capsule results in stretching out and loosening of the capsule and subsequent increased range of motion.

Consistent with the second hypothesis, it was found that both viscoelastic and elastic mechanical parameters were significantly diminished. Specifically, tendon (biceps and supraspinatus) percent relaxation was increased and the mid-substance elastic modulus was significantly decreased, indicative of inferior tissue properties. The location specific tendon changes (mid-substance region) may be due to its anatomic location under the acromial arch during forward flexion, resulting in impingement.

Additionally, results demonstrated changes in cell morphology, cell density, organization, and composition (for collagen III and decorin) due to scapular dyskinesis. For the supraspinatus, the SD group had greater disorganization at the insertion site (2 weeks), increased Col III at the insertion site (4 + 8 weeks) and mid-substance (8 weeks), a less rounded cell shape and increased cell density at the insertion site (8 weeks), and increased decorin at the mid-substance (8 weeks) compared to control. These changes support the diminished mechanical properties observed and are consistent with a tendinopathic condition (e.g., disorganized structure, accumulation of Col III and proteoglycan, and increased cell density). For the biceps, the SD group had greater organization at the intra-articular space (2 + 4 weeks) and proximal groove (4 weeks), decreased decorin at the insertion site and distal groove (4 weeks), greater disorganization at the insertion site (8 weeks), a more rounded cell shape at the insertion, intra-articular space, proximal groove, and distal groove (8 weeks), increased Col III at the insertion site (8 weeks), decreased Col III at the distal groove (8 weeks), and increased decorin at the insertion site (8 weeks). The biceps tendon passes from the extra-articular space through the biccipital groove, enters the intra-articular space where it wraps around the humeral head, and ultimately inserts on the scapula. As a result, the

biceps experiences complex loading and nutritional environments along its length, resulting in unique structure and composition at each location. The findings observed at the insertion site are consistent with a tendinopathic condition and a compressive loading environment (e.g., greater disorganization, more rounded cell shape, accumulation of Col III and proteoglycan) due to scapular dyskinesis. However, the findings observed at the other locations (that do not pass under the acromial arch) are differential (e.g., increased organization, altered composition) and indicate an adaptive response due to the altered loading observed in the presence of scapular dyskinesis.

In summary, this is the first study to directly identify scapular dyskinesis as a causative mechanical mechanism for the development of pathological changes in the supraspinatus and biceps tendons. Through creation of an animal model, we were able to rigorously evaluate the effect of scapular dyskinesis in a controlled manner. Identification of scapular dyskinesis as a mechanism of pathological changes will help inform and guide clinicians in developing optimal prevention and long-term rehabilitation strategies.

C. Overuse Activity in the Presence of Scapular Dyskinesis Leads to Shoulder Tendon Damage in a Rat Model

Shoulder injuries are debilitating conditions and are particularly common in individuals who perform repetitive overhead activities due to their occupation or sport. Individuals who perform these activities may also develop abnormal shoulder mechanics, due to muscular adaptations or fatigue. However, the long term consequences associated with overuse activity in the presence of abnormal scapular kinematics are unknown. Therefore, the objective of this study was to determine the effect of overuse in

combination with scapular dyskinesis on joint mechanics and properties of the rotator cuff and biceps tendon in this rat model.

We utilized our animal model of scapular dyskinesis and prescribed overuse activity, which has previously been demonstrated to induce tendinopathy.[26] We hypothesized that scapular dyskinesis in combination with repetitive overuse will alter joint function and diminish tendon properties when compared to scapular dyskinesis alone (H1) and when compared to overuse alone (H2).

Contrary to our first hypothesis, overuse activity did not alter joint function and consistent with our second hypothesis, scapular dyskinesis significantly altered joint function. Specifically, vertical force and braking force were decreased while propulsion force was increased with scapular dyskinesis. The scapular rotators (i.e., the trapezius and serratus anterior) are particularly important in abduction, acting to upwardly rotate the scapula and allow for clearance of the rotator cuff under the acromion. In the presence of scapular dyskinesis in this model, these muscles are not functioning, resulting in changes in braking and propulsion force, which correlate with human abduction. The increased propulsion force may place increased stresses on the joint, resulting in subacromial impingement and compromising tendon properties. The decreased vertical force suggests decreased weight-bearing potentially due to increased pain associated with scapular dyskinesis.

Additionally, passive joint mechanics were altered. Specifically, decreased external range of motion was observed in the SD + OV group compared to both groups, SD (at 2 and 8 weeks) and OV (at 2 weeks). Shoulder range of motion in overhead athletes is typically characterized by increased external range of motion and limited

internal range of motion due to stretching of the anterior capsule and tightening of the posterior capsule.[5] Surprisingly, in this study, we observed decreased external range of motion, indicative of tightening in the anterior structures. These changes may be indicative of over-compensation by the surrounding anterior muscles, such as the subscapularis, pectoralis major, teres major, and latissimus dorsi, or joint capsule, leading to subsequent tightening.

Consistent with our first hypothesis, overuse activity in the presence of scapular dyskinesis led to compromised tendon properties. Specifically, tendon (supra and biceps) percent relaxation was increased, elastic modulus was decreased, and organization was more disorganized with the addition of overuse activity. These changes may be a result of microtrauma caused by mechanical compression and shear of the tendons due to repetitive excursion of the tendons under the acromion during overuse activity. Additionally, a more rounded cell shape was present in the supraspinatus, consistent with a tendinopathic condition, and altered matrix synthesis was observed in both tendons (increased collagen II in biceps, decreased collagen III in biceps and supraspinatus, and increased and decreased decorin in biceps and supraspinatus, respectively). Histologic and compositional changes supported the mechanical changes observed. Due to the altered loading environment observed in the presence of scapular dyskinesis, cellular function and subsequent matrix deposition was altered, leading to abnormal collagen metabolism and greater disorganization. These changes diminished the material properties of the tendon, altering the cellular microenvironment and further affecting cellular morphology and function, as previously described.[8]

Consistent with our second hypothesis, scapular dyskinesis did further diminish tendon properties, compared to overuse alone. Specifically, supraspinatus and biceps mid-substance modulus were diminished, supraspinatus cell density was increased, and altered matrix synthesis was observed (decreased collagen III in biceps). However, the tendon changes due to scapular dyskinesis were not as dramatic (a few parameters) as changes due to overuse (several parameters). These findings indicate that overuse activity alone may have a greater effect on tendon properties than scapular dyskinesis alone.

In summary, we elucidated tendon mechanical damage through two distinct mechanisms: 1) tendon overuse and 2) tendon overload (i.e. abnormal joint mechanics). While each independently lead to tendon injury, overuse activity in the presence of scapular dyskinesis resulted in significantly more structural and biological adaptations (such as decreased range of motion, diminished tendon properties, and altered matrix synthesis) than scapular dyskinesis alone. Taken together, results suggest that the risk for shoulder injury in patients with scapular dyskinesis may be higher in an active population. Identification of overuse activity as a risk factor for shoulder injury in individuals with scapular dyskinesis will help inform and guide clinicians in developing prevention and treatment programs. Specifically, activity levels of athletes and laborers could be monitored in order to prevent permanent shoulder injury. Additionally, early detection and intervention programs can be developed, such as preventative neuromuscular training and scapular movement screens, which could assist in prevention of further detrimental changes due to scapular dyskinesis.

D. Effect of Scapular Dyskinesis on Supraspinatus Tendon Healing in a Rat Model

Rotator cuff tears often require surgical repair in order to improve function and relieve pain. Unfortunately, failure of repairs is common (5-95% of patients), resulting in decreased strength and function. Several factors may contribute to repair failure including age, tear size, and time from injury. Mechanical loading also plays an important role in tendon-to-bone healing; however, the mechanical mechanisms behind repair failure are not well-established. We have previously demonstrated that scapular dyskinesis alters joint mechanics and diminishes tendon properties. However, the consequences on rotator cuff tendon healing in the presence of scapular dyskinesis have never been evaluated. Therefore, the objective of this study was to determine the effect of scapular dyskinesis on supraspinatus tendon to bone healing following tendon repair.

We utilized our animal model of scapular dyskinesis and performed acute transection of the supraspinatus followed by tendon repair to evaluate healing. We hypothesized that scapular dyskinesis would result in H1) diminished joint function and passive joint mechanics and H2) decreased supraspinatus tendon to bone healing following tendon repair due to the compromised mechanical environment present during healing.

Consistent with our first hypothesis, scapular dyskinesis significantly altered joint function (specifically, propulsion was increased and braking force was decreased, at later time points). These changes indicate an alteration in the loading environment at the shoulder due to scapular dyskinesis and may place increased stresses on the healing supraspinatus tendon, increasing risk for re-injury. The decreased braking force present at later time-points may be indicative of a functional adaptation to prevent further

damage. Interestingly, no changes in vertical force were observed, as seen in previous studies. It is likely that vertical force, which corresponds to weight-bearing and pain, was affected more by the repair surgery, masking any underlying alterations due to scapular dyskinesis.

However, no effect on passive joint mechanics was observed. Previous studies have demonstrated that increased stiffness and decreased range of motion is observed following cuff repair.[25] It is likely that the excessive scar formation present following repair surgery may mask any underlying changes in passive motion due to tendon stiffening or capsular tightening.

Consistent with our second hypothesis, scapular dyskinesis was detrimental to supraspinatus tendon properties for some parameters (decreased mid-substance modulus, increased percent relaxation, more rounded cell shape, greater disorganization). Surprisingly, decreased cross-sectional area was observed in the SD group compared to control at 4 weeks. This finding may be related to the reduced subacromial space present in the SD group, allowing less space for tissue proliferation and matrix production. These adaptations in the presence of scapular dyskinesis may compromise tendon repair functionality and integrity. Interestingly, no differences in tendon composition were identified. The excessive cell proliferation and increased matrix synthesis present following tendon repair may mask the effect of scapular dyskinesis on tendon composition in this study.

In summary, results highlight the functional consequences associated with scapular dyskinesis that may impair healing potential by diminishing tendon mechanical properties. Identification of abnormal joint mechanics as a potential mechanical

mechanism of failed rotator cuff healing will help guide clinicians in prescribing treatment strategies for patients with cuff tears. This study supports the need for evaluation and correction of abnormal joint kinematics prior to rotator cuff repair in order to optimize the mechanical loading environment of the tendon and improve healing rates.

E. Final Conclusions

We developed a model of scapular dyskinesis in an established rat shoulder model. We then utilized this model to characterize the functional consequences and mechanical, histological, organizational, and composition changes to the supraspinatus and biceps tendon in the presence of scapular dyskinesis compared to a sham control surgery. We found that scapular dyskinesis is detrimental to shoulder function and mechanical properties and alters histological and compositional properties as well. Next, we utilized this model to investigate the effect of overuse activity in the presence of scapular dyskinesis on function and the supraspinatus and biceps tendons. We found that overuse activity does not affect shoulder function but is further detrimental to the supraspinatus and biceps tendon in mechanical and organizational properties and some histological and compositional properties. Finally, we utilized this model to investigate the effect of scapular dyskinesis on supraspinatus tendon healing. We found that scapular dyskinesis affects joint function and is detrimental to tendon properties for some parameters (mechanical, histological, compositional).

We conclude that scapular dyskinesis is a causative mechanical mechanism for shoulder tendon injury, as demonstrated in a rat model. Previous studies have demonstrated a strong association between scapular dyskinesis and shoulder pathology. However, the cause and effect relationship between these pathologies has never been

fully elucidated. Results indicate that scapular dyskinesis can lead to tendon injury if left untreated. This information will help guide clinicians in identifying rehabilitation strategies, such as early screening and preventative neuromuscular training, in order to prevent tendon injury and improve tendon healing potential following repair.

F. Future Directions

Based on these results, several possible future directions should be considered for this animal model. These include 1) further elucidating the role of altered joint mechanics as a mechanism of supraspinatus and biceps tendon pathology through use of additional biologic, mechanical, and functional assays and using this model 2) to investigate the effect of scapular dyskinesis on the joint capsule and 3) the shoulder musculature, 4) to investigate the role of subacromial impingement in tendon pathology, and 5) to assess treatment strategies.

a. Additional biologic assays

For this study, we examined the distribution of extra-cellular matrix proteins using immunohistochemical techniques. We chose to localize a chondrogenic marker (col II), a tendon proteoglycan marker (decorin), a marker for scar/healing (col III), and an inflammatory marker (IL-1β). However, additional markers should be examined in order to further elucidate the biologic mechanisms involved in tendon injury in the presence of scapular dyskinesis. Tendon's initial response to changes in loading is to adapt to the environment by altering matrix composition while attempting to maintain a rate of degradation that is equal to the rate of synthesis. When the mechanical demands placed on the tendon are excessive, the rate of degradation may exceed the rate of synthesis, which may diminish mechanical properties. Specifically, additional

chondrogenic markers (such as ACAN, SOX-9), matrix markers (such as type I collagen, biglycan, versican, and fibronectin), and inflammatory markers (such as TNF-α, IL-10, TGFβ) should be examined. TGFβ, which has known roles in cell proliferation and matrix synthesis, may be responsible for some of the changes in cell density and matrix composition observed in Chapter 2.[14] Previous studies have demonstrated altered regulation of chondrogenic markers within tendon, due to a change in the mechanical loading environment (e.g., compressive, shear).[1, 28] Additionally, altered production of small-leucine rich proteoglycans (e.g., biglycan) may play a role in tendon's response to injury through interactions with collagen and could diminish mechanical properties.[7] The ratio of type III collagen to type I is particularly important in injured tendon and could impact tendon function. Lastly, the role of inflammation in tendon injury is poorly understood. Some studies suggest that both acute and chronic tendinopathies are absent of inflammation while others have identified an early inflammatory response.[23] Additionally, matrix metalloproteases (MMPs), a family of enzymes responsible for degradation of extracellular matrix components (including collagen and proteoglycans), should also be examined.

In this dissertation and in previous studies,[24, 26] we have demonstrated that tendon overload is a key component of pathology; however, the biologic mechanism by which pathology is mediated is not fully understood. Therefore, the objective of this study would be to examine biological changes in the supraspinatus and biceps in the presence of scapular dyskinesis. This could be achieved by evaluating biological changes through immunohistochemical techniques at 2, 4, and 8 weeks following induction of scapular dyskinesis. The associated hypothesis would be that the altered mechanical loading

environment due to scapular dyskinesis would result in increased tendon degradation (e.g., increased presence of degradative factors, proteoglycans, chondrogenic, and inflammatory markers) in the scapular dyskinesis group compared to control. Specifically, the altered loading environment will lead to abnormal cellular metabolism and behavior, particularly involving maintenance, repair, and remodeling of the tendon matrix. Proteins involved in chondrogenesis (such as ACAN, SOX-9) will be increased, matrix markers (such as biglycan, versican, and fibronectin) will be increased while Col I (the primary tensile load bearing component in tendon) will be decreased, inflammatory markers (such as TNF-α, IL-10, TGFβ) will be increased, and degradative enzymes (such as MMP1 and MMP3) will be increased. In order to test this hypothesis, rats would be randomized into two groups: scapular dyskinesis and sham control. This study would provide important information in characterizing the biologic response to mechanical tendon injury. Additionally, this model system could be used to assist in identification of potential therapeutic interventions (e.g., non-steroidal anti-inflammatories, MMP inhibitors) in tendon injury treatment, attenuation, or prevention. The proposed study would provide a better understanding of the tendon's biologic response to abnormal loads and will aid in the identification of appropriate treatment for tendon injuries.

b. Additional mechanical testing assays

Previous basic tendon research has focused on tendon failure and quasi-static mechanical properties (i.e., modulus, stiffness, cross-sectional area) to assess tendon injury and healing. Results from this study demonstrated that quasi-static tendon mechanical properties are altered in the presence of scapular dyskinesis and in the presence of scapular dyskinesis in combination with overuse activity and following

repair. However, tendon undergoes dynamic loading during daily activity and therefore dynamic loading measurements (i.e., dynamic modulus, phase shift) may provide additional information in elucidating tendon mechanical damage. The testing protocol would consist of preconditioning, recovery, and then dynamic loading (sinusoidal displacements at various frequencies and various strains).[6, 18]

In addition to dynamic mechanical evaluation, fatigue properties (i.e., tangent modulus, tangent stiffness, and cycles to failure) may provide additional information regarding tendon damage, particularly with respect to overuse and with respect to healing. Specifically, due to the repetitive nature of rotator cuff tendon loading during overhead activities, fatigue loading measurements may allow for early detection of damage accumulation. Additionally, due to the importance of the mechanical loading environment in tendon-to-bone healing, fatigue loading measurements may provide critical information for establishing optimal treatment and rehabilitation protocols. A previous study in the Achilles tendon found that the most sensitive measure to detect tendon injury and healing was cycles to failure, a fatigue parameter.[9]

In this dissertation and in previous studies,[21, 24] we have demonstrated that abnormal joint mechanics is a key component of shoulder tendon pathology; however, the mechanical mechanism by which pathology is mediated is not completely defined. Tissue mechanical properties only assessing quasi-static loading may provide an incomplete description of tendon injury and healing. Therefore, the objective of this study would be to determine the mechanical and structural properties during dynamic loading and throughout fatigue life of the supraspinatus and biceps tendon in the presence of scapular dyskinesis compared to control. The associated hypotheses would be that

scapular dyskinesis would decrease mechanical properties (dynamic and fatigue parameters) compared to control. Specifically, the altered mechanical environment will disrupt tendon mechanical integrity and dynamic parameters such as phase shift (a viscoelastic parameter) would increase and dynamic modulus (an elastic parameter) would decrease while fatigue parameters such as cycles to failure and tangent modulus would both decrease. In order to test this hypothesis, rats would be randomized into two groups: scapular dyskinesis and sham control. This study would provide insight into the mechanical consequences of abnormal loading on tendon. Alterations in the dynamic and fatigue mechanical properties of tendon may place them at increased risk for mechanical failure (i.e., tears). Information from the proposed study could assist in identification of optimal structured rehabilitation regimes (e.g., loading conditions, number of repetitions, and timing of mobilization) in order to optimize outcomes and increase healing rates.

c. Additional functional assays

Additional functional parameters such as forelimb grip strength and joint kinematics could be used to further assess changes due to scapular dyskinesis. Forelimb grip strength, a measure of neuromuscular function and muscular strength, could be measured in the injured limb as previously described.[4] Reduction in grip strength has been observed previously due to tissue injury, inflammation, and fibrosis in the forearm and shoulder muscles.[4, 22] The objective of this study would be to examine the effect of scapular dyskinesis on motor performance. The associated hypothesis would be that scapular dyskinesis will decrease grip strength compared to control. Specifically, compensatory adaptations in the muscles at the forearm and shoulder due to scapular

dyskinesis will lead to tissue injury and subsequent diminished function and strength. In order to test this hypothesis, rats would be randomized into two groups: scapular dyskinesis and sham control. This study would provide important information in characterizing the functional consequences of scapular dyskinesis.

Although the method of functional assessment used in the current study is very sophisticated, we were only able to quantify kinetics (i.e., ground reaction forces) and not joint kinematics (i.e., 3D motion and position of shoulder). This would provide additional information and direct quantification of important measures such as tendon forces and acromiohumeral distance, which when altered, are likely to contribute to tendon injury in this model. Specifically, future studies should be performed to quantify and/or classify the position of the scapula in this model in order to allow for a closer comparison to the clinical situation. This could be achieved through use of biplane fluoroscopy, which allows for accurate quantitative 3D motion assessment through direct visualization of bone motion.[27] Through this technology, we would be able to project the ground reaction forces from the paw to the shoulder in order to assess shoulder joint reaction forces. Additionally, we would be able to quantitatively describe how the humerus articulates with the scapula. For example, estimation of tendon forces and quantification of acromiohumeral distance would allow for direct assessment of the mechanical mechanism (e.g., overload or compressive loading) by which tendon changes occur in this model.

In this dissertation, we have demonstrated there are functional consequences associated with scapular dyskinesis; however, we have not quantified the altered loading pattern present at the shoulder joint. Therefore, the objective of this study would be to

determine the effect of scapular dyskinesis on shoulder joint kinematics and joint reaction forces. The associated hypotheses would be that scapular dyskinesis will decrease the acromiohumeral distance and would increase the reaction force observed at the shoulder joint compared to control. Specifically, scapular dyskinesis (induced by denervation of the trapezius and serratus anterior) would prevent upward rotation of the scapula during forward locomotion, reducing the acromiohumeral distance and disrupting clearance of the supraspinatus under the acromial arch, leading to tendon impingement. Additionally, the abrupt compression between the humeral head and acromion would result in increased reaction forces at the shoulder joint. In order to test this hypothesis, rats would be randomized into two groups: scapular dyskinesis and sham control. This study would directly elucidate the mechanical loading conditions present at the shoulder joint and provide insight into the mechanical mechanism (i.e., subacromial compression, tendon overload) by which tendon injury occurs. This information could assist in identification of optimal structured rehabilitation regimes (e.g, programs aimed at maximizing acromiohumeral distance by optimizing scapular mechanics).

d. Effect on joint capsule

Results from this study demonstrated changes in passive joint mechanics. These changes may be an indirect assessment of changes in the static restraints, such as the joint capsule, due to scapular dyskinesis. However, future studies should directly examine biologic and mechanical changes in the joint capsule due to scapular dyskinesis.

The joint capsule is a loose, fibrous membrane (reinforced by the glenohumeral ligaments) attached on the outside ring of the glenoid cavity and on the head of the humerus. Shoulder capsule pathology, due to injury (e.g., subluxation or dislocation) or

sport-specific adaptations, could result in increased tightening or loosening of the joint capsule (i.e., frozen shoulder or instability, respectively). For example, the joint capsule may become inflamed and fibrotic, leading to stiffness, pain, and diminished range of motion. However, the underlying changes present in the joint capsule due to alterations in joint mechanics (e.g., scapular dyskinesis) are poorly understood and can be evaluated in this animal model. Following injury, fibroblasts in the joint capsule may undergo a phenotypic change into contractile myofibroblasts, characterized by the expression of α-SMA.[10, 19] Several pro-fibrotic factors may induce this change including mechanical stimuli, fibronectin, CTGF, Col III, and TGF-β.[11, 19] Future studies could localize these factors using immunohistochemical techniques. Additionally, the material properties of the joint capsule could also be assessed by performing uniaxial tensile testing.

In this dissertation, we have demonstrated that scapular dyskinesis alters shoulder passive range of motion (which provides an indirect assessment of the joint capsule); however, a direct assessment of the joint capsule was not performed. Therefore, the objective of this study would be to determine the effect of scapular dyskinesis on the biologic and mechanical properties of the joint capsule compared to control. The associated hypotheses would be that scapular dyskinesis will diminish the biologic and mechanical properties of the joint capsule. Specifically, the unstable scapula may not allow the rotator cuff to effectively compress the humeral head into the glenoid fossa thereby requiring the joint to rely on static restraints, such as the joint capsule for stability. The resulting increased stress on the capsule could lead to microtrauma and altered cellular function such as altered matrix synthesis and deposition. Specifically, in response to the increased stresses, scapular dyskinesis would lead to increased presence

of pro-fibrotic factors (such as α-SMA, fibronectin, CTGF, Col III, and TGF-β) in the joint capsule and diminished mechanical properties (such as decreased modulus and increased tissue thickness). In order to test this hypothesis, rats would be randomized into two groups: scapular dyskinesis and sham control. Pathology of the joint capsule (i.e., frozen shoulder, laxity) is not well understood. This study would provide important information in characterizing the capsular response to abnormal joint mechanics. Results would provide insight into the biologic mechanism which mediates capsule pathology following mechanical injury and could assist in identification of treatments for this condition.

e. Effect on muscle

The rotator cuff muscles and biceps originate and insert on the scapula, respectively. In order to achieve proper function and maximal strength, an appropriate length-tension relationship must be maintained. Muscle length-tension relationship is the relationship between the length of muscle and the force it produces at that length. In the case of scapular dyskinesis, the scapula is misaligned, which may result in an altered length-tension relationship and inefficient rotator cuff and biceps muscle function and weakness. Fiber morphology (size and type) is also an indicator of muscle function. The isometric contractile properties and morphology of the supraspinatus and biceps muscles could be measured, as previously described.[16, 17] Briefly, each muscle could be activated through electrical stimulation of their respective nerves (suprascapular and musculocutaenous) and contractile properties measured. Additionally, histological and immunohistochemical techniques, such as staining using myosin ATPase or myosin heavy chain antibodies, could be used to assess fiber diameter and type.

In this dissertation, we have demonstrated that scapular dyskinesis is detrimental to the supraspinatus and biceps tendons; however, the consequences on their associated muscles has not been studied. Therefore, the objective of this study would be to determine the effect of scapular dyskinesis on supraspinatus and biceps muscle function. The associated hypothesis would be that scapular dyskinesis will diminish muscle function and morphology. These changes will result due to the altered length-tension relationship present with the scapula misaligned and due to the increased reliance on the rotator cuff and biceps for dynamic stability at the joint, resulting in overload and tissue damage. Specifically, contractile properties of the supraspinatus and biceps muscles will be diminished and fiber type would be altered due to scapular dyskinesis. In order to test this hypothesis, rats would be randomized into two groups: scapular dyskinesis and sham control, and assessed at 2, 4, and 8 weeks. This study would provide important information in identifying the muscular adaptations that occur in the presence of scapular dyskinesis. These changes could be compared to tendon adaptations in order to determine the sequence of responses for both muscle and tendon. Results would help guide physical therapy evaluation and interventions (i.e., neuromuscular control and strength training).

f. Effect of subacromial impingement

Results from this study led us to speculate that subacromial impingement may be the mechanism by which scapular dyskinesis alters supraspinatus and biceps tendon properties. Additionally, previous studies have demonstrated that this extrinsic factor [subacromial impingement] may contribute to tendinopathy and tendon tears.[2, 3, 20] However, other studies have suggested that intrinsic factors, such as eccentric overload,

may be to blame. Therefore, in order to verify this, studies could be done, using this model, to decrease the role of the acromion in order to determine its effect. Specifically, an acromioplasty (surgical removal of the acromion) could be performed to remove the acromion and evaluate its effect in the presence of scapular dyskinesis.

In this dissertation, we have demonstrated that scapular dyskinesis is detrimental to shoulder tendon properties; however, the role of the acromion in causing those changes is unclear. Therefore, the objective of this study would be to determine the role of subacromial impingement in biceps and supraspinatus tendon pathology in the presence of scapular dyskinesis. The associated hypothesis would be that scapular dyskinesis would have no effect on tendon properties (mechanical, histological, immunohistochemical) following acromioplasty. Specifically, the induction of scapular dyskinesis (through denervation of the trapezius and serratus anterior muscles) will prevent upward rotation of the scapula, resulting in subacromial impingement and mechanical compression of the suprasinatus and biceps tendons. However, removal of the acromion may prevent impingement, despite the presence of scapular dyskinesis. In order to test this hypothesis, all rats would undergo acromioplasty and would then be randomized into two groups: scapular dyskinesis and sham control. Results of this study would provide important information in identifying the role of subacromial impingement in tendon injury. In addition, this study will provide an assessment of acromioplasty as a potential treatment strategy for patients with subacromial impingement in order to prevent long term shoulder injury.

g. Potential treatment strategies

Results from this study suggest that scapular dyskinesis is detrimental to shoulder tendon properties. Clinically, scapular dyskinesis is treated using rehabilitation strategies to re-educate scapular muscles, improve neuromuscular control, and correct positional abnormalities. However, it is unclear if rehabilitation would prevent further shoulder injury. In order to assess this in our model, we could induce temporary paralysis (using nerve compression or botulinum toxin) of the trapezius and serratus anterior followed by functional recovery (to model rehabilitation) in order to assess injury prevention. Specifically, we could induce scapular dyskinesis for 4 weeks (which has been shown to induce tendon injury) followed by functional recovery and evaluation at 8 and 16 weeks.

In this dissertation, we have identified a modifiable factor, scapular dyskinesis, as a causative mechanical mechanism of shoulder tendon injury; however, the effect of modifying that factor in preventing tendon injury has not been directly described. Therefore, the objective of this study would be to determine the role of rehabilitation in injury prevention. The associated hypothesis would be that restoration of scapular kinematics will prevent injury to the shoulder (in the form of improved mechanical, biological, compositional, and organizational properties). Specifically, restoration of scapular kinematics will increase tendon modulus and organization and will suppress the heightened cellular response to injury (i.e., decreased cell density, less rounded cell shape). In order to test this hypothesis, all rats would be randomized into two groups: permanent scapular dyskinesis and temporary scapular dyskinesis. This study would provide evidence for the benefits of scapular rehabilitation aimed at restoring the balance of forces at the shoulder joint. Evaluation of dyskinesis and subsequent rehabilitation

could allow for more effective treatment strategies for shoulder injuries by preventing further shoulder tendon pathology and improving outcomes.

h. Futures uses of this model

Several factors can contribute to scapular dysfunction clinically including muscle imbalance, nerve injury, postural abnormality, anatomical disruption, capsular contracture, or proprioceptive dysfunction.[12, 13] For this model, we utilized a nerve injury mechanism and were able to successfully and repeatably create scapular "winging", which is consistent with observations found clinically in patients with scapular dyskinesis. Specifically, in order to create scapular dyskinesis, we denervated both the serratus anterior and trapezius muscles, which are the primary muscles involved in rotation of the scapula. However, dysfunction of both muscles does not exactly mimic all clinical scenarios and the independent contributions of each muscle to shoulder injury have never been evaluated. In isolation, dysfunction of each muscle results in unique position and motion of the scapula and therefore the independent contributions of each muscle to shoulder injury should be examined. Specifically, isolated serratus anterior muscle dysfunction creates a prominent superior medial border of the scapula and depresses the acromion, while isolated trapezius muscle dysfunction results in a protracted inferior border and elevated acromion.[15]

In this dissertation, we have demonstrated that scapular dyskinesis (cause by denervation of the serratus anterior and trapezius muscles) leads to shoulder tendon injury; however, the independent contribution of each muscle to tendon injury was not evaluated. Therefore, the objective of this study would be to independently assess the role of trapezius dysfunction and serratus anterior dysfunction in shoulder injury. The

associated hypothesis would be that denervation of the serratus anterior alone would be more detrimental to joint function and shoulder tendon properties than denervation of the trapezius alone. Specifically, the reduced subacromial space present (due to depression of the acromion following denervation of the serratus anterior muscle) will result in subacromial impingement and compressive loading of the supraspinatus and biceps tendons. In order to test this hypothesis, all rats would be randomized into two groups: denervation of the spinal accessory nerve only (i.e., trapezius dysfunction) and denervation of the long thoracic nerve only (i.e., serratus anterior dysfunction). This study would increase our understanding of the mechanical mechanisms involved in tendon injury by identifying the role of each muscle. This knowledge will help guide physical therapy evaluation and interventions (e.g., targeted rehabilitation and strength training) in order to prevent the progression of tendon injury and improve outcomes.

i. Final conclusions

Several future directions have been presented here to further elucidate the role of scapular dyskinesis in shoulder pathology and to assess potential treatment strategies in a multi-disciplinary manner, including the use of sophisticated quantitative immunohistochemical techniques to localize ECM proteins, rigorous mechanical testing techniques to further characterize tissue properties, and in vivo assessments to further quantify joint kinematics and muscle function. Further characterization of the pathological changes present in this model due to scapular dyskinesis will help inform and guide clinicians in developing optimal prevention and long-term rehabilitation regimens.

G. References

1. Archambault JM, Jelinsky SA, Lake SP, Hill AA, Glaser DL, Soslowsky LJ. Rat supraspinatus tendon expresses cartilage markers with overuse. *J Orthop Res.* 2007;25(5):617-624.

2. Balke M, Schmidt C, Dedy N, Banerjee M, Bouillon B, Liem D. Correlation of acromial morphology with impingement syndrome and rotator cuff tears. *Acta Orthop.* 2013;84(2):178-183.

3. Bigliani LU, Ticker JB, Flatow EL, Soslowsky LJ, Mow VC. The relationship of acromial architecture to rotator cuff disease. *Clin Sports Med.* 1991;10(4):823-838.

4. Clark BD, Al-Shatti TA, Barr AE, Amin M, Barbe MF. Performance of a high-repetition, high-force task induces carpal tunnel syndrome in rats. *J Orthop Sports Phys Ther.* 2004;34(5):244-253.

5. Crockett HC, Gross LB, Wilk KE, et al. Osseous adaptation and range of motion at the glenohumeral joint in professional baseball pitchers. *Am J Sports Med.* 2002;30(1):20-26.

6. Dourte LM, Pathmanathan L, Jawad AF, et al. Influence of decorin on the mechanical, compositional, and structural properties of the mouse patellar tendon. *J Biomech Eng.* 2012;134(3):031005.

7. Dunkman A, Buckley M, Mienaltowski M, et al. The Tendon Injury Response is Influenced by Decorin and Biglycan. *Annals of Biomedical Engineering.* 2013;42(3):619-630.

8. Engler AJ, Sen S, Sweeney HL, Discher DE. Matrix elasticity directs stem cell lineage specification. *Cell.* 2006;126(4):677-689.

9. Freedman BR, Sarver JJ, Buckley MR, Voleti PB, Soslowsky LJ. Biomechanical and structural response of healing Achilles tendon to fatigue loading following acute injury. *J Biomech.* 2013.

10. Gabbiani G. The myofibroblast in wound healing and fibrocontractive diseases. *J Pathol.* 2003;200(4):500-503.

11. Hildebrand KA, Zhang M, Hart DA. Myofibroblast upregulators are elevated in joint capsules in posttraumatic contractures. *Clin Orthop Relat Res.* 2007;456:85-91.

12. Kibler WB. The role of the scapula in athletic shoulder function. *Am J Sports Med.* 1998;26(2):325-337.

13. Kibler WB, McMullen J. Scapular dyskinesis and its relation to shoulder pain. *J Am Acad Orthop Surg.* 2003;11(2):142-151.

14. Kjaer M. Role of extracellular matrix in adaptation of tendon and skeletal muscle to mechanical loading. *Physiol Rev.* 2004;84(2):649-698.

15. Kuhn JE, Plancher KD, Hawkins RJ. Scapular Winging. *J Am Acad Orthop Surg.* 1995;3(6):319-325.

16. Lieber RL, Friden J. Muscle damage is not a function of muscle force but active muscle strain. *J Appl Physiol (1985).* 1993;74(2):520-526.

17. Lieber RL, Woodburn TM, Friden J. Muscle damage induced by eccentric contractions of 25% strain. *J Appl Physiol (1985).* 1991;70(6):2498-2507.

18. Lujan TJ, Underwood CJ, Jacobs NT, Weiss JA. Contribution of glycosaminoglycans to viscoelastic tensile behavior of human ligament. *J Appl Physiol (1985).* 2009;106(2):423-431.

19. Mattyasovszky SG, Hofmann A, Brochhausen C, et al. The effect of the pro-inflammatory cytokine tumor necrosis factor-alpha on human joint capsule myofibroblasts. *Arthritis Res Ther.* 2010;12(1):R4.

20. Nicholson GP, Goodman DA, Flatow EL, Bigliani LU. The acromion: morphologic condition and age-related changes. A study of 420 scapulas. *J Shoulder Elbow Surg.* 1996;5(1):1-11.

21. Perry SM, Getz CL, Soslowsky LJ. After rotator cuff tears, the remaining (intact) tendons are mechanically altered. *J Shoulder Elbow Surg.* 2009;18(1):52-57.

22. Rani S, Barbe MF, Barr AE, Litivn J. Role of TNF alpha and PLF in bone remodeling in a rat model of repetitive reaching and grasping. *J Cell Physiol.* 2010;225(1):152-167.

23. Rees JD, Stride M, Scott A. Tendons - time to revisit inflammation. *Br J Sports Med.* 2013.

24. Reuther KE, Thomas SJ, Tucker JJ, et al. Disruption of the anterior-posterior rotator cuff force balance alters joint function and leads to joint damage in a rat model. *J Orthop Res.* 2014;32(5):638-644.

25. Sarver JJ, Peltz CD, Dourte L, Reddy S, Williams GR, Soslowsky LJ. After rotator cuff repair, stiffness--but not the loss in range of motion--increased transiently for immobilized shoulders in a rat model. *J Shoulder Elbow Surg.* 2008;17(1 Suppl):108S-113S.

26. Soslowsky LJ, Thomopoulos S, Tun S, et al. Neer Award 1999. Overuse activity injures the supraspinatus tendon in an animal model: a histologic and biomechanical study. *J Shoulder Elbow Surg.* 2000;9(2):79-84.

27. Tashman S, Anderst W. In-vivo measurement of dynamic joint motion using high speed biplane radiography and CT: application to canine ACL deficiency. *J Biomech Eng.* 2003;125(2):238-245.

28. Wren TA, Beaupre GS, Carter DR. Mechanobiology of tendon adaptation to compressive loading through fibrocartilaginous metaplasia. *J Rehabil Res Dev.* 2000;37(2):135-143.

Appendix A: Experimental Protocols

A1. Surgical Protocol: Nerve Transection for Scapular Dyskinesis and Supraspinatus Repair

Instruments Needed (sterile):

Hemostat (1)
Needle driver (1)
Blade holders (2)
Castroviejos (2)
Iris scissors (1)
Curved forceps (1)
Straight forceps (1)

Materials Needed (sterile):

#11 blades
#15 blades
4-0 vicryl suture
5-0 polypropylene suture
Surgical gowns
Surgical drape
Fire stick
Staple gun
Sodium Chloride
10 cc syringe

Materials Needed (non-sterile):

Scale
Clippers
Permanent Marker
Ear Punch
Knockout box (Tupperware container with two holes in side)
Lab notebook
Spray bottle filled with betadine/alcohol solution
Anesthesia machine with oxygen and isofluorane
Heat lamp
Cages filled with white alpha-chips
Nose-cone (2)

Pre-operative Analgesia and Anesthesia Protocol:

1. Administer buprenorphine (0.05 mg/kg) subcutaneously 30 minutes prior to surgery.
2. Place the rat in the Knockout box.
3. Insert the tubes for oxygen (or air) and isoflourane into each hole.
4. Turn the isofluorane on the flow level 5 until the rat falls asleep and does not respond to the pinch test.
5. Remove the tubes from the Knockout box and place them on the nose-cone.
6. Quickly take the rat out of the Knockout box and insert his nose into the nose-cone.
7. Decrease the isofluorane to flow level 2.
8. Shave the rats upper torso using the clippers.
9. Inject a few drops of lidocaine (1 mg/kg) at both sites of incision.
10. Weigh the rat.
11. If it is an odd numbered rat, use the ear-punch to clip a hole in the ear and mark his tail with permanent marker.
12. Clean the rats upper torso with alcohol-betadine solution using gauze.

Surgical Protocol for Spinal Accessory Nerve Transection:

1. Make a 2 cm vertical incision is made 1 cm posterior to the left ear.
2. Identify the cervical nerve, clavo-trapezius, and acromio-trapezius muscles.
3. Separate the clavo-trapezius and acromio-trapezius muscles cranial to the cervical nerve using blunt dissection with Iris scissors to expose the spinal accessory nerve, located above the omotransversarius muscle.
4. Transect the spinal accessory nerve 2 mm and 5 mm proximal to the acromio-trapezius and remove.
5. Irrigate the surgical site with sterile saline.
6. Close the overlying skin with staples.

Surgical Protocol for Long Thoracic Nerve Transection:

1. Abduct and internally rotate the rat’s forelimb.
2. Make a 3 cm axillary incision in the caudal direction along the abdominal fascia, exposing the serratus anterior muscle.
3. Identify the latissimus dorsi muscle and make an incision along the fascial interface.
4. Perform a blunt dissection between the latissimus dorsi muscle and serratus anterior to gain proximal exposure to the serratus anterior muscle and long thoracic nerve.
5. Transect the long thoracic nerve 2 mm and 5 mm proximal to the serratus anterior and remove.
6. Suture the abdominal fascia closed with 4-0 Vicryl suture.
7. Irrigate the surgical site with sterile saline.
8. Close the overlying skin with staples.

Surgical Protocol for Supraspinatus Tendon Transection and Repair:

1. Make a 2 cm skin incision over the craniolateral aspect of the scapulohumeral joint and dissect through the deltoid, down to the rotator cuff musculature.
2. Identify the rotator cuff tendons as the subscapularis, the most anterior and broadest rotator cuff tendon, the supraspinatus, the tendon that passes under the bony arch created by the acromion, coracoid, and clavicle, the infraspinatus, posterior to the other tendons with a similar insertion to the supraspinatus.
3. Grasp the supraspinatus using a 5-0 poplypropylene suture using a modified Mason-Allen technique.
4. Detach the supraspinatus at its insertion point on the humerus using a sharp blade and allow the tendon to freely retract.
5. Use a 5mm diameter high speed burr (Multipro 395, Dremel, Mt. Prospect, IL) to remove any remaining fibrocartilage at the insertion site.
6. Drill a 0.5 mm anterior/posterior hole through the humerus just below the insertion site.
7. Secure the suture through the bone tunnel and reappose the tendon to the insertion site.
8. Suture the deltoid muscle closed with 4-0 Vicryl suture.
9. Close the overlying skin with staples.

Surgical Recovery and Post-Operative Analgesia Protocol:

1. Place rats in the cages with alpha-dry chips under a heat lamp until they awaken.
2. Administer buprenorphine (0.05 mg/kg) 6-8 hours following surgery and then every 12 hours for following 2 days.
3. Remove staples 1 week post-surgery.

A2. Overuse Protocol

All overuse protocols are performed with the treadmill position at a 10˚ decline.

Training Protocol:

Week	Day	Protocol
1	Mon	(0-10 min) <= 37 rpm
1	Tue	(0-15 min) <= 40 rpm
1	Wed	(0-20 min) <= 43 rpm
1	Thu	(0-25 min) <= 46 rpm
1	Fri	(0-30 min) <= 49 rpm
2	Mon	(0-30 min) <= 51 rpm
2	Tue	(0-5 min) <= 51 rpm, (5-40 min) <= 54 rpm
2	Wed	(0-5 min) <= 51 rpm, (5-45 min) <= 57 rpm
2	Thu	(0-5 min) <= 51 rpm, (5-10 min) <= 57 rpm, (10-50 min) <= 60 rpm
2	Fri	(0-5 min) <= 51 rpm, (5-10 min) <= 57 rpm, (10-60 min) <= 63 rpm

Overuse Protocol:

Week	Day	Protocol
1,2,3,4	Mon	(0-5 min) <= 51 rpm, (5-10 min) <= 57 rpm, (10-60 min) <= 63 rpm
1,2,3,4	Tue	(0-5 min) <= 51 rpm, (5-10 min) <= 57 rpm, (10-60 min) <= 63 rpm
1,2,3,4	Wed	(0-5 min) <= 51 rpm, (5-10 min) <= 57 rpm, (10-60 min) <= 63 rpm
1,2,3,4	Thu	(0-5 min) <= 51 rpm, (5-10 min) <= 57 rpm, (10-60 min) <= 63 rpm
1,2,3,4	Fri	(0-5 min) <= 51 rpm, (5-10 min) <= 57 rpm, (10-60 min) <= 63 rpm

A3. Dissection Protocol: Biceps and Supraspinatus

Materials Needed:

#11 blade
Blade holder
Rat toothed pick-ups
Curved hemostats

Dissection Procedure:

1. Clamp hemostats to paw with curved side facing rat and handles facing anteriorly. Externally rotate limb by flipping hemostats over and tucking underneath rat's abdomen.
2. Using the flat portion of the blade, make an incision along the spine of the scapula and expose shoulder and arm
3. Using flat edge of blade, make a transverse and slightly oblique incision inferior to the cephalic vein until bone is exposed
4. Follow the posterior border of the deltoid and incise downward and visualize fascia. Incise along anterior edge of bony tuberosity to expose the biceps muscle and peel away the deltoid
5. Starting at the cephalic vein, incise up along the posterior border of the scapular spine and peel away the trapezius anteriorly.
6. Laterally cut away the bursa, cut the AC joint, and peel away clavicle
7. Grab the acromion with the pick-ups, lift off of the body and cut away connective tissue, then twist pick-ups to break away acromion.
8. Incise along the posterior border of the biceps tendon and free tendon from humerus, being careful not to damage the supraspinatus. Cut any exposed ligaments around the humeral head.
9. Incise along the edges of the supraspinatus and peel back until joint capsule is exposed.
10. Incise along the inferior border of the subscapularis muscle and cut away excess muscle and connective tissue. Lift the coracoid process from the subscapularis and cut away the connective tissue. Peel the subscapularis away from the scapula and detach the subscapularis at its insertion on the humeral head.
11. Peel away posterior deltoid to expose the infraspinatus muscle. Incise along the borders of the infraspinatus and peel away from the scapula. Detach any remaining connecting ligaments. Detach the infraspinatus at its insertion on the humeral head.
12. Detach scapula from body.
13. Cut away excess muscle from the humeral head and expose down to the elbow joint. Dislocate the homers at the elbow and remove.

For mechanical testing:

1. Place the humerus and intact supraspinatus in small vial filled with 1X PBS until fine dissection.
2. To preserve the biceps tendon, cut away a square (~5 cm X 5 cm) of skin, fascia, and muscle from the dorsal area of the rat, adjacent to the shoulder.
3. Place scapula and biceps in tissue, spray with PBS, wrap with gauze, and place in separate Ziploc bag with specimen number labeled.
4. Place in -20˚C freezer until needed for mechanical testing

For histology:

1. Fold a Kimwipe to fit into a plastic cassette.
2. Using pins, secure the bone-tendon-muscle complex (for both the biceps and supraspinatus) to the Kimwipe in a flattened and straight position before placing the tissue in the cassette.
3. Place the cassette in Formalin for 7 days to allow for proper tissue fixation.

A4. Stain Line Protocol: Biceps and Supraspinatus

Materials Needed:

6-0 braided silk suture
Verhoeff's stain
Ruler
Small curved forceps

1. Place a small amount of Verhoeff's stain in a weighing boat. Allow a piece of 6-0 silk suture to rest in stain for approximately 20 minutes.
2. Fan the tendon out next to the ruler.
3. Blot the tendon with a Kimwipe to prevent the stain from running.
4. Use the suture to apply stain lines on the tendon at the tendon insertion then at 1.5, 3.5, 8.5, and 11.5 mm from the insertion for the biceps and at 2, 4, and 8 mm from the insertion for the supraspinatus.
5. Wait about 60 seconds and blot the tendon with the Kimwipe to prevent the stain from running.
6. Place the specimens back in the vials with PBS.

A5. Potting and Sand Paper Protocol: Biceps and Supraspinatus

Materials Needed:

Plastic tubing
Paper towel
Masking tape
PMMA (orthojet)
Sand Paper
Cyanoacrylate (superglue)
Curved forceps

1. Cut plastic tubing at ~1.5 inch intervals.
2. Cover bottom of tube with masking tape and label with specimen number.
3. Place a small amount of paper towel in the bottom of the pot.
4. Make PMMA (orthojet) following the manufacturer's directions.
5. Place each sample (scapula or humerus) in their respective pots and wait for the PMMA to cure.
6. Place the samples in a cup of PBS and place in refrigerator until hardened (~30 minutes).
7. Place the tendon between a small piece of sandpaper with superglue, lining up the edge of the sandpaper with the last stain line.

A6. Area Data Collection and Analysis

Data Capture:

1. Allow the laser to warm up for 20 minutes prior to use. Do this by turning on the switch box next to GisMO.
2. When ready to begin taking measurements, run Labview and open the Mogware program.
3. Remove tendon from PBS and dab briefly on both sides with Kimwipe.

For the supraspinatus:

1. Place tendon bursal side down and ensure tendon is lying flat with no space between tendon and base; if necessary, angle humerus.
2. The tendon should be oriented in the direction that it will be loaded; this will ensure that the area measurements correspond to the stain line regions and the loading direction.
3. Press the RUN (→) button in Mogware with the oval Capture button not activated.
4. Zero all positions (X, Y, Z) at first (insertion) stain line. Move laser to just after humeral head and note distance (A). This distance will vary between specimens.
5. Press the STOP button.
6. Press the RUN (→) button and click the oval Capture button to activate.
7. At distance (A), make first pass across the width of the tendon. The remaining passes are indicated by the distance (in millimeters) from the start (where the laser was zeroed).
8. Pass over tendon 1, 2, 3, 4, 6, and 8 mm.

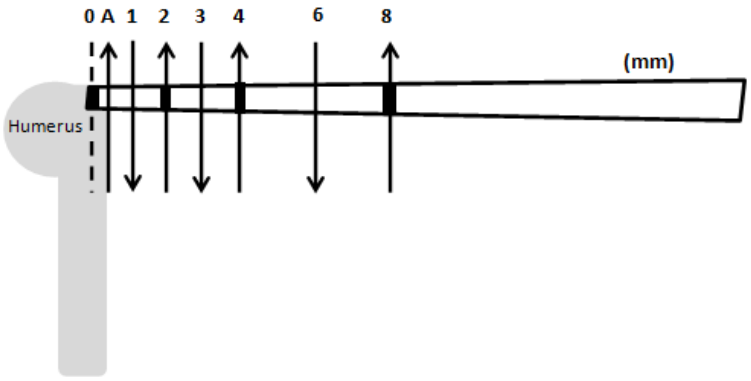

For the biceps:

1. Place the tendon bursal side down and ensure the tendon is lying flat with no space between the tendon and base; if necessary, prop up the scapula.
2. The tendon should be oriented in the direction that it will be loaded; this will ensure that the area measurements correspond to the stain line regions and the loading direction.
3. Press the RUN (→) button in Mogware with the oval Capture button not activated.
4. Zero all positions (X, Y, Z) at first (insertion) stain line, located just after the supraglenoid tubercle (at bony insertion of the glenoid).
5. Press the STOP button.
6. Press the RUN (→) button and click the oval Capture button to activate.
7. At 0.5 mm, make first pass across the width of the tendon. The remaining passes are indicated by the distance (in millimeters) from the start (where the laser was zeroed).
8. Pass over tendon at 1, 1.5, 2.25, 3.5, 4.75, 6.0, 7.25, 8.5, 10, and 11.5 mm.

Data Analysis:

1. Run the Matlab GUI named "gismo_area" (located in \\medfiles\ort\McKay_Lab_Folders\SoslowskyLab\Software-Released\gismo_area).
2. Load GisMO file.
3. Click "Mark GisMO" and select beginning and end of each pass over the tendon.
4. Label Pass 1 (mm) and Pass 2 (mm) with a negative sign before each number (e.g., -0 and -2 for supraspinatus insertion).
5. Click "Local Area" to calculate area for insertion, mid-substance, and the entire tendon.
6. Copy output from command window and save in Excel.

A7. Tendon Mechanical Testing Protocol: Biceps and Supraspinatus

1. Turn on equipment for at least 30 minutes before testing.
2. Fill the tank with 1X PBS and heat to 37˚C.

Data Capture for Images:

1. Load Digivlepo on image capture computer.
2. Position the camera to see from the insertion site to the upper grip.
3. Enter the name of the specimen in the appropriate field.

Data Capture for Instron:

1. Set up fixtures in Instron testing machine and use a 100 N load cell.
2. Load Bluehill and calibrate load cell with fixture attached. This only needs to be done once, at the beginning of the testing day.
3. Choose testing protocol.

For Biceps:

Block 1|absolute ramp: absolute ramp to 0.1 N at 0.115 mm/s
Block 2|preconditioning: 10 triangle cycles from 0.1 to 0.5 N at 0.0115 mm/s
Block 3|hold: 300 sec hold
Block 4|ramp: relative ramp to delta = 0.46 mm at 0.575 mm/s (4% strain)
Block 5|hold: 600 sec hold
Block 6|ramp: relative ramp to delta = 0.46 mm at -0.575 mm/
Block 7|hold: 60 sec hold
Block 8|ramp to failure: relative ramp to delta = 50 mm at 0.0345 mm/s (0.3%/s)

For Supraspinatus:

Block 1|absolute ramp: absolute ramp to 0.1 N at 0.03 mm/s
Block 2|preconditioning: 10 triangle cycles from 0.1 to 0.5 N at 0.03 mm/s (1%/s)
Block 3|hold: 300 sec hold
Block 4|ramp: relative ramp to delta = 0.4 mm at 0.4 mm/s (5% strain)
Block 5|hold: 600 sec hold
Block 6|return ramp: relative ramp to delta = 0.4 mm at -0.4 mm/s
Block 7|hold: 60 sec hold
Block 8|ramp to failure: relative ramp to delta = 50 mm at 0.024 mm/s (0.3%/s)

Running Test:

1. Zero load when tendon is slack.
2. Manually pre-load tendon to 0.08 N.
3. Zero extension when load reads 0.08 N.
4. Simultaneously begin loading protocol and image capture program.
5. After pre-conditioning cycles have completed, set timer for 4.5 minutes.
6. Once timer alarms, set image capture mode to "on" and capture images at 2 frames per second until the peak of the stress relaxation.
7. Turn off image capture and set timer for 10.5 minutes.
8. When timer alarms, set image capture mode to "on" to capture images at 2 frame per second until the specimen fails.
9. Stop image capture program and stop/finish loading protocol.
10. Manually raise Instron to better visualize how specimen failed (e.g., at grip, at mid-tendon, at insertion, etc.).
11. Acquire calibration image by taking image of ruler (millimeter side).
12. Remove specimen.
13. Save Instron data and images to Data folder on computer by date.

A8. Tendon Mechanical Testing Analysis Protocol: Biceps and Supraspinatus

General Analysis Protocol:

1. Run the Matlab GUI named "rawful" (located in \\medfiles\ort\McKay_Lab_Folders\SoslowskyLab\Software-Released\rawful).
2. Load Instron Data.
3. Select failure load.
4. Set GUI to Block #25 and Block #29 to highlight appropriate peak and equilibrium loads from Stress-Relaxation curve.
5. Click "Text Output" to export Instron Data, Relaxation Data, and Failure Data.
6. Copy output from command window and paste in Excel.

QLV Analysis Protocol:

1. Run the Matlab code "qlv_lmfit.m" (located in \\medfiles\ort\McKay_Lab_Folders\SoslowskyLab\Software-Released\qlv-lanir).
2. Open rlx.txt file.
3. Copy output from command window and paste in Excel.

Optical Strain Protocol:

1. Run the Matlab GUI named "optikos" (located in \\medfiles\ort\McKay_Lab_Folders\SoslowskyLab\Software-Released\optikos).
2. Load images.
3. Set GUI to Contrast Enhanced to filter images.
4. Click "Instron Restrict" and select corresponding Instron data to isolate ramp-to-failure curve (and corresponding images) from data.
5. Click "Choose ROIs" and draw an ROI on the left edge (L) and right edge (R) of each stain line (S).
6. Click "Track ROIs". The program will track the stain lines.
7. Click "Text Output" and save file with original extension (trk.txt) and add stain line number and LR (e.g., Specimen_S1-LR_trk.txt).
8. Repeat to track each stain line and displacement of the pot (or bone).
9. Run the Matlab code "apply_disp.m" in order to apply displacements from the pot (or bone) to the insertion stain line (S1).
10. Save applied displacement and indicate it is synthetic (SYN) (e.g., Specimen_SYN-S1-LR_trk.txt).
11. Run the Matlab code "LRtrk_element.m" in order to track strain between adjacent stain lines.
12. Save tracking and indicate which stain lines were tracked (e.g., Specimen_S1-S2_eopt2D.txt).
13. Run the Matlab code "el2d_stiffness.m" in order to create load vs. strain curve.
14. Load tracking and Instron data.
15. Select linear region of load vs. strain curve using the Data Selector.

16. Save XY-plot and copy output from command window and paste in Excel.
17. Repeat for each specimen.

Image Calibration Protocol:

1. Run the Matlab code "calib_image.m".
2. Select calibration image (image of ruler).
3. Draw line over 5 mm on ruler and enter calibration object length of 5 mm.
4. Copy output from command window and paste in Excel.

Calculate Percent Relaxation, Modulus, and Stiffness:

1. For percent relaxation, divide equilibrium load from peak load and subtract this value from 1.
2. For modulus, multiply stiffness value [Kstrn (N/%)] by 100% and divide by cross-sectional area of specimen.
3. For stiffness, multiply stiffness value [Kopt (N/pix)] by calibration (pix/mm).

A9. Cartilage Thickness Ultrasound and Analysis Protocol

Ultrasound Scanning Protocol:

1. Plug in and turn on machine
2. Switch on computer, using large black lever located on back of machine AND black button on left side
3. Attach Vevo 770 window to 55 MHz ultrasound probe.
4. Using a flat-head screw-driver, remove screw and fill transducer container with DI water using squirt bottle. Be sure that no bubbles are present in container.
5. Plug probe into machine, aligning the red dot on the probe with the red dot on the port.
6. Initialize probe.
7. Open Software and indicate operator.
8. Click "New".
9. Type in study name
10. Set-up 3D Motor and plug in port labeled "3D motor" on rear of machine.
11. Position longitudinal portion of motor transverse to the scapular plane.
12. Position the transducer in plane with the scapula.
13. Initialize 3D motor. Be sure nothing is in range of motor travel distance (probe will move the full range).
14. Orient the central portion of the glenoid to be flat in both the coronal and sagittal planes and centralized in the fixture. The glenoid should be positioned such that the inferior portion is closest to you and the superior portion is furthest away.
15. The probe should be centered over the glenoid. It then translates to the LEFT and then acquires images from LEFT to RIGHT (for a left shoulder, anterior to posterior).
16. Position the transducer in plane with the scapula.
17. Lower the transducer until the glenoid is visible and 'flat' in the focal zone (adjust glenoid positioning as necessary).
18. Click on "Mode" and "3D Mode".
19. Adjust settings: Step size (0.250 mm) and Range (10 mm).
20. Press scan on keyboard (images will be acquired throughout range.
21. Save by selecting "Export Image" (as .rdb).
22. Close session and select commit session data.
23. Repeat for additional specimens.

Data Analysis Protocol:

1. Run the Matlab code "rdb_writestack.m" (located in \\medfiles\ort\McKay_Lab_Folders\SoslowskyLab\Software-Released\gac_us).
2. Select .rdb file created by ultrasound machine and program will convert to stack of .tif files. These images will be segmented in next step.
3. Run the Matlab code "cart_segment.m" (located in \\medfiles\ort\McKay_Lab_Folders\SoslowskyLab\Software-Released\gac_us).
4. Select .tif file. Start with first file in which cartilage is visible
5. Segment top and bottom of cartilage (double click last selected point)
6. Save SEG#_seg.txt file
7. Continue segmenting .tif files until cartilage is no longer visible (i.e., all cartilage has been segmented for the specimen).
8. Repeat process a total of 3 times. Label # as 1, 2, or 3
9. Save in folders labeled [SEG1, SEG2, SEG3] for each specimen.
10. Run the Matlab code "make_thickmap.m" (located in \\medfiles\ort\McKay_Lab_Folders\SoslowskyLab\Software-Released\gac_us).
11. Select folder with _seg.txt files
12. Double click one _seg.txt (this will grab all .txt files in folder).
13. Prompt will ask for location of metal post which was originally used to determine orientation (i.e., anterior/posterior) (Note: If you don't have metal post and you scanned anterior to posterior, choose "anterior")
14. Calculate thickness map from series of segmented images
15. Save _thmap.txt file in folder labeled THMAPS.
16. Run the Matlab code "rot_thmap.m" (located in \\medfiles\ort\McKay_Lab_Folders\SoslowskyLab\Software-Released\gac_us).
17. This program automatically rotates thickness map in plane with the scapula
18. Save ROT_thmap.txt file in folder labeled THMAPS.
19. Run the Matlab code "regional_mask.m" (located in \\medfiles\ort\McKay_Lab_Folders\SoslowskyLab\Software-Released\gac_us).
20. This program automatically divides glenoid into regions and calculates area in each region.
21. Copy and paste output from command window into Excel file for SEG1, SEG2, and SEG3.

Calculate Regional Thickness:

1. Average SEG1, SEG2, SEG3.
2. Determine thickness for each region.

Calculate Local Thickness:

1. Run the Matlab code “thmap_circregions.m” ” (located in \\medfiles\ort\McKay_Lab_Folders\SoslowskyLab\Software-Released\gac_us).
2. This will determine the thickness in each of the regions for mechanical testing.
3. If not accurate, run the Matlab code “adjust_regions.m” (located in \\medfiles\ort\McKay_Lab_Folders\SoslowskyLab\Software-Released\gac_us) and re-position regions.

A10. Cartilage Mechanical Testing and Analysis Protocol

Protease Inhibitor Cocktail:

Ingredients:

Benz-HCl (MW 156.6): 500mM stock = 0.0783g in 1 ml meth; working concentration 5mM
PMSF (MW 174.1):100mM stock = 0.0174g in 1ml meth; working concentration 1mM
NEM (MW 125.1):1M stock = 0.125g in 1ml meth; working concentration 10mM

1. To get your working concentrations, add 10ul stock for every 990ul buffer (1:100 dilution)
2. Make sure to mix your buffer solutions well after adding the inhibitors.
3. Example of Working Concentration:

   198mL PBS (approximate size of dissection cups)
   2 mL methanol + 0.1566 g Benz-HCl + 0.0348 g PMSF + 0.25 g NEM

4. Example of 5 mL Stock Solution:

   5 mL methanol + 0.3915g Benz-HCl + 0.087 g PMSF + 0.625 g NEM

Mechanical Testing Protocol:

1. Clamp spherical indentor tip (500 um) with pin vice
2. Attach pin-vice to fixture
3. Attach fixture to 5 N load cell and calibrate load cell. This only needs to be done once, at the beginning of the testing day.
4. Load Blue-Hill and testing protocol:
   Block 1|Relative ramp with a delta of 0.008 mm at 0.002 mm/sec
   Block 2|Hold 300s
   Block 3|Repeat 1st block
   Block 4|Repeat 2nd block
   Block N|NOTE: N= (Number of Indentations)*2
5. Label the specimen name and location to save file
6. Place potted scapula in fixture
7. Start with rotational stage and angular stages at 0°.
8. Orient the superior portion of the glenoid to be flat in both the coronal and sagittal planes and centralized in the fixture. The glenoid should be positioned such that the inferior portion is closest to you and the superior portion is furthest away
9. Position the indentor over the superior region of the glenoid
10. Use a syringe to add the PBS w/ protease inhibitor such that the top of the pin vice is completely submerged

11. Preload tissue to approximately 0.005 N using the manual gauge
12. Begin test. Finish and save test
13. Readjust testing protocol for number of indentations for center region
14. Orient the center portion of the glenoid to be flat in both the coronal and sagittal planes and centralized in the fixture (*Use PBS line as a level). The glenoid should be positioned such that the inferior portion is closest to you and the superior portion is furthest away
15. Position the indentor over the center region of the glenoid
16. Preload tissue to approximately 0.005 N using the manual gauge
17. Begin test. Finish and save test
18. Readjust testing protocol for number of indentations for antero-superior region
19. Rotate the stage to 45˚.
20. Reorient the center portion of the glenoid to be flat in both the coronal and sagittal planes (try to keep angle at 45˚, use PBS line as a level)
21. Angle the platform to [15˚] and translate in the x-y axes, bringing the antero-inferior portion of the glenoid orthogonal to the indentor
22. Preload tissue and begin test. Finish and save test
23. Readjust testing protocol for number of indentations for antero-superior region
24. Angle the platform to [0˚]
25. Rotate the stage to 315˚.
26. Reorient the center portion of the glenoid to be flat in both the coronal and sagittal planes (try to keep angle at 315˚, use PBS line as level)
27. Angle the platform to [15˚] and translate in the x-y axes, bringing the antero-superior portion of the glenoid orthogonal to the indentor
28. Preload tissue and begin test. Finish and save test
29. Repeat steps 12-14, subtracting 90˚each time for the postero-superior and postero-inferior regions, respectively.

Positioning and Indentation Summary:

Region	Rotation	Indentations
Superior	0˚	4
Center	0˚	6
Anterior-Inferior	45˚	6
Anterior-Superior	315˚	6
Posterior-Superior	225˚	6
Posterior-Inferior	135˚	6

Analysis Protocol:

1. Run the Matlab code “load_mask.m” (located in \\medfiles\ort\McKay_Lab_Folders\SoslowskyLab\Software-Released\gac_indent) and include output information: [P,wo,EqLoad,EqDisp,thick,pth,PkDisp,PkLoad].
2. Select Instron File.
3. Select corresponding thickness file located in THMAPS folder (e.g., Specimen_circregion.txt)
4. Select indentation region.
5. Select equilibrium loads and displacements on graph.
6. Run the Matlab code “hayes_modulus.m” (located in \\medfiles\ort\McKay_Lab_Folders\SoslowskyLab\Software-Released\gac_indent) and include input information: (P,wo,thick,pth).
7. Copy and paste output from command window into Excel file.

A11. Histology Protocol: Processing, Embedding, Sectioning

Fixation and Decalcification:

1. Remove tissue in cassette from Formalin after 7 days.
2. Transfer cassettes to Immunocal for 7 days (change immunocal every few days
3. On the 7th day, check the specimens for complete decalcification using the fluoroscope.
4. If decal is complete, transfer cassettes to 70% EtOH

Processing:

For Biceps:

Day 1 (7.5 hrs total)
1) 70% EtOH for 45 min at 37˚C (~ 1 notch) and vacuum at 15 psi
2) 95% EtOH for 45 min at 37˚C and vacuum at 15 psi
3) 100% EtOH for 3 hrs at 37˚C and vacuum at 15 psi
4) Xylene for 3 hrs at 37˚C and vacuum at 15 psi
5) Leave at room temperature in xylene overnight

Day 2 (3 hrs. total)
1) Change cup and place cassettes in paraffin wax tray while you heat the oven to 62˚
2) Paraffin for 2.5 hrs at 62˚C (~ 1) and vacuum at 15 psi
3) Cut glenoid from biceps (leaving bone chip), and then put both sections back in paraffin for 40 min at 62˚C

For Supraspinatus:

Day 1 (7 hrs total)
1) 70% EtOH for 60 min at 37˚C and vacuum at 15 psi
2) 95% EtOH for 60 min at 37˚C and vacuum at 15 psi
3) 100% EtOH for 5 hrs at 37˚C and vacuum at 15 psi
4) Leave at room temperature in xylene overnight

Day 2 (9.5 hrs total)
1) Xylene for 4.5 hrs at 37˚C and vacuum at 15 psi
2) Change cup and place cassettes in paraffin wax tray while you heat the oven to 62˚C
3) Paraffin for 3.5 hrs at 62˚C and vacuum at 15 psi
4) Cut sample in half, and then put both sections back in paraffin for 1.5 hrs at 62˚C

Embedding:

1. Place cassettes in the paraffin wax tray.
2. Fill a paraffin casting mold half way with paraffin and place on the cold block.
3. When a small layer of wax on the bottom is solidified, place the sample in the wax and flatten it to the bottom.
4. Place cassette on the top of the mold and fill with paraffin.
5. Tap bubbles out of the wax.
6. Place on cool block to harden.

Sectioning:

1. Make an ice bath.
2. Soak the ice bath for at least 20 minutes prior to sectioning.
3. Turn the water bath on to 1.5 (optimal temperature is 37-40˚C).
4. Make sure the angle of sectioning is at 15 (this should not change).
5. Mount the block in the microtome and align it so it sections evenly across the surface.
6. Make sure the section is being cut from bone to tendon.
7. Face off the block using a thickness of 10 µm until you start sectioning tissue.
8. Adjust the tilt so that you are sectioning the tissue evenly.
9. Remove the block and allow it to cool in the ice bath again.
10. Once cooled, place back on the microtome and switch the sections to 7 µm.
11. Place ribbons in the water bath to remove wrinkles in paraffin and put 2 sections per slide.
12. Collect a 10-15 slides per specimen.
13. Verify integrity of section using light microscope.
14. Bake slides for 1 hour at 60˚C.

A12. Histology Protocol: H&E Staining

De-waxing:

3 minutes	Xylene
3 minutes	Xylene
3 minutes	Xylene

Dehydration:

2 minutes	100% Ethanol
2 minutes	100% Ethanol
2 minutes	100% Ethanol
2 minutes	95% Ethanol
2 minutes	95% Ethanol
2 minutes	70% Ethanol
2 minutes	DH2O

Stain:

10 minutes	Hematoxylin

Rinse:

Until water is clear	DH2O
3 Dips	Clarifier
2 minutes	DH2O
3 Dips	Bluing
2 minutes	DH2O
2 minutes	95% Ethanol

Stain:

10 seconds	Eosin

Rehydration:

2 minutes	95% Ethanol
2 minutes	95% Ethanol
2 minutes	100% Ethanol
2 minutes	100% Ethanol
2 minutes	100% Ethanol
3 minutes	Xylene
3 minutes	Xylene

3 minutes Xylene

A13. Histology Protocol: Bioquant for Cellularity and Cell Shape

To open existing data set:

1. File>> Open Data Set>> select your data volume>> select a data set>> press "Open"

   Note: Data Directory should be on C:\BQDATA\ in order for the name of your data volume to appear in the scroll menu. If you click "Browse" and search within the BQDATA folder there will only be numbered folders, e.g. "DATA170".

To create new data volume:

1. Open existing data set, which has functions you desire (e.g., Supra_8wk_SD>>27-027_S20_Insertion). This allows you to keep functions that calculate total area, cell count, cell shape, and cell area.
2. File>> New Data Set>> Create New Data Volume. This allows you to create new Data Volume that has aforementioned prewritten function.
3. Keep Data Directory as C:\BQDATA\
4. Finish Wizard. Note which Data Volume you created (e.g., "DATA170"). This will information will be needed to save data later.

To create a new data set within the same data volume:

1. Image>>Type: Image File>> Open Single>> Select Image to Analyze
2. On Large Image Navigator, set it to 1:2.
3. Before doing anything else, create a new data set. File>>Quick Data Set>>Rename the New Data Set >> Current Data Set >>Create
4. Choose correct camera magnification/calibration. Parameters >> Mag (Nikon "N")>>Assign. To switch cameras, Image>>Calibration>>File>>Load>>e.g., Nikon.cal

To analyze image:

1. Define ROI (Region of Interest). Usually full screen, but if not: Irregular>> Click "Spacebar to End" >> Define>>Select ROI with mouse and push spacer bar and RIGHT click to end. There will be a green outline. Unclick "Space Bar to End".
2. Select Array: Double Click on A2 Area. Notice value will be (1).
3. Select Array: Double Click on A1 Cell Area. Notice value will be (0).
4. Adjust Threshold: Press "Select">>Click on cells> Same color regions will turn pink. Once satisfied, right click.

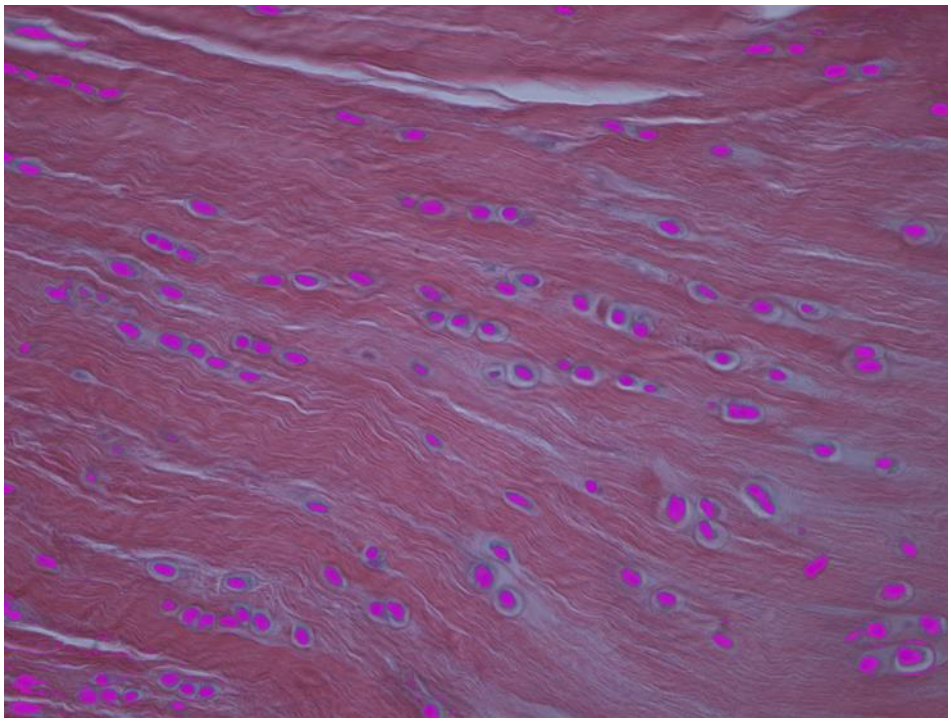

5. Press “Preview” and a yellow outline will form around each cell. Note: Each yellow-bordered region is what Bioquant will recognize as a cell, not the pink. Numbers next to “Preview” control smoothness and filtering of yellow border. Click apply, then preview to test.

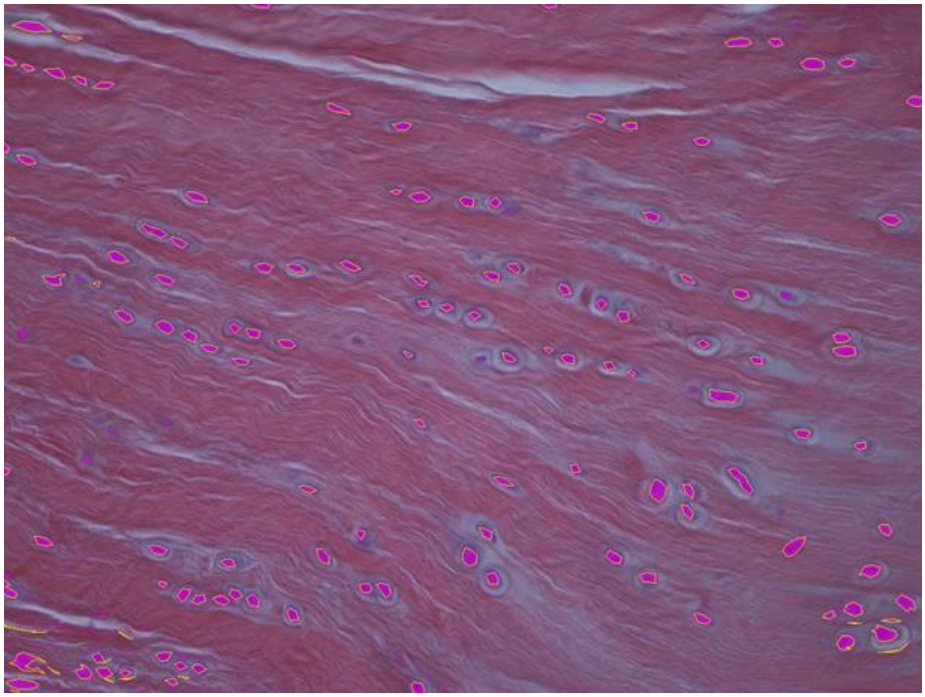

6. Fine-Tune Selection: Color-in cells. Click “Draw Threshold”>>Use mouse to color in cells>>Use mouse scroller to adjust marker size>> Right click to end. Note: Right clicking allows your cursor to exit the picture window and it also creates a yellow border around each cell. Bioquant only registers these yellow bordered regions as cells, not the pink.
7. Fine-Tune Selection: Draw cells. To increase accuracy of cell shape drawings, decrease cursor speed by pressing the negative shortcut on the mouse. Using the smallest marker size of the paintbrush, draw an enclosed border for each cell instead of filling in the entire cell.
8. Fine- Tune Selection: Erase cells. Click “Erase Threshold”>>Use mouse to color over unwanted regions>> Use mouse scroller to adjust eraser size>> Right click to end. Note: Watch out for small, yellow regions that Bioquant picks up without your knowledge. Erase these and look at text file for cells with area ~0. These “cells” are actually noise.
9. When satisfied, click “Preview”>> click “Measure”.
10. File >> Save

Useful Tools:

1. Press “Show” and pink fill will disappear. This will allow for qualitative evaluation of accuracy of pink on cells. Press “Show” again to make pink fill reappear.

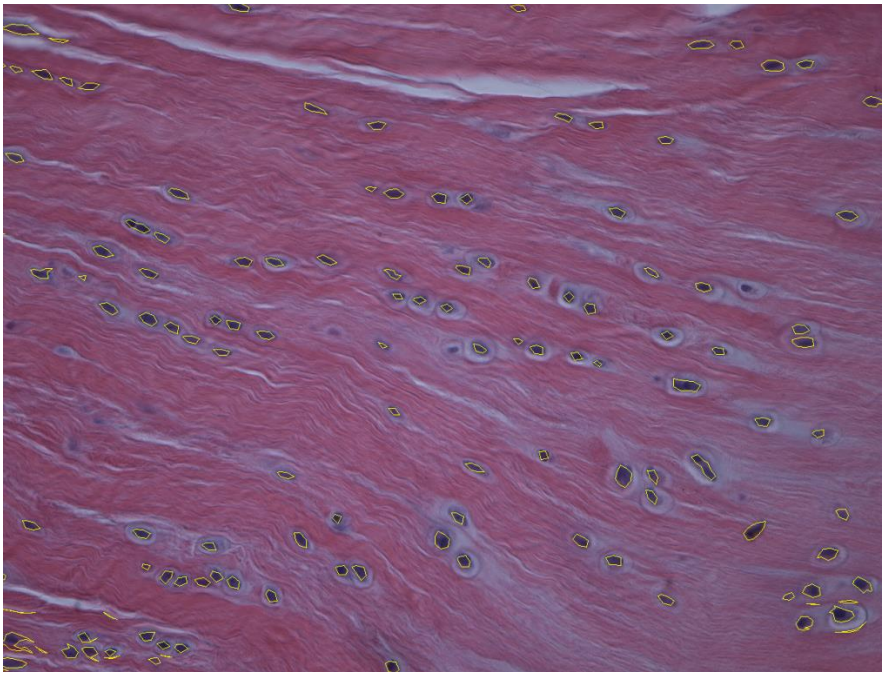

2. To more quickly switch between the Eraser tool and Paintbrush tool, press either of the two arrows located by your thumb. You must already have selected either the paintbrush or eraser for this shortcut to work.

To Export Data as a .txt File:

1. File>> Data Manager
2. Uncheck: Desktop>> My Computer>> OS(C:)>>BQDATA>>Click “DATA###”
3. Click on the icon of a folder with binoculars on top
4. Select which Data Set you require>>Right Click>>Click “Save to File”

A14. Histology Protocol: Grading for Supraspinatus Repair

1. Before you begin, you must rename all H&E stained pictures with a letter in order to blind the graders. Be sure to keep track of the original specimen name and associated letter.
2. Open a blank PowerPoint presentation.
3. Place each stained image into the PowerPoint file, arranging from most elongated to most rounded cell shape (or least to most cellular).
4. After all images have been placed into the file, break images into 3 equal sections.
5. Choose the middle image (approximately) in each section to represent that grade (for example 1,2,3).
6. Create a separate PowerPoint slide with these standard images and associated grades.
7. Instruct each blinded grader to set this image as their desktop, and then open each image to be graded against it.
8. Have them record their grade for each image.
9. After all 3 blinded graders are finished; assign the mode of the grades among them to each sample.
10. Repeat for each tendon location.
11. Repeat for cellularity.

A15. Histology Protocol: Polarized Light and Analysis

Image Acquisition:

The setup on the microscope from top to bottom should be: eyepiece, rotating analyzer, objective, slide, stage, condenser, compensator (only for compensated images as described below), rotating polarizer

1. Turn on the microscope and the camera (plug fire wire cable into either input on side of camera)
2. Using the 5X objective, focus the condenser so that the edges of the hexagon are sharp. (Dial at bottom left of microscope, on the base, changes the size of the hexagon. Condenser is focused using black knobs under stage)
3. Find the region of interest (e.g., injury) and focus the specimen
4. As you change objectives to 10X, ensure that the edges of the hexagon are still in focus and that the specimen is still in focus
5. Upon reaching the desired magnification, move the condenser hexagon out of view.
6. On the computer connected to the microscope, load Capture Pro software. Click on the camera icon to bring up the capture menu. Click Preview to view the image.
7. Rotate the stage until the tendon is at a ~45˚ angle (bottom left to top right) and then lightly tighten the stage.
8. Set the analyzer to 180˚ and the polarizer to 270˚. This position will be considered 45˚ when saving the images.
9. Turn the light all the way up and ensure that all light is directed toward the camera.
10. Take the noncompensated images first. With the 10X objective in place, load the PolLightUncomp profile. Without the analyzer and polarizer, click Auto White Balance and select a region of the slide that does not contain the specimen. Slide the analyzer and polarizer in place and click Auto Exposure.
11. Rotate both the analyzer and polarizer in a clockwise direction by the same increment (10˚). For both noncompensated and compensated images, pictures need to be taken across a 90˚ range in 10˚ increments.
12. Press Snap and save each picture as a .tiff file. For each specimen, create a folder with the specimen number. Within this, create separate folders for compensated and noncompensated images. Save pictures using a 3 digit filename format. For example, a picture taken at 45˚ should be saved as 045. Repeat until a span of 90˚ (image named 135) has been reached.
13. Insert the compensator in its slot above the polarizer with the nail pointing down. The compensator must be oriented 45˚ counterclockwise from analyzer and polarizer (i.e., compensator nail should be pointing at 225˚ – the blue dot – on the polarizer).
14. Load the PolLightComp profile and adjust exposure as needed.

15. Repeat steps l and m; however, this time rotate the compensator in a clockwise direction with the analyzer and polarizer (make sure that compensator is always oriented 45° from the analyzer and polarizer while you are rotating). Instead of going from light to dark (or vice-versa) as you rotate analyzer compensator and polarizer, the images should go from blue to red (or vice versa).
16. Turn off camera by unplugging fire wire cable and turn off microscope lamp.

Data Analysis:

1. Run the Matlab code "polarware_gui.m" (located in \\soslowskylab\max\software cooker-freezer\polarware\released).
2. Press button "NON-compensated".
3. Navigate to the correct directories where the noncompensated and compensated images are saved and click on a noncompensated image.
4. Change parameters to desired values (suggested values below):

   Bundle spacing determines the pixel distance between adjacent bundles (left, right, top, bottom)

   Bundle spacing = 50 (for non-repaired tendon)
   Bundle spacing= 30 (for repaired supraspinatus)

   Bundle size determines the size of each bundle. This value must be odd.

   Bundle width = 7 (for non-repaired tendon)
   Bundle spacing= 5 (for repaired supraspinatus)

5. Input desired file prefix in the Output File Prefix box.
6. Press button "NON-Bundle" and save the INTD file.
7. Press button "NON-Fit" and save the NNF file.
8. Press button "COM-Bundle" and save the INTD file.
9. Press button "COM-Fit" and save the CNF file.
10. Press button "Shift noncomp" and save the SNF file.
11. Press button "Apply Mask". Change automask parameters to desired values:

    Phi-CI Threshold = 10 (for non-repaired tendon)
    Phi-Sensitivity Threshold = 0.5 (for non-repaired tendon)
    P2P Int Threshold= 20 (for repaired supraspinatus ONLY)

12. Go through each pixel bundle and ensure that the noncompensated and compensated light intensity graphs look good. If the noncompensated or compensated light intensity graphs do not look good (i.e., very noisy) and/or are on a section of the slide that is not tendon, press button "Manual Mask" and click on the bundles to mask, then hit "Enter" on keyboard when finished.
13. Press button "Save Mask" and save the MSK file
14. Press button "OUTPUT RESULTS" and copy the data to an Excel file.

A16. Immunohistochemical Staining Protocol: Collagen II

Preparation:

Antibody Preparation:

1. Primary: Col II (antibody II-II6B3)
    a. Store in refrigerator
2. Secondary: Biotin Rat Anti-Mouse IgG1 (antibody 550331)
    a. Store in refrigerator

Solutions Needed:

1. H_2O_2
    a. 3% solution
    b. Dilute 30% hydrogen peroxide in methanol
    c. 100 ul H_2O_2 in 900 ul methanol
2. Hyaluronidase
    a. Dilute 0.5mg of Hyaluronidase in 1 mL PBS (aliquots stored at -20°C)
3. Acetic Acid
    a. Dilute 1.43 mL of Acetic Acid in 48.57 mL DI H_2O
4. Skim Milk
    a. 0.5 g skim milk powder in 10 mL PBS
5. Horse serum
    a. 1:100 dilution
    b. 1 ml serum in 99 ml 1x PBS
6. Primary Antibody
    a. 1:4 dilution
    b. Dilute 250 µl Ab in 750 µl Horse serum
7. Secondary Antibody
    a. 1:100 dilution
    b. Dilute 10 µl Ab in 990 µl Horse serum
8. Vectastain
    a. Prepare 30 minutes prior to use
    b. Mix 1 drop Reagent A in 2.5 mL PBS, vortex. Add 1 drop Reagent B, vortex.
9. DAB
    a. Remove DAB tablets from freezer 30 min prior to use (warm to room temp)
    b. Add 1 gold + 1 silver to 5 ml dH_2O and vortex to dissolve tablets

Other supplies needed:

1. PAP pen
2. IHC slide chamber
3. 1 ml pipette

4. 20 µl pipette

DAY 1

Deparaffanize sections:

1. CitriSolv®	5min×3 times
2. 100% EtOH	5min
3. 95% EtOH	5min
4. 70% EtOH	5min
5. 50% EtOH	5min
6. DI H_2O	5min

7. Mark around samples using water-proof pen.

Digestion (antigen retrieval; unmasking):

1. Incubate samples in 200µl of Hyaluronidase (Solution 2) for 60 min at 37°C.
2. Rinse 3X with PBS for at least 5 min each.
3. Line IHC chambers with wet paper towels (close lid during incubation).
4. Incubate samples in 0.5 N Acetic acid- DI H_2O (Solution 3) for 4 hours at 4°C.
5. Rinse 2X with PBS for at least 5 min each.

Block for endogenous peroxidase:

1. Incubate samples in 3% H_2O_2-Methanol (Solution 1) for 10 min at room temperature.
2. Rinse with PBS for at least 5 min.

Block non-specific binding:

1. Apply 5% skimmilk-PBS (Solution 4) for 30 minutes to eliminate background staining.

Primary Antibody:

1. Apply primary antibody II-II6B3 (Solution 6) to cover samples. For negative control, apply the same amount of 1% Horse Serum-PBS (Solution 5).
2. Close the lid of the moist chamber.
3. Incubate overnight (approximately 16 hours) at 4°C.

DAY 2

1. Rinse 3X with PBS for at least 5 min each.

Secondary Antibody and Vectastain:

1. Apply secondary antibody 550331 (Solution 7) to cover samples and incubate for 30 min at room temp.
2. Rinse 2X with PBS for at least 5 min each.
3. Apply VECTASTAIN ABC reagent (Solution 8) to cover samples and incubate for 30 min at room temp.
4. Rinse with PBS for at least 5 min.

DAB enzymatic reaction:

1. Incubate in DAB (Solution 9) under hood for 4 min at room temp.
2. Immediately rinse with tap water to end reaction

Dehydration and coverslip:

1. Rinse 3X with PBS for at least 5 min.
2. DI H_2O 1min
3. 70% EtOH 2min×2 times
4. 95% EtOH 2min×2 times
5. 100% EtOH 2min×2 times
6. CitriSolv® 5min×2 times
7. Add four drops of Cytoseal, coverslip, and dry slides overnight.

A17. Immunohistochemical Staining Protocol: Collagen III

Preparation:

Antibody Preparation:

1. Primary: Col III (antibody C7805)
    a. Aliquot 10 ul into small eppendorf tubes (store at -20°C)
2. Secondary: Biotin Rat Anti-Mouse IgG1 (antibody 550331)
    a. Store in refrigerator

Solutions Needed:

1. H_2O_2
    a. 3% solution
    b. Dilute 30% hydrogen peroxide in methanol
    c. 100 ul H_2O_2 in 900 ul methanol
2. Protease K
    a. Dilute 0.4 mg of Pro K in 1 mL of 30mM Tris HCL
3. Hyaluronidase
    a. Dilute 0.5mg of Hyaluronidase in 1 mL PBS (aliquots stored at -20°C)
4. Acetic Acid
    a. Dilute 1.43 mL of Acetic Acid in 48.57 mL DI H_2O
5. Horse serum
    a. 1:10 dilution
    b. 1 ml serum in 9 ml 1x PBS
6. Primary Antibody
    a. 1:500 dilution
    b. Dilute 10 µl Ab in 4990 µl PBS
7. Secondary Antibody
    a. 1:100 dilution
    b. Dilute 10 µl Ab in 990 µl Horse Serum
8. Vectastain
    a. Prepare 30 minutes prior to use
    b. Mix 1 drop Reagent A in 2.5 mL PBS, vortex. Add 1 drop Reagent B, vortex.
9. DAB
    a. Remove DAB tablets from freezer 30 min prior to use (warm to room temp)
    b. Add 1 gold + 1 silver to 5 ml dH_2O and vortex to dissolve tablets

Other supplies needed:

1. PAP pen
2. IHC slide chamber
3. 1 ml pipette
4. 20 µl pipette

DAY 1

Deparaffanize sections:

1. CitriSolv®	5min×3 times
2. 100% EtOH	5min
3. 95% EtOH	5min
4. 70% EtOH	5min
5. 50% EtOH	5min
6. DI H_2O	5min

7. Mark around samples using water-proof pen.

Digestion (antigen retrieval; unmasking):

1. Incubate samples in 200µl Protease K (Solution 2) for 4 min at room temperature.
2. Rinse 2X with PBS for at least 5 min each.
3. Incubate samples in 200µl of Hyaluronidase (Solution 3) for 60 min at 37°C.
4. Rinse 2X with PBS for at least 5 min each.
5. Line IHC chambers with wet paper towels (close lid during incubation).
6. Incubate samples in 0.5 N Acetic acid- DI H_2O (Solution 4) for 4 hours at 4°C.
7. Rinse 2X with PBS for at least 5 min each.

Block for endogenous peroxidase:

1. Incubate samples in 3% H_2O_2-Methanol (Solution 1) for 10 min at room temperature.
2. Rinse with PBS for at least 5 min.

Block non-specific binding:

1. Apply 10% Horse serum-PBS (Solution 5) to cover samples and incubate for 20 min to eliminate the background staining.

Primary Antibody:

1. Apply primary antibody C7805 (Solution 6, *modified from Peltz protocol according to Barbe protocol) to cover samples. For negative control apply the same amount of PBS.
2. Close the lid of the moist chamber.
3. Incubate two nights and three days (approximately 34-38 hours) at 4°C.

DAY 3

1. Rinse 3X with PBS for at least 5 min each.

Secondary Antibody and Vectastain:

1. Apply secondary antibody 550331 (Solution 7) to cover samples and incubate for 30 min at room temp.
2. Rinse 2X with PBS for at least 5 min each.
3. Apply VECTASTAIN ABC reagent (Solution 8) to cover samples and incubate for 30 min at room temp.
4. Rinse with PBS for at least 5 min.

DAB enzymatic reaction:

3. Incubate in DAB (Solution 9) under hood for 4 min at room temp.
4. Immediately rinse with tap water to end reaction

Dehydration and coverslip:

1. Rinse 3X with PBS for at least 5 min.
2. DI H_2O 1min
3. 70% EtOH 2min×2 times
4. 95% EtOH 2min×2 times
5. 100% EtOH 2min×2 times
6. CitriSolv® 5min×2 times
7. Add four drops of Cytoseal, coverslip, and dry slides overnight.

A18. Immunohistochemical Staining Protocol: Decorin

Preparation:

Antibody Preparation:

1. Primary: Decorin (antibody LF-113)
    a. Aliquot 6 ul into small eppendorf tubes (store at -20°C)
2. Secondary: Biotin Goat Anti-Rabbit Ig (antibody 550338)
    a. Store in refrigerator

Solutions Needed:

1. H_2O_2
    a. 3% solution
    b. Dilute 30% hydrogen peroxide in methanol
    c. 100 ul H_2O_2 in 900 ul methanol
2. Chondroitinase-ABC
    a. Dilute 0.2 Units/ mL buffer
    b. Add 1 mg BSA per 1 mL of 0.1 Tris Acetate
    c. Example: 0.056 g BSA + 56 mL 0.1 M Tris Acetate + 11.2 U of cABC)
3. Acetic Acid
    a. Dilute 1.43 mL of Acetic Acid in 48.57 mL DI H_2O
4. Goat serum
    a. 1:10 dilution
    b. 1 ml serum in 9 ml 1x PBS
5. Horse serum
    a. 1:10 dilution
    b. 1 ml serum in 9 ml 1x PBS
6. Skim Milk
    a. 0.5 g skim milk powder in 10 mL PBS
7. Primary Antibody
    a. 1:300 dilution
    b. Dilute 10 µl Ab in 2990 µl PBS
8. Secondary Antibody
    a. 1:200 dilution
    b. Dilute 10 µl Ab in 1990 µl Horse Serum
9. Vectastain
    a. Prepare 30 minutes prior to use
    b. Mix 1 drop Reagent A in 2.5 mL PBS, vortex. Add 1 drop Reagent B, vortex.
10. DAB
    a. Remove DAB tablets from freezer 30 min prior to use (warm to room temp)
    b. Add 1 gold + 1 silver to 5 ml dH_2O and vortex to dissolve tablets

Other supplies needed:

1. PAP pen
2. IHC slide chamber
3. 1 ml pipette
4. 20 µl pipette

DAY 1

Deparaffanize sections:

1. CitriSolv® 5min×3 times
2. 100% EtOH 5min
3. 95% EtOH 5min
4. 70% EtOH 5min
5. 50% EtOH 5min
6. DI H_2O 5min
7. Mark around samples using water-proof pen.

Digestion (antigen retrieval; unmasking):

1. Incubate samples in 200µl 0.2 U/mL Chondroitinase-ABC (Solution 2) for 60 min at 37°C.
2. Rinse 2X with PBS for at least 5 min each.
3. Line IHC chambers with wet paper towels (close lid during incubation).
4. Incubate samples in 0.5 N Acetic acid- DI H_2O (Solution 3) for 4 hours at 4°C.
5. Rinse 2X with PBS for at least 5 min each.

Block for endogenous peroxidase:

1. Incubate samples in 3% H_2O_2-Methanol (Solution 1) for 10 min at room temperature.
2. Rinse with PBS for at least 5 min.

Block non-specific binding:

1. Apply 5% skim milk-PBS (Solution 6) for 30 min to eliminate background staining.
2. Rinse with PBS for at least 5 min.
3. Apply Goat serum-PBS (Solution 4) to cover samples and incubate for 20 min to eliminate the background staining.

Primary Antibody:

1. Apply primary antibody LF-113 (Solution 7) to cover samples. For negative control apply the same amount of 10% Horse Serum (Solution 5).
2. Close the lid of the moist chamber.
3. Incubate two nights and three days (approximately 34-38 hours) at 4°C.

DAY 3

1. Rinse 3X with PBS for at least 5 min each.

Secondary Antibody and Vectastain:

1. Apply secondary antibody 550338 (Solution 8) to cover samples and incubate for 30 min at room temp.
2. Rinse 2X with PBS for at least 5 min each.
3. Apply VECTASTAIN ABC reagent (Solution 9) to cover samples and incubate for 30 min at room temp.
4. Rinse with PBS for at least 5 min.

DAB enzymatic reaction:

1. Incubate in DAB (Solution 10) under hood for 4 min at room temp.
2. Immediately rinse with tap water to end reaction

Dehydration and coverslip:

1. Rinse 3X with PBS for at least 5 min.
2. DI H_2O 1min
3. 70% EtOH 2min×2 times
4. 95% EtOH 2min×2 times
5. 100% EtOH 2min×2 times
6. CitriSolv® 5min×2 times
7. Add four drops of Cytoseal, coverslip, and dry slides overnight.

A19. Immunohistochemical Staining Protocol: IL1-β

Preparation:

Antibody Preparation:

1. Primary: 1L-1β (Chemicon AB1832)
    a. Reconstitute powder in 50 ul sterile water
    b. Aliquot 10 ul into small eppendorf tubes, store at -20C
2. Secondary: Peroxidase Goat anti-Rabbit IgG (Jackson Co. 111-035-003)
    a. Reconstitute powder in 2 ml with sterile water
    b. Aliquot 50 ul into small eppendorf tubes, store at -20C

    **Keep one tube of each in fridge (label with date and 6 week expiration)

Solutions Needed:

1. H_2O_2
    a. 3% solution
    b. Dilute 30% hydrogen peroxide in methanol
    c. 100 ul H_2O_2 in 900 ul methanol
2. Pepsin
    a. Make 0.01N HCl (dilute in water)
    b. Dilute 35 µl pepsin (prepared aliquot) with 965 µl HCl
3. Goat serum
    a. 1:8 dilution
    b. 1 ml serum (aliquoted) in 7 ml 1x PBS
4. Milk solution
    a. 2% solution
    b. 1 g dry milk in 50 ml 1x PBS
5. Combined serum and milk solutions
    a. 250 µl goat serum in 10 ml milk
6. Primary Antibody
    a. 1:250 dilution
    b. Dilute 5 µl Ab in 1245 µl PBS
7. Secondary Antibody
    a. 1:100 dilution
    b. Dilute 10 µl Ab in 990 µl PBS
8. DAB
    a. Remove DAB tablets from freezer 30 min prior to use (warm to room temp)
    b. Add 1 gold + 1 silver to 5 ml dH_2O and vortex to dissolve tablets

Other supplies needed:

1. PAP pen
2. IHC slide chamber
3. 1 ml pipette
4. 20 ul pipette

DAY 1

Deparaffinize sections:

1. Xylene	5 min. x 2
2. 100% EtOH	2 min. x 2
3. 95% EtOH	2 min. x 2
4. 70% EtOH	2 min. x 1
5. PBS	5 min. x 1

6. Circle sections with pap pen
7. Line plastic chambers with wet paper towels (close lid during incubations)

Block for endogenous peroxidase:

1. Incubate in 3% H_2O_2 (solution 1) for 30 min at room temp.
2. Rinse with PBS for 5 min.

Pepsin digest (antigen retrieval; unmasking):

1. Incubate in pepsin (solution 2) for 20 min at room temp.
2. Rinse with PBS 5 min x 3

Block non-specific binding:

1. Incubate in serum/milk mixture (solution 5) for 20 min at room temp
2. Vacuum off solution (without rinsing)

Primary antibody:

1. Incubate with primary antibody (solution 6) overnight at room temperature
2. For 1 section, incubate with PBS overnight at room temperature (neg ctrl)

DAY 2

1. Rinse with PBS 5 min x 3

Secondary antibody:

1. Incubate with secondary antibody (Solution 7) for 2 hours at room temp
2. Rinse with PBS for 5 min x3

DAB enzymatic reaction:

1. Incubate in DAB (Solution 8) under hood for 3 min at room temp.
2. Immediately rinse with tap water to end reaction

Dehydration and coverslip:

1. Rinse with PBS for 5 min x3
2. dH_2O 1 min
3. 70% EtOH 2 min x2 times
4. 95% EtOH 2 min x2 times
5. 100% EtOH 2 min x2 times
6. Xylene 5 min x2 times

A20. Immunohistochemical Staining Protocol: Grading

1. Before you begin, you must rename all Immuno stained pictures with a letter in order to blind the graders. Be sure to keep track of the original specimen name and associated letter
2. Open a blank PowerPoint presentation
3. Place each stained image into the PowerPoint file, arranging from least stained to most stained.
4. After all images have been placed into the file, break images into 4 equal sections (0-undetectable, 1=low, 2=medium, 3=high).
5. Choose the middle image (approximately) in each section to represent that grade (for example 0,1,2,3)
6. Create a separate PowerPoint slide with these standard images and associated grades.
7. Instruct each blinded grader to set this image as their desktop, and then open each image to be graded against it.
8. Instruct each grader to record their grade for each image.
9. After all 3 blinded graders are finished; assign the mode of the grades among them to each sample.
10. Repeat for each tendon, each location, and each target.

A21. Joint Function: Ground Reaction Force Measurement and Analysis

Measurement

1. Acclimate animals prior to measurement.
2. All lights should be off (except light under lane) and the room should be silent.
3. ZERO the load cells.
4. Type in Animal ID, Measurement #, and Walk #. NOTE: Measurement # and Walk # should be switched due to bug in software.
5. Place animal in lane and allow for unrestricted movement across lane at own will.
6. Press Record and Save.
7. Record letter grade for walk and indicate which plate the paw is isolated on.
8. At minimum, record 2 walks per animal (at least one should be an "A" and isolated on one plate).

Analysis

1. Run the Matlab GUI "drw.m" " (located in \\medfiles\ort\McKay_Lab_Folders\SoslowskyLab\Software-Released\DRW).
2. Load forcetorque.txt file to be analyzed.
3. Use scroll bar to scan to start of first front paw down (corresponds with initial spike in force).
4. In PawDown window, click which paw is down (e.g., LF) and on which force plate (e.g., 1).
5. Scroll through until paw is lifted and unclick which paw is down.
6. Repeat for each paw.
7. Export AnimalID_grf.txt file.
8. When complete, summarize data and copy and paste into Excel.
9. NOTE: Use best run for each rat (based on notebook chart) and normalize each force by animal bodyweight.

A22. Joint Function: Spatio-Temporal Parameter Analysis

Analysis

1. Run the Matlab GUI "tiptoe.m" " (located in \\medfiles\ort\McKay_Lab_Folders\SoslowskyLab\Software-Released\Tiptoe).
2. Load images to be analyzed.
3. Calibrate by drawing length of first force plate (68 mm) and save calibration.
4. Use scroll bar to scan to first paw down (entire paw is spread wide and fully on plate).
5. Mark toes by selecting the correct foot (e.g., LF) and correct order (e.g., 1).
6. Repeat for each paw.
7. Export AnimalID_toes.txt file.
8. When complete, summarize data and copy and paste into Excel.
9. NOTE: Use best run for each rat (based on notebook chart).

A23. Passive Joint Mechanics Measurement and Analysis

Measurement

1. Unclick "Remove Bias".
2. To calibrate device, start at ZERO (forelimb fixture is parallel to ground).
3. Press record and rotate through internal and external rotation 3 times.
4. Save file as Cal_Left_M#_rdf.txt.
5. Click "Remove Bias".
6. Place the rat in the Knockout box.
7. Insert the tubes for oxygen (or air) and isofluorane into each hole.
8. Turn the isofluorane on the flow level 5 until the rat falls asleep and does not respond to the pinch test.
9. Remove the tubes from the Knockout box and place them on the nose-cone.
10. Quickly take the rat out of the Knockout box and insert his nose into the nose-cone.
11. Decrease the isofluorane to flow level 2
12. Fasten forelimb (forearm and upperarm) using tie wrap fasteners (2).
13. Position animal at proper height (upper arm should be parallel to ground) and proper orientation (upper arm should be at 90˚ from forearm and scapula should be in resting position on thorax).
14. Start at ZERO.
15. Manually stabilize scapula with thumb, index, and middle finger. Close eyes and rotate through internal and external rotation until scapula begins to lift off thorax (this is the end-range of rotation).
16. Once you have the proper "feel" of end-range, you are ready to record data.
17. Press record.
18. Close eyes and repeat step 15. Repeat three times.
19. Save file as AnimalID_rdf.txt.

Analysis

1. Run the Matlab code "rdf2cyc.m" " (located in \\medfiles\ort\McKay_Lab_Folders\SoslowskyLab\Software-Released\Ratonalysis).
2. Load data file (_rdf.txt).
3. Following prompts, select the beginning and end of each cycle (3 total). The beginning and end should be at 0 on the y-axis and after a full internal and external rotation.
4. Save AnimalID_cyc.txt file.
5. Run the Matlab code "cycle_results.m" " (located in \\medfiles\ort\McKay_Lab_Folders\SoslowskyLab\Software-Released\Ratonalysis).
6. Input peak torque as 100 N-mm.
7. Save AnimalID_result.txt file and paste into Excel.
8. NOTE: Normalize each measurement by baseline.